NASA Contractor Report 189584

Evaluation of Human Response to Structural Vibrations Induced by Sonic Booms

L.C. Sutherland and J. Czech

WYLE RESEARCH
128 Maryland St.
El Segundo, California 90245

NASA

National Aeronautics and
Space Administration

Langley Research Center
Hampton, Virginia 23665-5225

ABSTRACT

This report addresses the topic of building vibration response to sonic boom and the evaluation of the associated human response to this vibration. Within this report, an attempt is made to reexamine some of the issues addressed in the previous extensive coverage of the topic, primarily by NASA, and offer, in some cases, fresh insight that may assist in reassessing the potential impact of sonic boom over populated areas.

The report first reviews human response to vibration and develops, for purposes of this report, a new human vibration response criterion curve as a function of frequency. The difference between response to steady-state versus impulsive vibration is addressed and a "vibration exposure" or "vibration energy" descriptor is suggested as one possible way to evaluate duration effects on response to transient vibration from sonic booms.

New data on the acoustic signature of rattling objects are presented along with a review of existing data on the occurrence of rattle. A fairly consistent pattern for the peak acceleration required to induce rattle is established.

Structural response to sonic boom is reviewed and a new descriptor, "Acceleration Exposure Level" is suggested which can be conveniently determined from the Fourier Spectrum of a sonic boom. Also included is a thorough re-analysis of the structural response data acquired previously by NASA, during the Edwards AFB sonic boom test program in 1966. The previously well-recognized sensitivity of peak acceleration response data to aircraft type is illustrated in more detail.

Lastly, a preliminary assessment of potential impact from sonic booms is provided in terms of human response to vibration and detection of rattle based on a synthesis of the preceding material.

INTRODUCTION

This report addresses the topic of building vibration response to sonic boom and the evaluation of the associated human response to this vibration. This topic has been addressed extensively in prior publications, primarily from NASA–Langley (e.g., Mayes and Edge, 1964; Findley, Huckel and Hubbard, 1966; Hubbard and Mayes, 1967; Carden and Mayes, 1970; Clarkson and Mayes, 1972; Clevenson, 1978; Hubbard, 1982). This extensive past coverage can obviously not be duplicated here. Rather, an attempt is made within this report to reexamine some of the issues addressed by these previous reports and, in some cases, attempt to offer a fresh insight into some aspects of the problems. Hopefully, this may assist in reassessing the potential impact of sonic boom exposure over populated areas that may ensue from overland commercial operations of a new generation supersonic transport.

The report first reviews, in Section 1, criteria for human response to vibration. For purposes of this report, a new human vibration response criterion curve is developed as a function of frequency which is a composite of kinesthetic and tactile vibration responses. Next, the difference between human response to steady-state versus impulsive vibration is addressed and a "vibration exposure" (i.e., vibration energy) descriptor is suggested as one possible way to evaluate duration effects on response to transient vibration.

Section 2 reexamines the problem of response to rattle with limited new data on the acoustic signature of rattling objects and summarizes criteria and data on the occurrence of rattle. A fairly consistent pattern for the peak acceleration required to induce rattle is established by this latter process.

Section 3 examines structural response to sonic boom in some detail, including a review of the Acceleration Shock Spectra for several sonic boom time histories. Also a new descriptor, "Acceleration Exposure Level" (see discussion above on human response and acceleration exposure), is suggested, which is an approximate measure of the maximum structural response that can be conveniently determined from the Fourier Spectra of a sonic boom. Also included is a thorough re-analysis of the structural response data acquired previously during the Edwards Air Force Base sonic boom test program in 1966 (Stanford, 1967; Blume et al., 1967). Sensitivity of the peak acceleration response data to aircraft type (i.e., sonic boom signature characteristics), which had been well recognized by the original NASA experimenters, is illustrated in more detail.

Finally, Section 4 provides a preliminary assessment of potential impact from sonic booms in terms of human response to vibration and detection of rattle based on a synthesis of the preceding three sections. Further research remains to be done to explore, more thoroughly, human response to transient vibration and the anticipated acceleration response of structure to generic boom-minimized sonic boom signatures.

TABLE OF CONTENTS

TABLE OF CONTENTS (Continued)

LIST OF TABLES

LIST OF FIGURES

LIST OF FIGURES (Continued)

Figure   **Page**

1.0 CRITERIA FOR HUMAN PERCEPTION OF BUILDING VIBRATION

Vibration of building surfaces can be perceived by humans in four ways: (1) by kinesthetic perception of whole-body vibration in any direction, (2) by tactile perception of vibration at the fingertips, (3) by acoustic detection of sound radiated by the vibrating surface itself or radiated by an object that rattles against the surface due to its vibration, or (4) by visual perception. Only the first three perception modes are addressed in this report.

1.1 Criteria for Whole-Body Vibration

Preliminary criteria for human response to whole-body vibration were summarized 30 years ago in Goldman and von Gierke, 1961, based on extensive research available in the late 1950s. They defined a range of criteria for the threshold of perception, unpleasantness and voluntary tolerance. The ranges for the first two criteria are shown in Figure 1.

More recently, an International Standard has evolved which defines criteria for acceptable vibration levels, as a function of time of exposure, at a "reduced comfort boundary" (ISO, 1985). Criteria are defined in the standard for longitudinal and lateral whole-body vibration. (The most recent 1985 version of this standard increased the criterion levels for the longitudinal direction by 2 dB over values specified in an earlier, 1974 version.) Longitudinal whole-body vibration is often called vertical vibration but actually corresponds to vibration excitation in the direction of a person's spine while sitting, standing or lying down. Lateral whole-body vibration is at 90° to this direction.

Stephens *et al.*, 1982, suggested a composite vibration perception threshold criterion based on an amendment (ISO, 1977) to ISO Standard 2631-1974 and another ISO guide for horizontal vibration (ISO, 1979). However, the latest addition to the ISO standards (ISO, 1989) indicates slightly (3 dB) higher vibration levels for this composite horizontal and vertical perception threshold criteria. Figure 1 compares these three sets of criteria: (1) Unpleasantness and Perception from Goldman and von Gierke, 1961; (2) Reduced Comfort (for 24-hour exposure) from ISO, 1985; and (3) Perception Threshold from ISO, 1989. The criteria for perception threshold, from Goldman and von Gierke and the various ISO criteria, lie within about a 30 dB-wide band of peak acceleration levels over the frequency range of 1 to 100 Hz. Not shown in the figure are values for a vibration detection threshold from Bekesy for horizontal motion which lie very close to the lower boundary of the "perception" threshold range from Goldman and von Gierke, 1961.
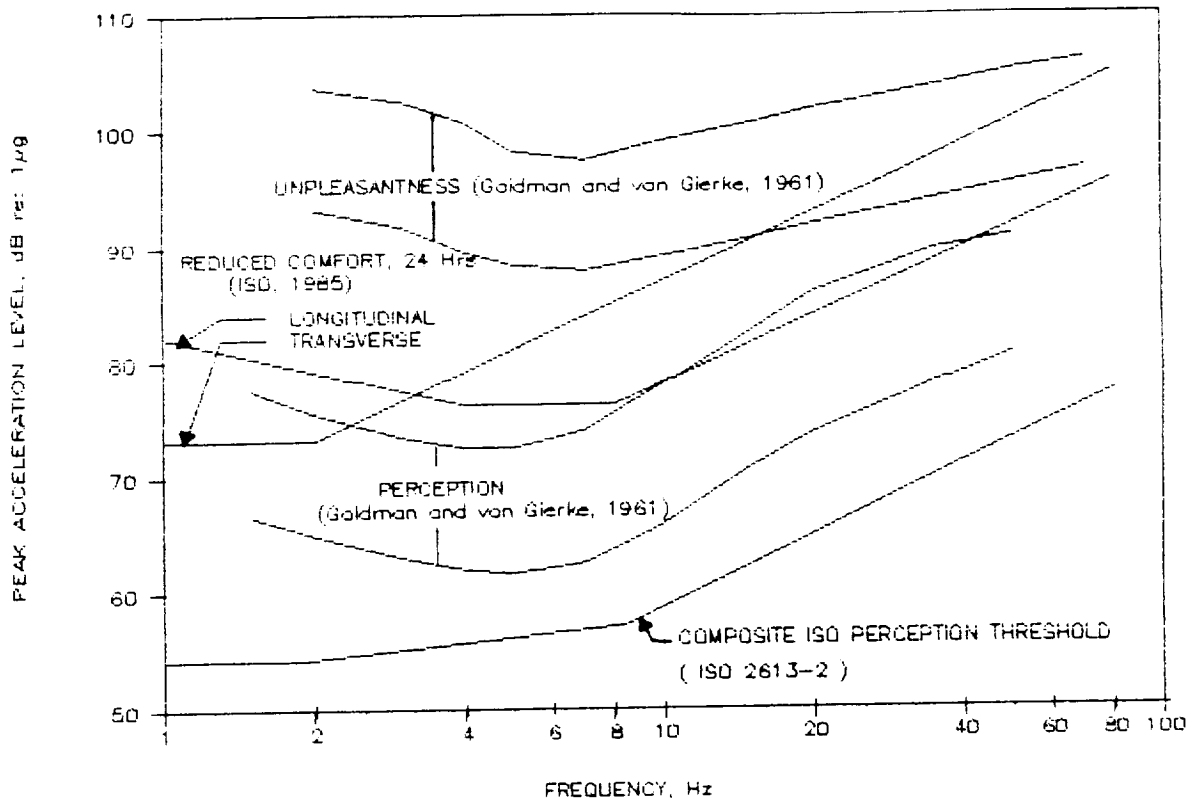
Figure 1.   Comparison of Human Response Criteria for Whole-Body Vibration.
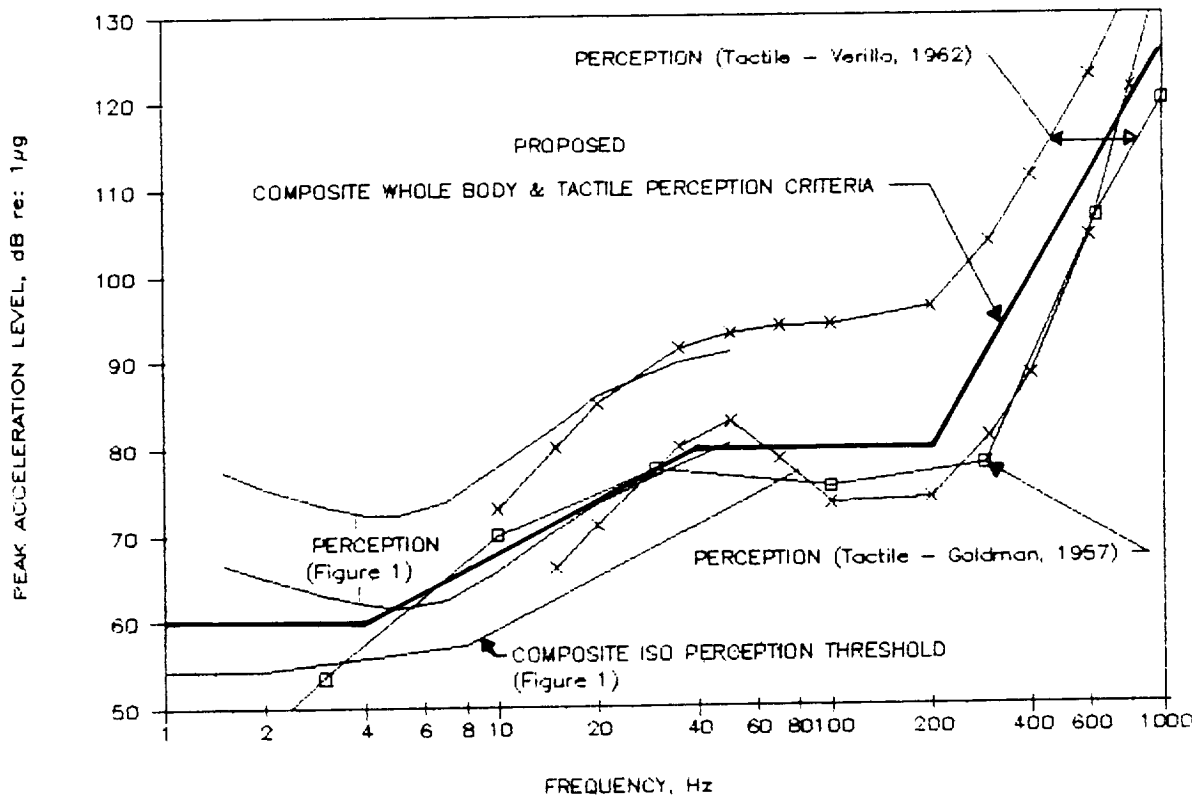
Figure 2.   Proposed Composite Whole-Body and Tactile Vibration Criteria.

1.2 Criteria for Tactile Vibration

Criteria for response to tactile vibration have been developed by Goldman, 1957 and from an extensive survey of six such studies summarized by Verillo, 1962. The criteria developed from these studies are compared, in Figure 2, to the criteria for perception and the composite ISO criteria for whole-body vibration from Figure 1. (The data from Verillo is shown as a range.) The vibration criteria for "Reduced Comfort for 24-Hr Exposure" in Figure 1 was omitted here since it was not at all certain that it was applicable for this study. It is clear that the whole-body vibration criteria tend to overlap the tactile vibration criteria over the frequency range where both criteria are specified, from about 2 to 80 Hz. Note, also, that Goldman's tactile vibration criteria are quite close to the lower range of the data from the survey by Verillo.

1.3 Composite Whole-Body and Tactile Vibration Perception Criteria

For purposes of this study, it was desirable to establish a single human vibration perception criteria curve. Such a curve, corresponding roughly to an average of all of the other criteria shown in Figure 2, is also shown by the heavy black line. This proposed simplified criteria curve for human whole-body (vertical and horizontal) and tactile vibration is defined by the following expressions for the peak vibration level, $L_{pk}(f)$ in decibels, re: 1 µg as a function of frequency.

$$L_{pk}(f) = \begin{cases} 60 & f < 4 \quad \text{Hz} \\ 60+20\lg(f/4) & 4 \le f < 40 \quad \text{Hz} \\ 80 & 40 \le f < 200 \quad \text{Hz} \\ 80+66\lg(f/200) & f \ge 200 \quad \text{Hz} \end{cases} \qquad (1)$$

It is important to recognize that this criteria is *only* intended to be applied as a convenient analysis guide for this study – it is *not* intended to represent a replacement for the currently well-defined ISO standards. However, the latter do not include tactile vibration and hence the need, in this study, for the proposed single criterion curve described by Eq. (1).

1.4 Response to Continuous vs Transient (Impulsive) Vibration

One might justifiably question the averaging process employed here to develop the preceding vibration sensitivity criteria. In particular, one could question including both the earlier (Goldman and von Gierke, 1961) and more recent (ISO, 1989) perception criteria in this averaging process since they differ substantially and the more recent version can be presumed

to be more reliable. However, there is another factor that has not been considered that would tend to support the values in the above expression. It is reasonable to assume that the whole-body vibration criteria presented so far represent human response to internal physiological stress due to dynamic stretching of connective body tissues. For example, given the simplified dynamic model of the human body (von Gierke, 1964) illustrated in Figure 3, one could expect that dynamic relative displacements between the various "lumped mass" elements of the body as a result of vibration input would represent such stretching of the connective tissue, i.e., the springs. The point is that for <u>continuous vibration input, the peak internal "stress" response, call it R(f), at any one frequency f of the input signal, would be equal to the vibration input, A(f) times a frequency-dependent vibration attenuation factor, K(f) times a Resonance Amplification Factor, Q</u> or:

$$R(f) = A(f) \cdot K(f) \cdot Q \qquad\qquad (2)$$

The factor Q is estimated to be relatively low, of the order of 2 to 4 (Goldman, 1957). In contrast, for a transient impulsive vibration input of the same peak magnitude at a given frequency, the internal physiological response would be governed by the same sort of expression except that the Resonance Amplification Factor Q would be replaced with a dynamic magnification (shock response) factor which will probably not exceed about 2 for sonic boom-type excitation. Thus one can crudely estimate that, all other things being equal, human vibration response criterion levels to impulsive transient vibration would be of the order of 1 to 2 times greater for sonic excitation than for steady-state continuous vibration. <u>Very limited information on the difference between human response criteria for continuous vs impulsive vibration is consistent with this very rough estimate (CHABA, 1977)</u>. For example, the following values are suggested as acceptable acceleration inputs to occupied residences (CHABA, 1977) for these two different types of vibration environments.

Acceptable Acceleration, m/sec^2
(CHABA, 1977)

Time of Day	Continuous rms	Impulsive peak
Day	$0.072/\sqrt{t}$	$0.1/\sqrt{N}$
Night	0.005	0.01

where t = duration of continuous vibration in seconds, or N = number of vibration impulses.
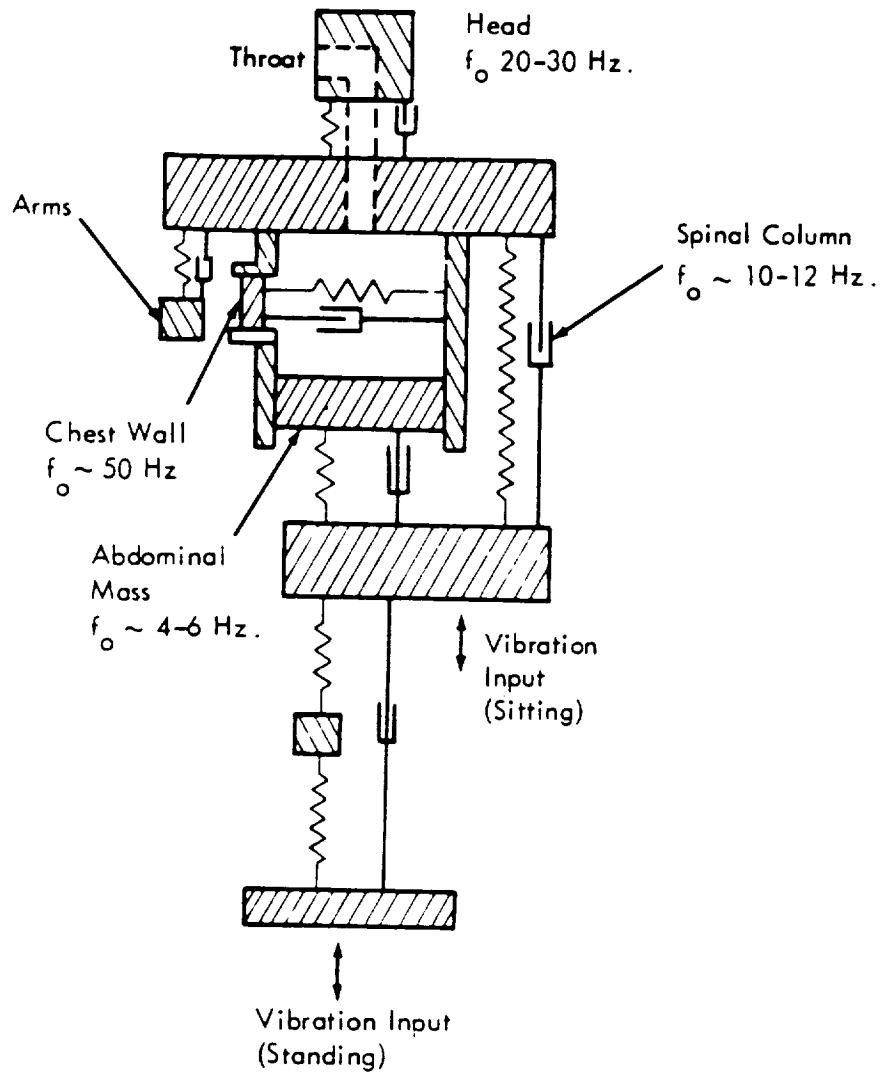
Figure 3.   Mechanical Model of Human Body Exposed to Vibration (from von Gierke, 1964).

In this case, allowing for a peak/rms ratio of $\sqrt{2}$ for the continuous vibration, the acceptable levels for a four-second "continuous" vibration would be about one half the acceptable level for one impulse for day-time exposure. This would support a value of 2 as the ratio between continuous vs an impulsive vibration input for this particular set of conditions. Clearly, however, application of this same rationale would support a wide range of values for this ratio depending on the duration of the continuous vibration versus the number of impulses for the transient vibration.

The overall point here is that if the earlier perception criteria line(s) from Goldman and von Gierke in Figure 2 are discarded, one could argue that the composite ISO perception criteria line should increase for impulsive vibration and hence more closely approach the tactile vibration criteria. Unlike the whole-body vibration criteria, the latter are *not* expected to have any significant difference between continuous versus impulsive vibration since, in this case, the physiological sensors are near the surface of the skin and should not have any significant dynamic response (i.e., resonance) characteristics in the low-frequency range of concern, so that impulsive vibration inputs would be perceived differently. Clearly, there is much speculation involved here that deserves a more careful evaluation. A cursory examination of the literature does not indicate anything substantial on this issue of human response to transient, low-level impulsive vibration and further research may be called for.

1.5 Duration Effects on Human Response to Vibration

The ISO standards on whole-body vibration (ISO, 1985) specify allowable levels of acceleration as a function of both frequency and time. The values shown in Figure 1 for the "Reduced Comfort" criteria were for a 24-hour exposure. Values for shorter exposure durations are simply increased in level by a constant amount at all frequencies. The resulting trade-off between level and duration of exposure is shown in Figure 4a in terms of the rms acceleration level, in decibels, relative to the value for a 24-hour exposure. Over a substantial portion of the range of shorter durations, the level vs duration trade-off follows an equal energy rule as, illustrated in the figure. Over the range of durations from 16 minutes to 4 hours, the allowable vibration exposure corresponds to a constant value of what will be called the Acceleration Exposure Level (abbreviated AEL and symbolized as L_{AE}), that is 4.1 ±0.5 dB above the Acceleration Exposure Level for a 24-hour exposure. This new quantity, Acceleration Exposure Level, is recognizable as equivalent to Sound Exposure Level in noise exposure and can be given, in decibels re: $(1\mu g)^2 \cdot sec.$, by:

(a)   Duration (from ISO-2631-1, 1985)
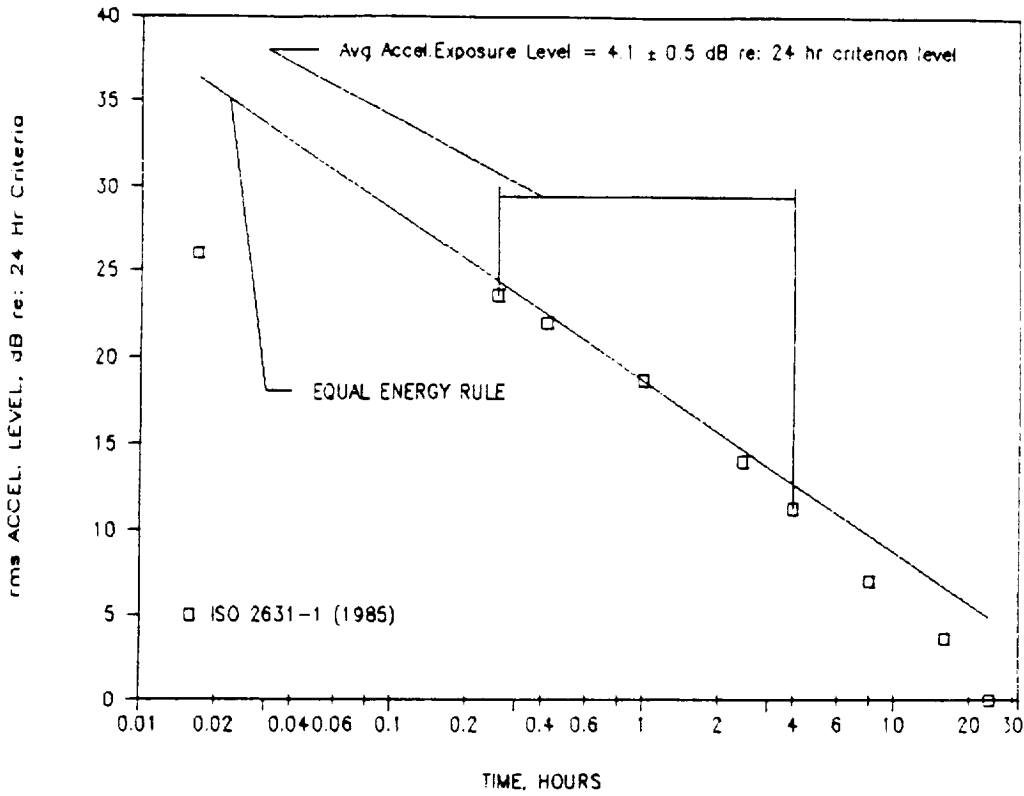
(b)   Number of Impulses (from CHABA, 1977)
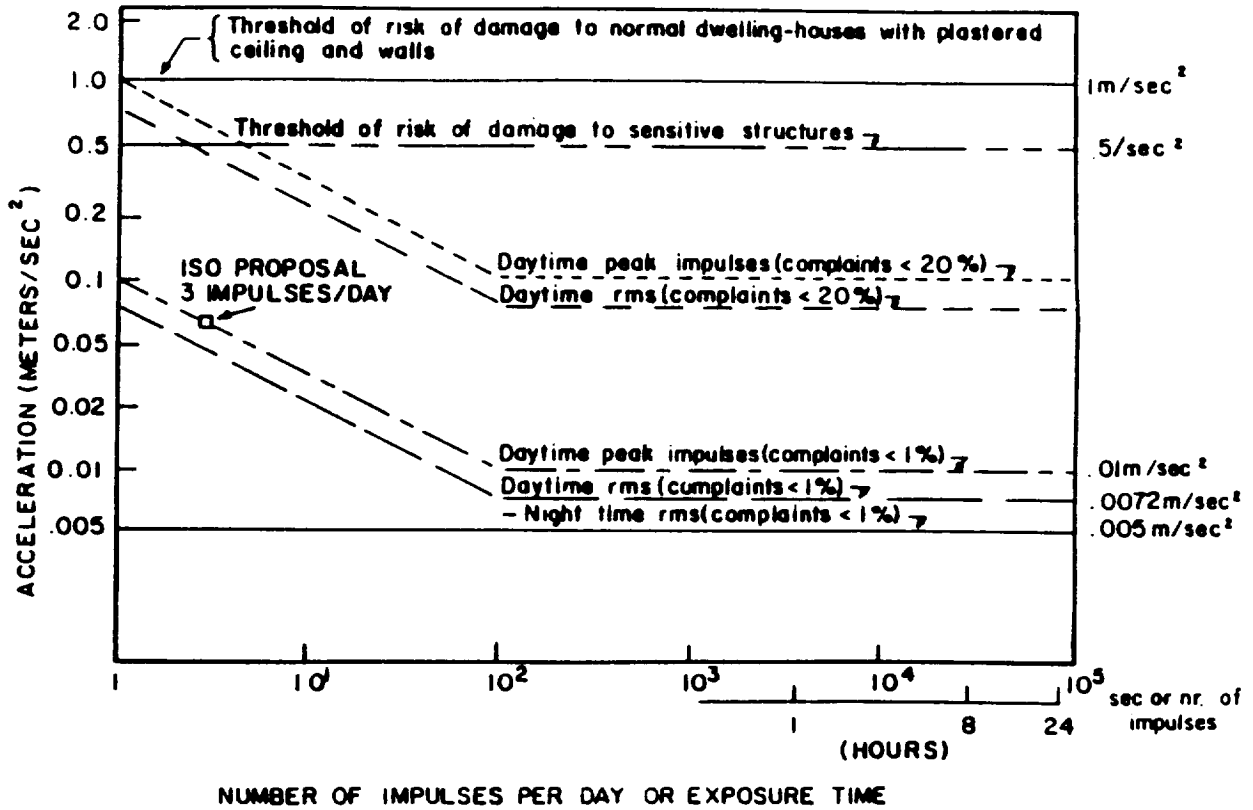
Figure 4.   Criteria for Exposure to Vibration as a Function of (a) Duration, or (b) Number of Impulses.

$$L_{AE} = 10 \cdot \lg \left[\int_{O}^{T} A^2(t)\, dt \,/\, [A_o^2 \cdot \delta t] \right] \qquad (3)$$

where A_o is a reference acceleration equal to 1 μg and δt is a reference duration equal to 1 second.

The failure of the criterion levels to follow this equal energy rule at the shortest durations can be attributed to the fact that the rms acceleration levels approach high, potentially intolerable, levels so that the acceleration amplitude, rather than the time-integrated acceleration exposure, becomes the limiting criteria. The basis for the deviation in the criteria from an equal energy rule for exposures between 4 and 24 hours is not clear. However, this deviation is not large – only about 4 dB. Thus the ISO whole-body vibration criteria (ISO, 1985) follow, approximately, an equal energy rule or constant value for AEL for durations greater than 16 minutes. However, this duration is clearly much greater than the durations on the order of 0.2 to 1 second that we are concerned with for response to sonic-boom-induced vibration from one event.

To explore this problem further, it is useful to examine the more conservative guidelines developed in 1977 by Working Group 69 of the Committee on Hearing, Bio-acoustics and Biomechanics (CHABA) for evaluation of environmental impact of vibration in residences (CHABA, 1977). These guidelines are shown in Figure 4b in terms of overall rms (continuous) or peak (impulsive) acceleration levels in residences that would be expected to be acceptable (i.e., less than 1 percent of people would complain). Although not pertinent here, it is desirable to point out that these overall acceleration levels are values that would be measured with a frequency-weighting network designed to approximate the complement of the average of the ISO criterion curves of acceleration versus frequency for horizontal and vertical whole-body vibration (CHABA, 1977).

Evaluation of the curves in Figure 4b indicate that for daytime exposure to continuous vibration lasting no more than 100 seconds, the allowable vibration is equivalent to a constant rms Acceleration Exposure Level (AEL) of 77.3 dB re $(1\mu g)^2 \cdot$ sec. for less than 1 percent complaints and 97.3 dB re: $(1\mu g)^2 \cdot$ sec. for less than 20 percent complaints. From the Composite Perception Threshold criteria curve in Figure 2, at frequencies in the range of 4 to 12 Hz (where the ISO frequency weighting is minimal and corresponding to the lowest biodynamic resonance frequencies indicated in Figure 3), the perception criteria correspond to an rms acceleration level of 57 to 67 dB re: 1μg. Assuming a minimum duration of the order of 1 sec for sonic boom-induced vibration, this perception threshold would correspond to an

Acceleration Exposure Level of 62 ±5 dB re: (1 μg)^2 • sec. Thus a range of about 20 dB (a factor of 10 in magnitude of acceleration), is suggested as the approximate range between a detection threshold and a lower limit for acceptability of whole-body vibration at low frequencies. This range appears to correspond to values of AEL from 62 to 77 dB re: (1 μg)^2 • sec. This wide range in an acceptable (or detectable) AEL is comparable to the wide range in acceleration magnitude for such levels as shown in Figure 1 and 2. A brief look at one specific study on response to transient vibration (Wiss and Parmelee, 1974) indicates similar results.

In a study of passenger vibration discomfort criteria, Clevenson *et al.*, 1978, found that the threshold for discomfort for vertical vibration was reached at a wide-band (1 to 20 Hz) random rms acceleration level of 0.027 g. This threshold was essentially independent of duration which varied from 0.25 minute to 60 minutes. At higher vibration levels, the discomfort rating by the subjects actually decreased slightly with increasing duration of exposure – a trend in the opposite direction from what would be expected on the basis of the "equal energy" rule suggested earlier. This trend was presumed to be due to adaptation by the subjects to the test stimuli. In contrast, a study by Young, 1975, indicates that an energy measure may be appropriate for evaluation of human response to impulsive-type vibration. Clearly, further research is needed to resolve the effects of duration on response to transient vibration. However, for purposes of this report, it will be assumed that the more conservative model associated with the use of an Acceleration Exposure Level (Equal Energy) criteria is appropriate.

2.0 CRITERIA FOR HUMAN PERCEPTION OF RATTLE

It is expected that "rattle" of interior furnishings in a room, such as wall-hung pictures, interior doors, loose windows or bric-a-brac on shelves, will be perceived primarily as an audible sound rather than as a visually detected vibration. This is not to say that human perception of a vibrating surface might not occur from a visual stimulus at a lower vibration level than from an acoustic stimulus. However, perception of a visual stimulus requires that one's visual field of view is oriented towards the vibrating surface while an auditory stimulus would not ordinarily require any such selective orientation of a listener. Thus, for purposes of this study, perception of rattle will be presumed to occur when: (1) an object will, in fact, "rattle" upon exposure of a building to sonic boom, and (2) the "rattle" sound will be clearly audible.

A number of studies have attempted to assess human response to rattle sounds as heard indoors and the following trend seems to apply. The subjectively judged magnitude of aircraft noise inside a room does not appear to be changed by the introduction of a typical rattle sound (Cawthorne, Dempsey and DeLoach, 1978). However, the subjectively judged annoyance of such a sound does appear to be increased when it generates an audible rattle or sound, or causes perceptible building vibration. For an aircraft noise-induced rattle or flow vibration stimulus, the increase in annoyance was equivalent to an increase in the aircraft noise of about 12 to 22 dB (Cawthorne, Dempsey and DeLoach, 1978). For helicopter noise, the equivalent increase in stimulus ranged from about 5 to 20 dB (Schomer and Neathammer, 1985). For a simulated blast sound, the presence of rattle indoors was equivalent to an increase in stimulus level in the range of 6 to 13 dB (Schomer and Averbuch, 1989). In all three studies, the effective (i.e., equal annoyance) stimulus level increased as the rattle-inducing noise level increased. In summary, there seems to be no question that the judged annoyance of a sound, able to excite rattle inside a building, is substantially greater than the judged annoyance in the absence of rattle. Consider, now, the criteria for the detection and generation of rattle sounds.

2.1 Acoustic Detection of Rattle Noise

It is expected that once rattle occurs, it will ordinarily be readily audible. To provide some minimum validation of this hypothesis, a very limited and relatively crude experiment was conducted. The sound level spectra of several wall-hung rattling objects were measured at a distance of 1 meter from the wall on which they were hung. The objects were wire-hung pictures of various sizes in a typical office. The pictures were manually "rattled" by pressing lightly but rapidly on a portion of the frame in order to displace it from a stable position and

2-1

allow the picture to impact the wall. The impact force was provided by the inherent inertia of the picture returning to its stable position and not by any manual vibration input. Although relatively crude, the experiment provided a reasonably consistent pattern, shown in Figure 5, for the one-third octave band sound pressure level spectrum from impact noise for six different pictures ranging in size from 17 x 21 inches to 29 x 35 inches. Two of the six pictures were glass-covered. For comparison, a bare wooden coat hanger hanging on a coat hook on a wooden door was also "rattled" in a similar manner. The sound level spectra, each measured as a 10 sec. L_{eq}, are compared in Figure 5 with the ambient sound level measured in approximately the same location. The "rattle" spectra shown in the figure have all been corrected for this ambient level. With the exception of most of the one-third octave band levels for the coat hanger rattle spectrum below 200 Hz and the average one-third octave band level at 40 Hz for the six pictures, the signal to noise ratio was sufficient, especially above 125 Hz, to obtain a clearly credible spectrum measurement. (Very limited, uncalibrated data on the sound level of "rattle sounds" – mostly artificially generated by rattling a 4 in x 4 in air filter frame and screen – exhibited comparable maximum spectral levels but shifted to a higher frequency of about 4 kHz [Schomer and Averbuch, 1989]).The general nature of the observed spectra do not appear to be inconsistent with theoretical expectations for impact noise (Richards, 1983; BBN, 1974). However, a more thorough study of the literature should be carried out relative to noise from rattling or impacting objects.

The average A-weighted sound levels measured from this limited study were as follows.

Ambient Background	39 dB(A)
Rattle Noise - Average ± 1 Std. Dev. for Six Pictures	60 dB(A) ± 2.6 dB
Coat Hanger Rattling Against Door	63 dB(A)

It does not require any sophisticated signal detection analysis to recognize that the rattle sounds would be clearly audible in this typical office background noise. However, even in a noisier environment with, for example, radio, TV, conversation or appliance noise in the background with average noise levels in the range of 56 to 62 dB(A) (e.g., Sutherland, 1978), it is still expected that rattle noise with levels such as reported herein would be clearly audible most of the time due to its unique character. Thus, for purposes of this report, perception of rattle will be assumed to occur whenever "rattle" physically occurs – that is, whenever wall-hung pictures or plaques rattle against a wall. Rattling of bric-a-brac (e.g., plates and dishes, etc.) on a shelf
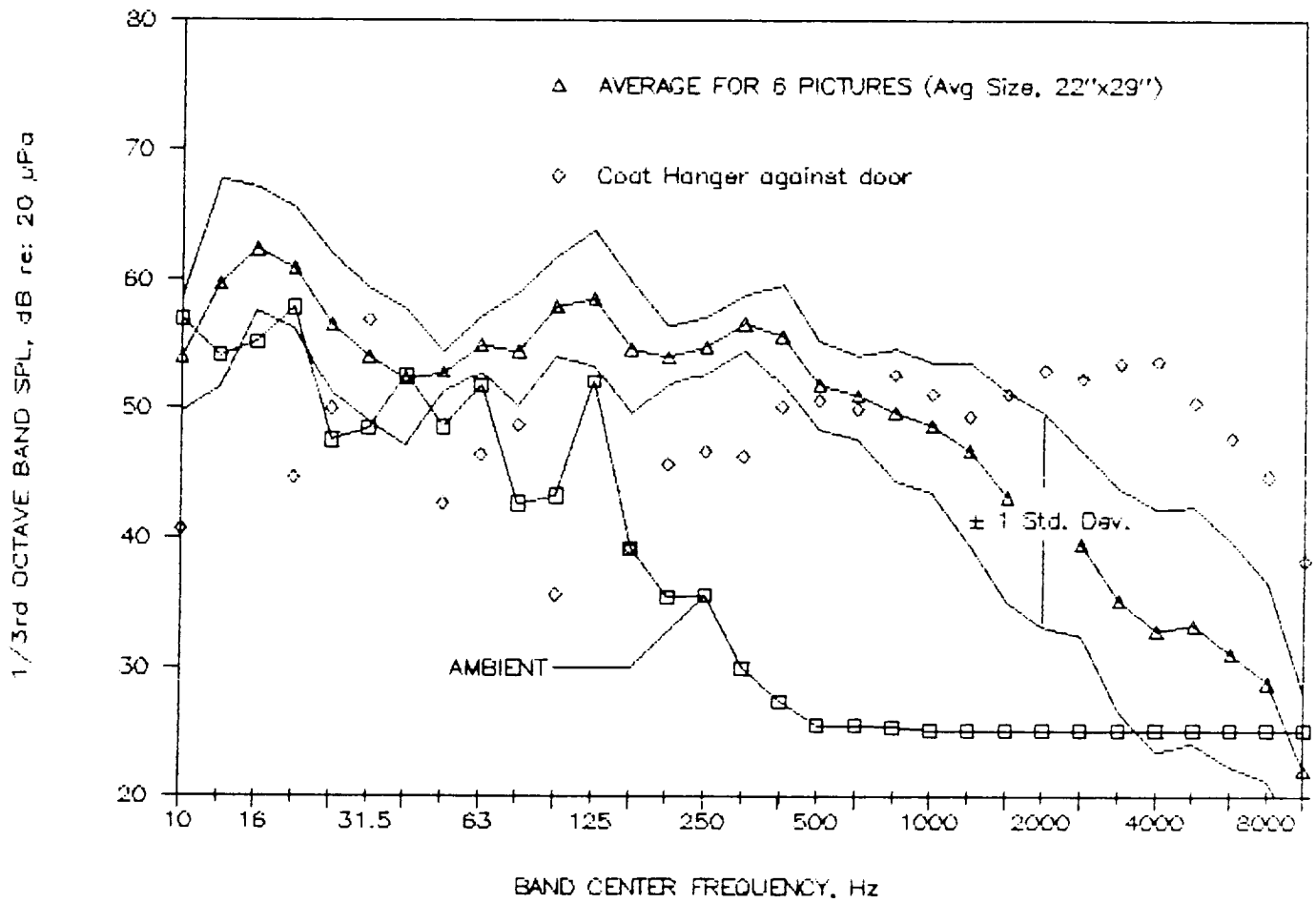
Figure 5.   10-Second Samples of One-Third Octave Band Sound Pressure Levels at 1 Meter from Rattling Objects on Walls.

is a less well-defined problem due to the wide range of randomly-occurring static stability conditions (i.e., the propensity for rattle) for such objects, and will not be treated here. More definitive data on all types of rattle noise obtained under more carefully controlled conditions would obviously be desirable.

2.2 Occurrence of Rattle from Acoustic Excitation

Several studies provide guidance relative to when rattle is expected to occur. One of the first citations of rattle from a sonic boom is in Hubbard and Mayes, 1967. Measurements of the interior response of a building to a sonic boom, shown in Figure 6, include a sound pressure time history (labeled NOISE in the figure) which was recorded with an audio frequency response microphone. According to the experimenters:

> "It is believed that this audible portion of the pressure signal is associated with the rattling of the building structure and furnishings because of the primary mode responses in the building."

A very rough analysis of the pressure signal indicates at least two peaks in its spectrum – one indicating a peak sound pressure level of about 97 dB at a fundamental frequency (probably a room mode) of about 7 Hz and another peak level of about 87 dB at 150 ± 20 Hz. Note that this latter level is considerably higher than any of the peaks in the "rattle noise" spectrum shown earlier in Figure 5. Even allowing for a 10 dB crest factor in this signature, it seems more likely that the "noise" record in Figure 6 is simply a record of the interior sound level of the sonic boom as it would appear when transmitted through the building structure. Rough estimates of this expected internal sound level based on the measured external acoustic signature in Figure 6 and a model for the exterior to interior noise reduction for a typical building (Brown and Sutherland, 1991) indicates that the measured internal "noise" level in Figure 6 would be consistent with this conjecture.

Other studies related to rattle provide information on:

1) Wall acceleration levels at which rattle occurs.

2) Prediction models for these rattle acceleration levels for windows, and for wall-hung pictures or plaques.

3) Measured sound pressure levels for which rattle occurred

4) Acceleration levels of walls or other building elements for acoustic excitation by random (e.g., aircraft noise) or impulsive (e.g., sonic boom or blast noise).
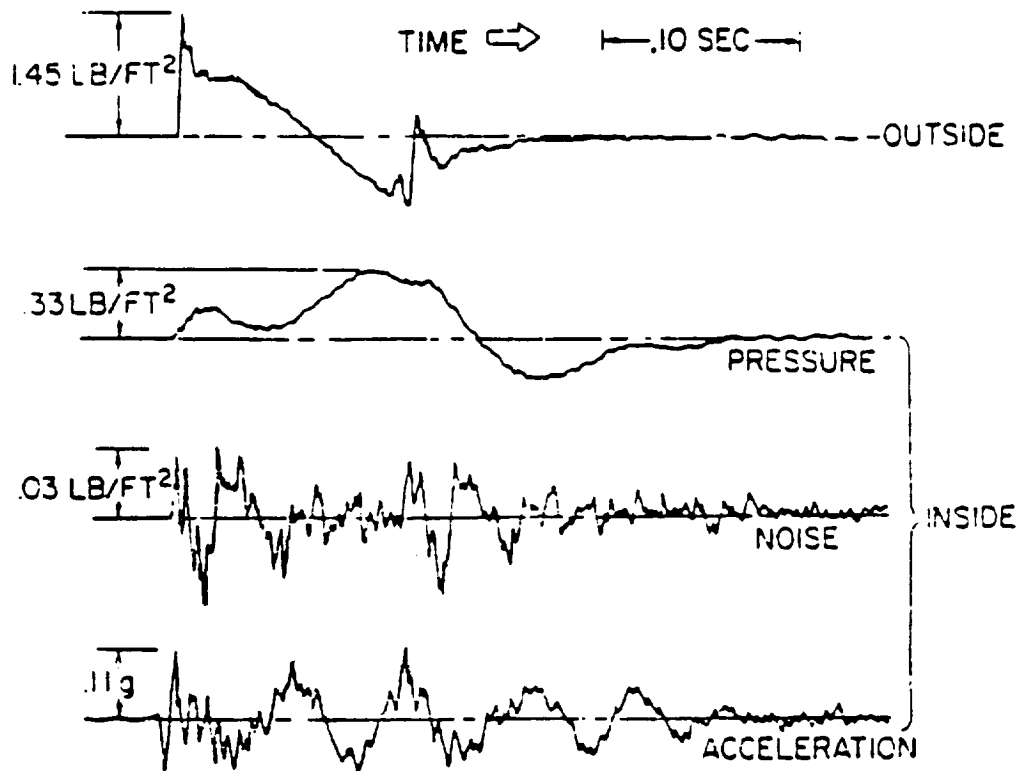
Figure 6. Outside and Inside Exposure Stimuli Due to Sonic Boom (from Hubbard and Mayes, 1967).

The following will attempt to tie together this clearly interrelated information to validate a criterion curve for sonic boom-induced rattle. The first three items are considered in this section.

2.3 Wall Acceleration Levels at Which Rattle Occurs

The most definitive experimental study of rattle of wall-hung plaques or pictures, carried out by Carden and Mayes, 1970, is summarized in Figure 7. Figure 7a shows the mechanical vibration-excited wall acceleration as a function of frequency that was measured, in each of two test buildings at Wallops Islands, near where, in each case, two plaques were mounted. The plaques, weighing 0.676 kg, were 0.502 m long and 0.146 m wide and were hung on a wall-mounted hanger from a small loop built in to the end of each plaque. The plaques hung in the normal fashion, very nearly vertical and close to the wall (Figure 3b in Carden and Mayes, 1970). Based on analysis of the data in Figure 7a and assuming sinusoidal motion, the mean peak wall acceleration at which rattle was first audible, for low-order wall resonance frequencies from 16 to 150 Hz, was about 0.028 g peak. The average lower bound for the wall acceleration threshold over this frequency range for plaque rattle was about 0.023 g peak. Note that in this low-frequency range, the rattle threshold for the plaques appears to be essentially independent of frequency. This will be shown later to be consistent with expected trends.

In the same test program, rattle was also measured for a mirror hung in two different ways in one structure. The results are summarized in Figure 7b in terms of the wall acceleration as a function of the applied mechanical vibration force with and without the mirror in place. The sinusoidal excitation was applied at a wall resonance frequency of 15 Hz. The mirror, weighing 6.5 kg, was 0.61 m high by 0.711 m wide and was apparently hung by two small frame-mounted metal loops from two wall-mounted picture hooks, one pair of each on each side of the mirror frame. Scaling from Figure 3b and 3c in Carden and Mayes, 1978, the distance of the hooks from the top of the picture frame was approximately 0.21 m. For one test, the wall-mounted hook was mounted directly against the wall providing a hanging angle for the mirror of 1.30°. For the second test, the picture hooks were moved out 1.27 cm from the wall to provide a larger hanging angle of 3.14°.

The results of this particular mirror test are shown later to be generally of the right order of magnitude but reversed from the expected trend of higher rattle acceleration thresholds for a higher hanging angle. (Note that the NASA authors indicate that the text on page 14 of Carden and Mayes, 1978, is incorrect in stating: "With the hanger flat against the wall, the rattling

(a) Rattle Threshold for Wall-Mounted Plaques

Wall acceleration (rms), g units

Rattle

No rattle

Structure No.3

Structure No.4

Frequency, Hz
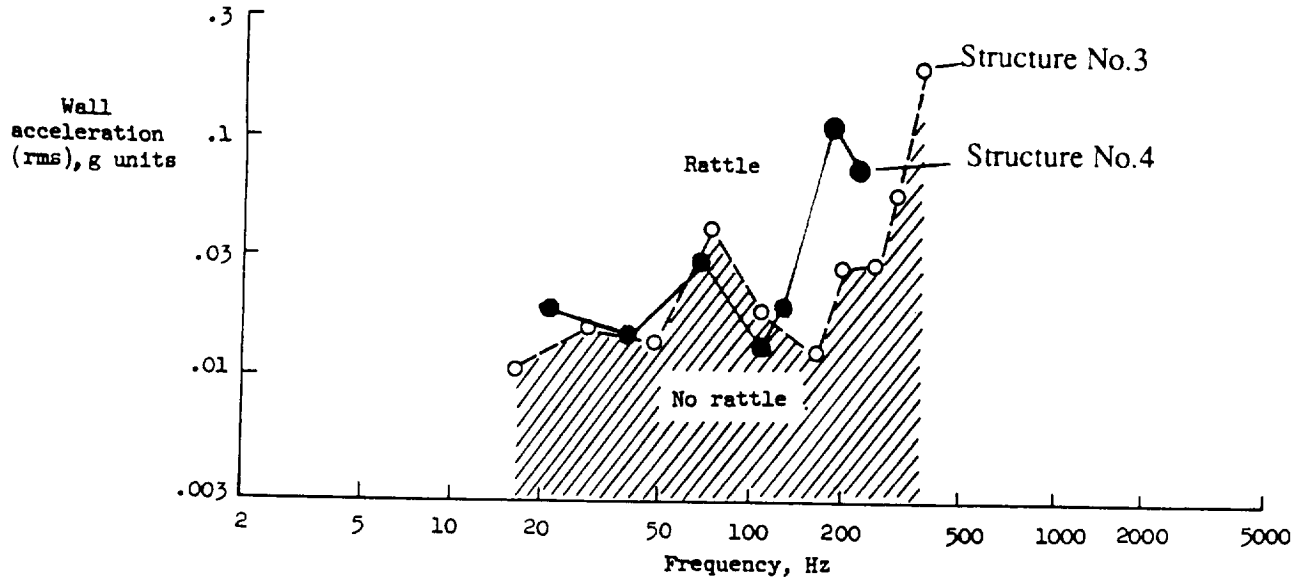
(b) Rattle Threshold for Mirror Hung at Two Different Angles

Wall acceleration (rms), g units

Wall (no mirror)
Wall with mirror (mirror angle 1.30°)
Wall with mirror (mirror angle 3.14°)

Normalized input force
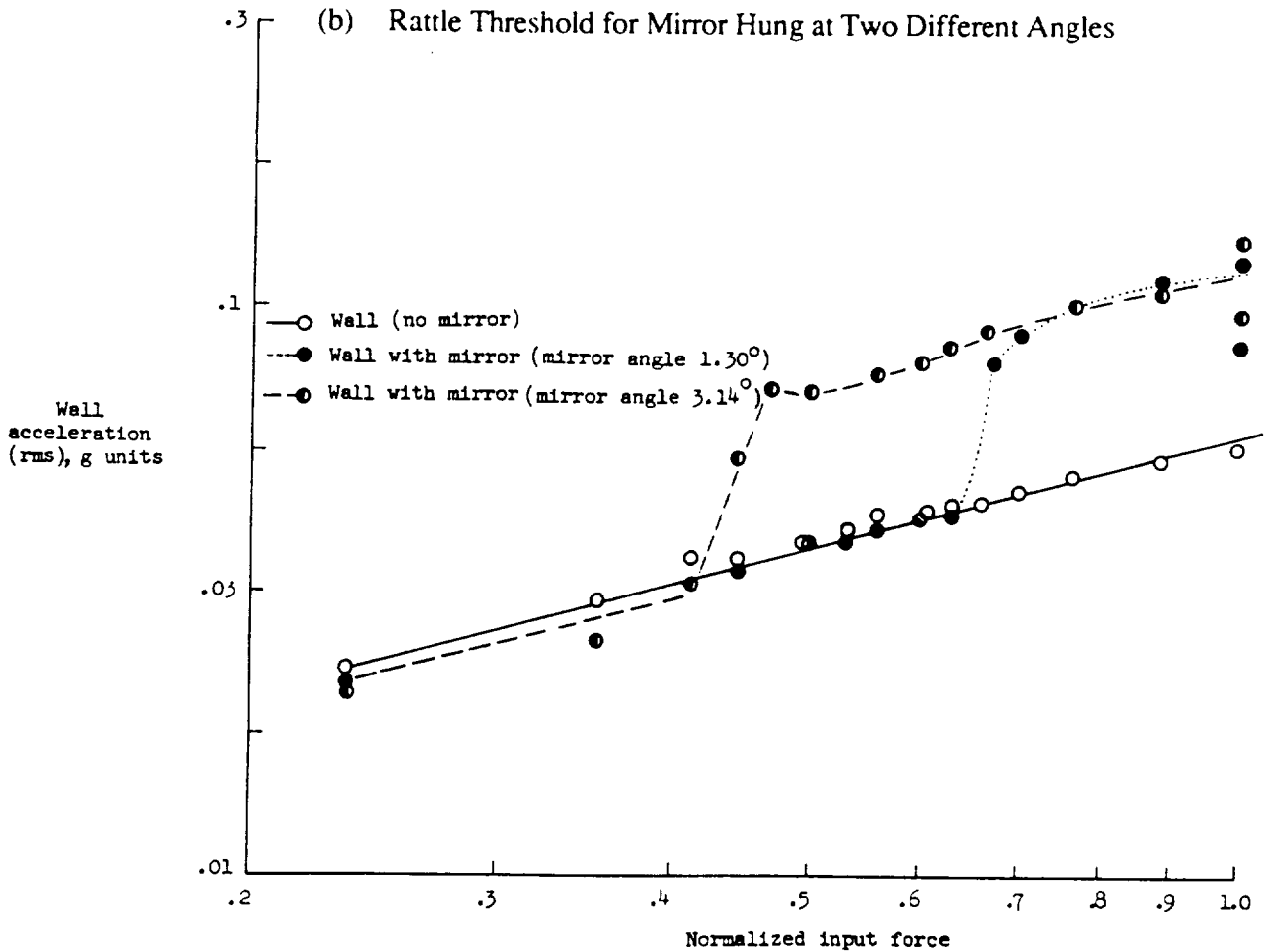
Figure 7. Mechanically Excited Wall Accelerations With and Without Rattle from NASA Tests at Wallops Island (Carden and Mayes, 1971).

2-7

(impacting) is initiated at a lower force level." The data in Figure 7b, taken from the report, correctly shows that, in this case, the lower force level is required to initiate rattle associated with the higher hanging angle.

2.3.1 Predicted Variation in Rattle Acceleration Threshold with Hanging Angle for Wall-Mounted Objects

The expected variation in rattle vibration threshold with the hanging angle of wall-mounted objects was evaluated experimentally by Clevenson, 1978. As shown in Figure 8, his tests of rattle threshold for a simple hanging ball resting against a mechanical vibrator indicated that the critical rattle acceleration magnitude varied directly with the hanging angle, a. In fact, for his particular configuration, he expected, as shown below, that the rattle threshold in peak g's would be numerically equal to the hanging angle (in radians) and independent of the mass of the "rattler." The experimental data partly confirm this theoretical trend. Although the rattle threshold exhibited a small mass effect, it did vary linearly with hanging angle for both masses. However, the average peak rattle acceleration for both masses was about 0.7 times the hanging angle (in radians). Note that the vibration excitation was at a frequency of 20 Hz, well above the natural pendulum frequency of the hanging ball and hence the rattler would act, dynamically, like a mass.

Referring to the insert in Figure 8, summing the moments about the pivot point of the hanging ball with a mass M, mass moment of inertia I_m about the stationary pivot point, and a pendulum length L, the rattle threshold can be defined as follows. (Note that this analysis only treats wall motion at the point of impact of the ball. The pivot point is assumed to be stationary.)

$$MLg \sin (\alpha) - F\ L = I_m\ \ddot{\alpha} \tag{4}$$

where α is the hanging angle in radians, F is the resisting force when the ball is resting against the wall and where $\ddot{\alpha}$ is the angular acceleration of the ball about pivot point P which is equal to $\ddot{x}/L$, where $\ddot{x}$ is the wall acceleration at the impact point. Neglecting the finite size of the ball, I_m is simply ML^2 and, when rattle occurs, F equals 0, so Eq. (4) gives for the rattle threshold acceleration a_r (= $\ddot{x}/g$) for small values of the angle, α:

$$a_r\ =\ \sin (\alpha) \approx \alpha$$
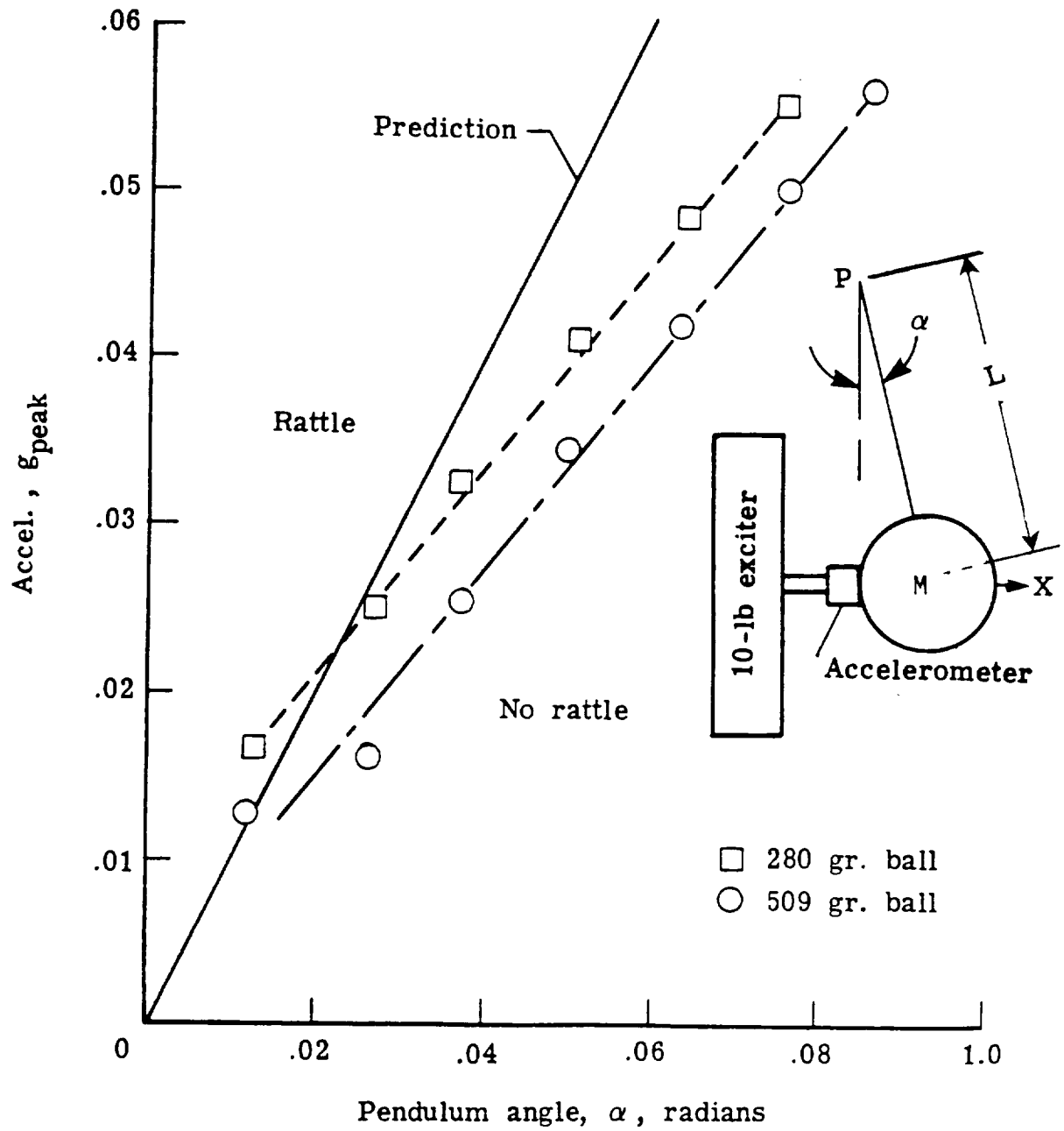
Figure 8.   Rattle Boundaries of Two Balls Suspended as Pendulums with Various Hang
Angles (from Clevenson, 1978).

A hanging mirror can be roughly represented as a homogeneous rectangular "plate" with mass density ρ_m, vertical length L, width W, and thickness T. If the center of gravity of this "plate" is assumed to be in the middle, and the plate is assumed to be hung from a fixed pivot "line" located at a distance L/3 from the top edge (an approximation to the estimated conditions for the data in Figure 7b) then, referring to the sketch, the mass Moment of Inertia, I_m can be shown to be given by:
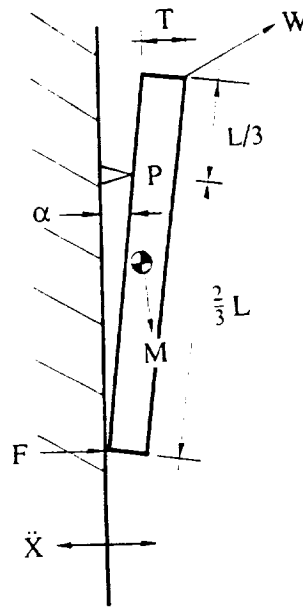
Sketch of Wall and Hanging Mirror

$$I_m = \int_O^T \int_{-L/3}^{2L/3} \rho_m \; W \; r^2 \; dx \; dy \;\; = \;\; \frac{M}{9} \; L^2 \; [\; 1 + 3(T/L)^2] \tag{6a}$$

where r^2 equals [$x^2 + y^2$] where x,y are coordinates in the length and thickness direction for the mirror, and M equals the mass [$\rho_m LWT$] of the plate. For this case, Eq. (4) must be modified for the moment of the mirror mass about the pivot line and the rotational acceleration about this line is modified by the shorter lever arm (2L/3) between the fixed pivot "line" and the impact "line" at the bottom of the picture. The modified moment for the mirror mass about the pivot point can be closely approximated by:*

$$\text{Moment} \simeq Mg \left[\frac{T}{2} - \frac{L}{6} \sin \alpha \right] \tag{6b}$$

---

* The authors are indebted to Kevin Shepherd of NASA–Langley for pointing out this modification.

Again, setting $F = 0$ at the onset of rattle, it can be shown that the "rattle" threshold for this case occurs when the horizontal acceleration a_r at the impact point is approximately equal to:

$$a_r \simeq [\, 3\, T/L - \sin(\alpha)\,] \cdot [1 + 3(T/L)^2]^{-1} \qquad (7)$$

where it is assumed that both T/L and α are $\ll 1$. Thus a very different result is obtained than the one for the simple lumped mass pendulum model.

For the mirror rattle data presented earlier in Figure 7b, assuming a value for T/L $\approx$ 1/32 for the mirror (e.g., T $\approx$ 3/4 in and L $\approx$ 24 in.), the predicted rattle threshold according to Eq. (7) would occur for an acceleration at the mirror impact point of about 0.071 g for the mirror hanging angle of 1.3° and 0.039 g for the hanging angle of 3.14°, less than that predicted for the smaller hanging angle. In fact the observed values indicated by the data in Figure 7b were 0.064 g peak and 0.047 g peak, respectively. These values differ by about -11 percent and -17 percent, respectively, from the expected values. However, the wall acceleration was not measured at exactly the same location as the plaque. Hence such an agreement is very reasonable considering the effect of the wall vibration mode shapes on the potential difference between the wall acceleration at the measurement point and at the plaque location.

Following the same type of analysis, it can be shown that if a plaque is also modeled as a uniform plate but supported from a pivot line at the top-back edge (as was the case for the plaques evaluated by the data in Figure 7a), then the mass moment of inertia would have been:

$$I_m = \frac{1}{3}\, M\, L^2\, [1 + (T/L)^2] \qquad (8)$$

For this case, the "lever arm" for rotational acceleration is the full length L of the plaque but the moment arm for the gravitational force is L/2 so that Eq. (7) is again modified to predict a rattle threshold for objects hung from their top edge as a peak acceleration given by:

$$a_r \simeq \frac{3}{2}\, \left[\, \frac{T}{L} - \sin(\alpha)\,\right] \cdot [1 + (T/L)^2]^{-1} \qquad (9)$$

where it is again assumed that T/L and α are $\ll 1$.

If it is assumed that T/L for the plaques was about 1/24 and typical "hanging angles" for the plaques evaluated in Figure 7a were about 1 to 2°, then the predicted rattle threshold should have been about 0.036 to 0.01 g, respectively, giving an average of about 0.023 g.

As stated earlier, the measured lower bound of the plaque rattle data in Figure 7a is also about 0.023 g.

2.3.2 Design Value for Minimum Rattle Threshold for Wall-Mounted Objects

Considering the many assumptions involved in this simplified analysis, there is, nevertheless, fair agreement between prediction and measurement for the minimum rattle threshold for the mirror and plaques and the simpler "point mass" model in Figure 8. Therefore it is concluded that Eq. (7) and (9) provide reasonable bases for estimating lower bounds for rattle thresholds for wall-hung objects within a factor of about ±50 percent (e.g., ±3.5 dB). For analysis purposes, it will be assumed that an absolute value for the minimum rattle threshold for wall-hung items will be the average of the measured values in Figure 7; i.e., 0.045 ± 0.021 g, peak. It will be further assumed that this rattle occurs in the frequency range of low-order wall resonances – about 15 to 150 Hz. It should be pointed out that this limited analysis makes no effort to consider the second-order effects of the mass of rattling objects and the type or area of contact surface (Clevenson, 1978).

2.4 Rattle Thresholds for Structural Elements

In addition to wall-hung items, sonic boom excitation can cause rattle by inducing vibration of windows and doors. For example, windows with panes that are loose in the sash, or window sashes that fit loosely in their frames, are readily prone to rattle from sonic boom excitation of a dwelling. External doors are not as likely to rattle due to weatherproofing or security provisions but interior doors, which ordinarily have some play between their stops and door latch, may be readily excited acoustically (i.e., rattled) by the sonic boom signature inside a dwelling.[*]

Two analytical studies of the (non-linear) rattling response of windows (Crandall and Kurzweil, 1968) and simple beam models for structural elements (Benveniste and Cheng, 1967) have focused on the increased stress in such structures due to the added effect of an impact load imposed when a structural element, initially driven by a sonic boom load, hits its stops. No experimental or theoretical studies could be found on the magnitude of peak

---

[*] A very striking example of this phenomenon was observed by a member of Wyle's staff recently when a military jet apparently went supersonic twice within a period of about 30 seconds, several miles west of Los Angeles. The observer heard no sonic boom (although some others in the community did hear a boom) but heard and saw a severe rattling of an interior door which died out after a period of several seconds. The rattling then recurred and he observed and heard a 4' x 3' aluminum sliding window rattling, again for several seconds. The acoustic stimulus, in this case, is believed to have been the type of rumbling sinusoidal-like transient that can occur near "cut-off" well to the side of a sonic boom track.

2-12

accelerations which trigger this type of rattle. The lack of analytical predictions is not surprising since unknown or unpredictable friction forces would probably control this rattle threshold for door and windows. However, data are available on the magnitude of impulsive blast and sonic boom peak pressures (Siskind *et al.*, 1980, and Eldred, 1985) and of steady state sound levels (Tokita and Nakamura, 1981) which tend to cause rattle of such elements.

The most useful is the analysis presented in Siskind *et al.*, 1980, and shown by the data on the right side of Figure 9. The data points represent measured community annoyance response vs estimated peak (linear) pressures for sonic boom tests conducted at Oklahoma City (Borsky, 1965) and Edwards Air Force Base (Stanford, 1967). The "highly annoyed" response level for these tests was dominated by "house rattle" as the strongest complaint. Accepting a "5 percent highly annoyed" as an approximate threshold, the mean peak pressure is 0.0046 psi (0.67 psf). From data on acceleration response to sonic boom evaluated by Hubbard, 1982, typical wall acceleration response levels to sonic booms can be specified in terms of a transfer function a_{pk}/P_{pk} of about 0.18 ±80 percent g(pk)/psf(pk). (See also Section 2.4.) Again, considering the lower bound of this range, or 0.036 g(pk)/psf(pk), the peak sonic boom pressure of 0.67 psf translates to a peak wall acceleration of 0.024 g – surprisingly in agreement with the values observed from the preceding test data for a rattle acceleration threshold for wall-hung objects.

The study by Eldred, 1985, involved analysis of measurements at the U.S. Army Civil Engineering Research Laboratory of the structural response of a partial mock-up of a residential building to simulated blast pressure pulses. The pulses had a duration of about 26 ms to 41 ms and peak pressures up to 121 dB (0.47 psf). Rattle rarely occurred when the free field peak pressure was less than 108 dB (0.11 psf), was almost always present when the peak pressure exceeded 113 to 115 dB (0.19 to 0.24 psf), and always occurred (for windows, bric-a-brac, and china) when the peak pressure was 121 dB (0.47 psf). Thus these data indicate a peak overall rattle threshold pressure of 0.11 psf for the type of simulated blast pulses employed for this program. While this threshold pressure for rattle onset is *not* necessarily representative for sonic booms, it is possible to utilize this information to deduce what the acceleration levels were on the structure at which rattle occurred. These acceleration values for rattle should be valid for sonic boom as well as the simulated blast pulse employed here.

Note that these data might also be used to help establish a statistical model for the onset of rattle. If it is assumed that the range in pressure between which rattle first occurs and always occurs corresponds to a "4 to 6 sigma" range of a Gaussian distribution of rattle
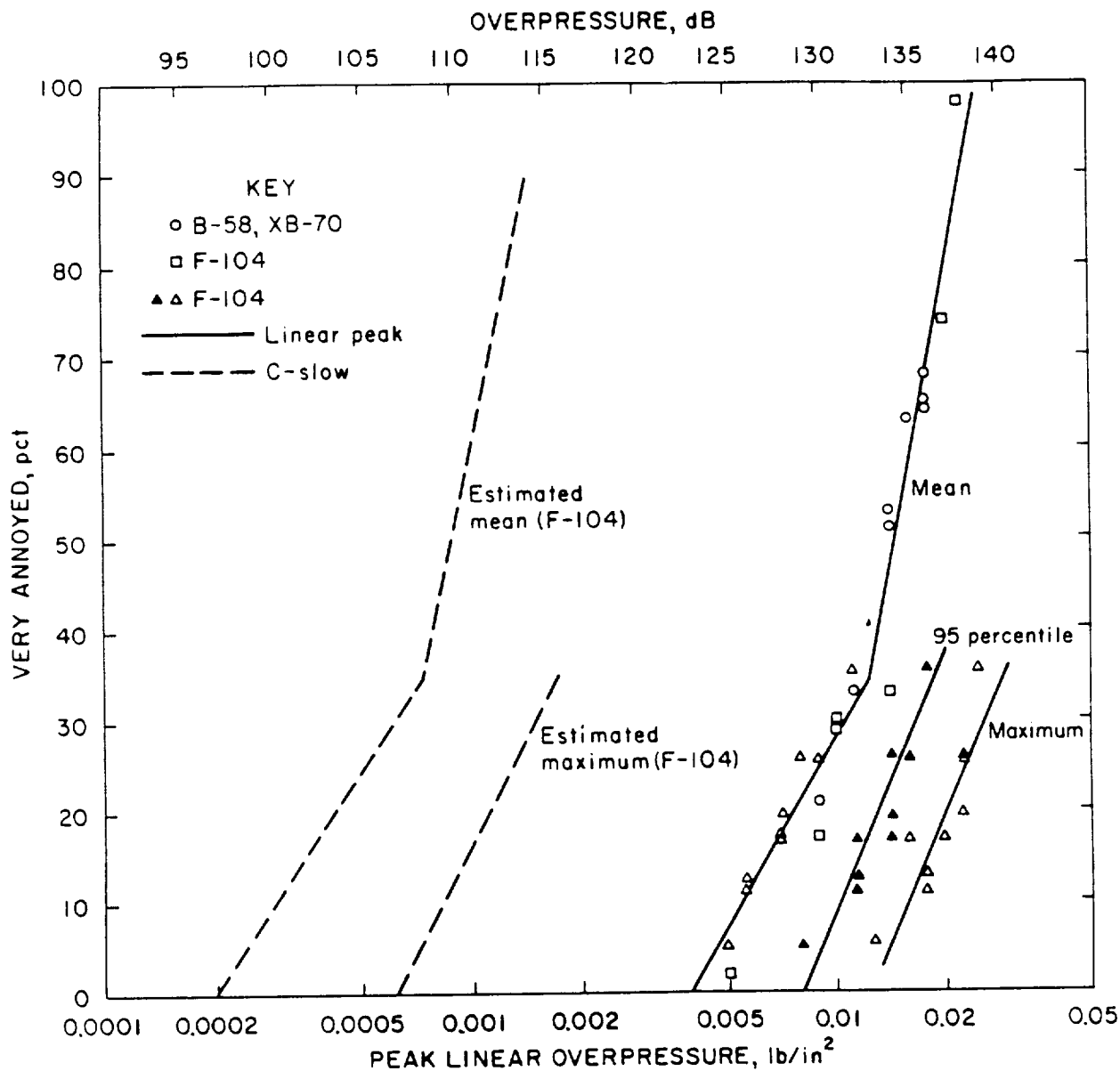
Figure 9. Population Very Annoyed by Sonic Boom-Produced House Rattle
(from Siskind *et al.*, 1980). (The dashed lines in the above figure
are not pertinent here, but were part of the original figure.)

excitation levels, these data would suggest that the standard deviation for the onset of rattle, in a given structure over all types of objects or structure that could rattle, would be about (121 - 108)/6 to (121 - 108)/4 or 2 to 3 dB.

For this test structure, the mean Specific Acoustic Mobility (the non-dimensional ratio of the acceleration response to acoustic loading times the surface weight divided by the incident pressure) for the storm windows, walls, door, and ceiling was about 18. This is the mean value at the fundamental resonance frequency of the various structural elements where the vibration response is greatest for acoustic loading and is well within the range of expected values, as will be shown later. The range in variation about this mean value was about ± 320 percent (± 10 dB). The threshold overall peak pressure of 108 dB (0.11 psf) corresponds to a peak pressure in the one-third octave band containing a typical wall resonance frequency of about 98 dB (0.035 psf). The average surface weight of the test structure walls, windows, door, and ceiling was 4.6 psf. Thus the mean acceleration expected at the rattle threshold peak pressure is estimated to have been $(18 \cdot 0.035/4.6) = 0.14$ g. Allowing for the variation about the mean value for the Specific Acoustic Mobility, a lower bound on this rattle acceleration threshold would have been about $0.14/3.2 = 0.044$ g, a value close to the previous estimates above for the minimum acceleration threshold for the onset of rattle.

Data on "steady-state" acoustic levels required to induce rattle in various structural elements are also available from measurements by Nakamura and Tokita, 1981. These data, shown in Figure 10, represent minimum sound pressure levels at which rattle occurred for the five different types of structural elements shown. The peak acceleration corresponding to these acoustic rattle thresholds can be roughly estimated as follows. The surface weight for all five of the various structures is estimated to be about 3 psf. An average Specific Acoustic Mobility (Acceleration x Surface Weight/Acoustic Pressure) of 18 is assumed based on the previous data from Eldred, 1985. An average lower bound for the rattle sound level threshold from Figure 10 is 75 dB rms or 0.0034 psf, peak. (This is the value for three of the five structures at the lower frequencies believed to represent the fundamental resonance frequency range of the element.) Thus, the estimated minimum peak acceleration, a_{pk}, in g's for the acoustic rattle threshold data in Figure 10 is estimated to be of the order of: $18 \cdot (0.0036/3) = 0.020$ g's, again, comparable to the previous estimates.

At higher frequencies, well above the fundamental mode, the required acoustic levels (and corresponding acceleration levels) required to cause rattle increase approximately with frequency squared.
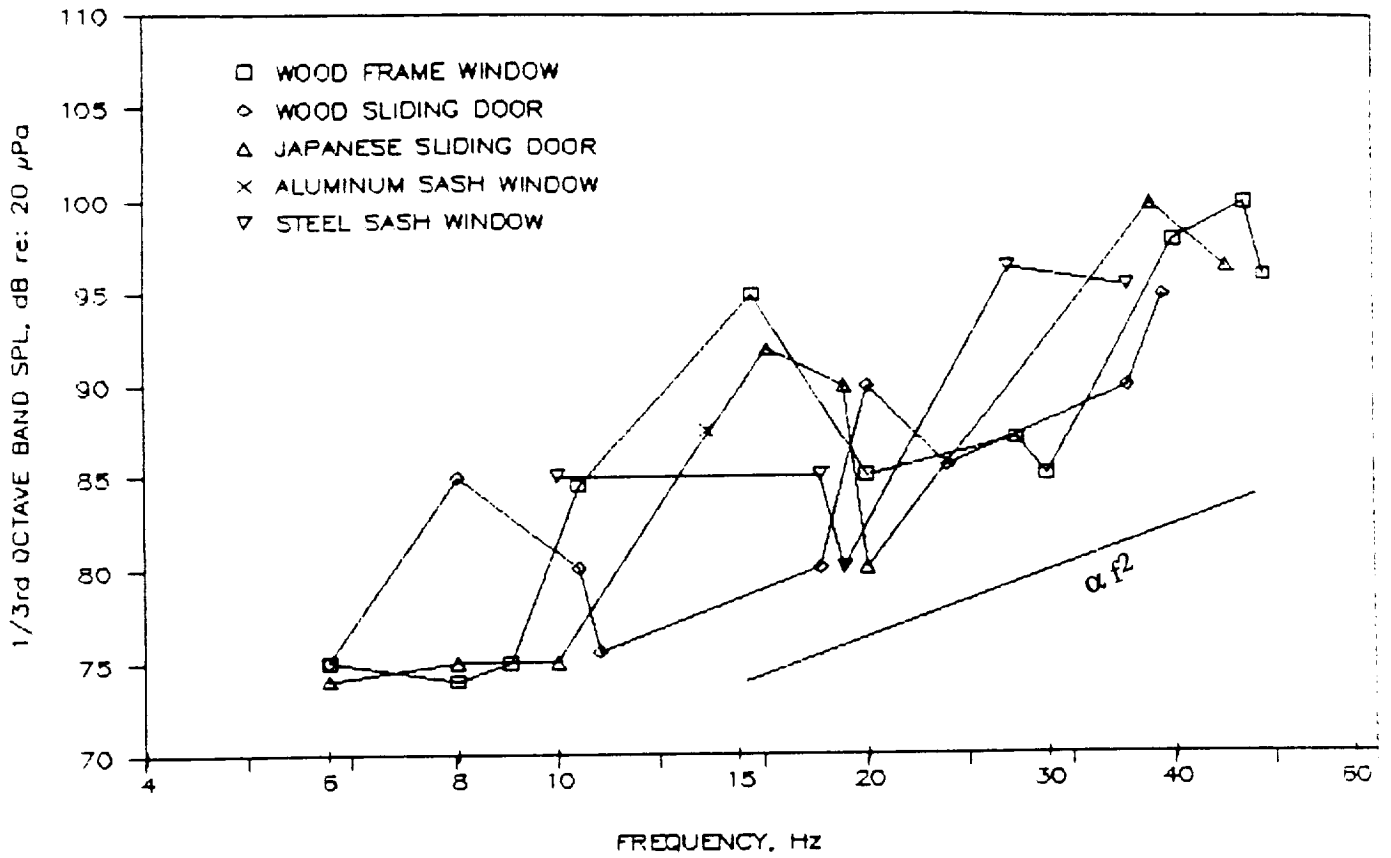
Figure 10. Acoustic Threshold for Rattle for Building Elements (Data from Nakamura and Tokita, 1981).

3.0 ACCELERATION RESPONSE OF BUILDING STRUCTURE FROM ACOUSTIC EXCITATION

The vibration response of building structure to sonic booms is evaluated for this report by two methods:

1. The well-known Shock Response Spectrum method which develops the transient response to a sonic boom in the time domain, and

2. A new variation on the approach based on the use of the Fourier Spectrum of any sonic boom wave form. This variation can employ an analytical or experimentally based model for the <u>absolute value</u> of the steady-state vibro-acoustic transfer function for a structure to evaluate its transient response to sonic booms. This approach can be used to compute the descriptor identified earlier which is a measure of the energy in an acceleration signal – the Acceleration Exposure Level. As explained later, this descriptor can also be used to define the equivalent peak acceleration magnitude of a damped sinusoidal acceleration signal with the same energy as that of the actual acceleration response to the sonic boom.

A key assumption required for application of both methods is that the vibro-acoustic response of structure is assumed to be linear. Such linear response behavior has been repeatedly shown by NASA and others, as illustrated, for example, in Figure 11 in terms of peak window acceleration levels versus sound pressure (Stephens *et al.*, 1982) and in Figure 12 by peak stresses in a dwelling wall stud versus peak acoustic pressure for noise, blast and sonic boom excitation (Mayes and Edge, 1964). Two exceptions to this linear behavior are: window response to steady-state random noise at one-third octave band sound levels above about 120 dB (Freynik, 1963) and rattle vibration responses (Crandall and Kurzweill, 1968). However, significant non-linear behavior for windows should not occur at the transient overpressures of concern for this report. The non-linear behavior of rattle is also ignored here since only the "linear" vibration response of structure up to the threshold of rattle is considered herein.

One important result of this assumption of linearity that is employed later is that the vibro-acoustic response or transfer function characteristics of structure developed experimentally or theoretically on the basis of steady state acoustic excitation can also be readily applied to the evaluation of transient response to sonic boom. This has been well demonstrated, experimentally, by comparison of response of a test structure to noise and simulated blast pulses (Eldred, 1985).

ACCELERATION
LEVEL, dB
REF. 1.0 μg ──── PROJECTED
\\\\\ AIRCRAFT AND HELICOPTER
NOISE
:::::: WIND TURBINE (KELLEY
UNPUBLISHED)
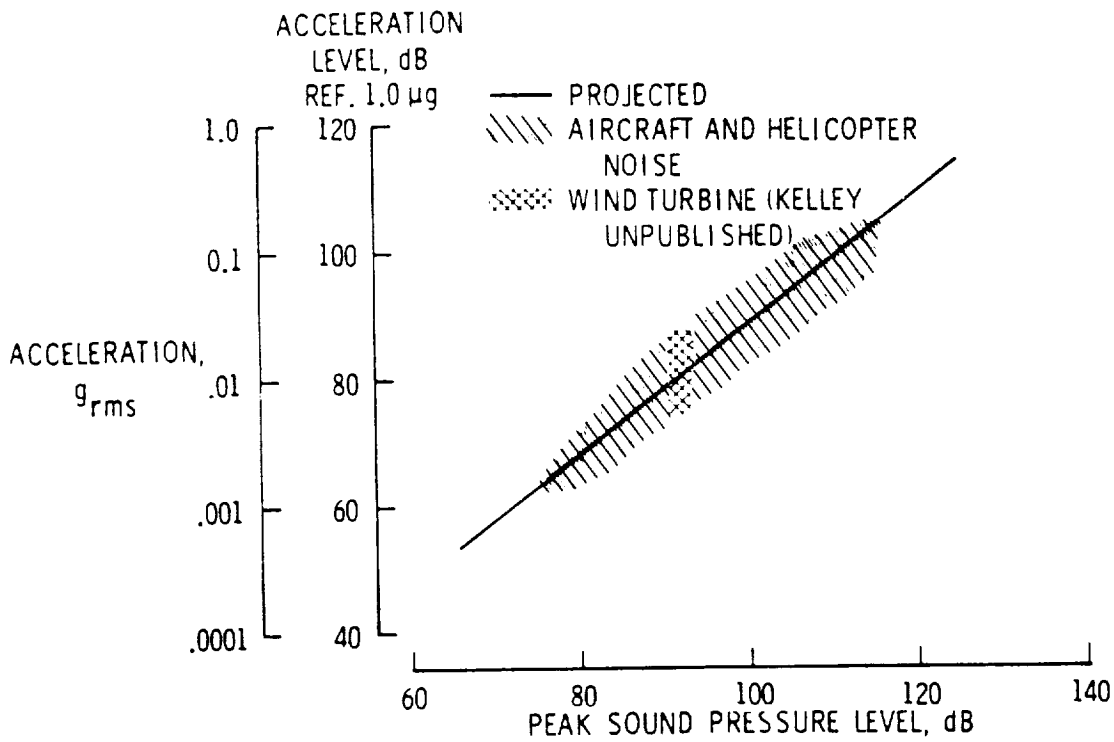
Figure 11. Measured House Window Acceleration Responses Due to Noise Excitation (from Stephens, et al., 1982).
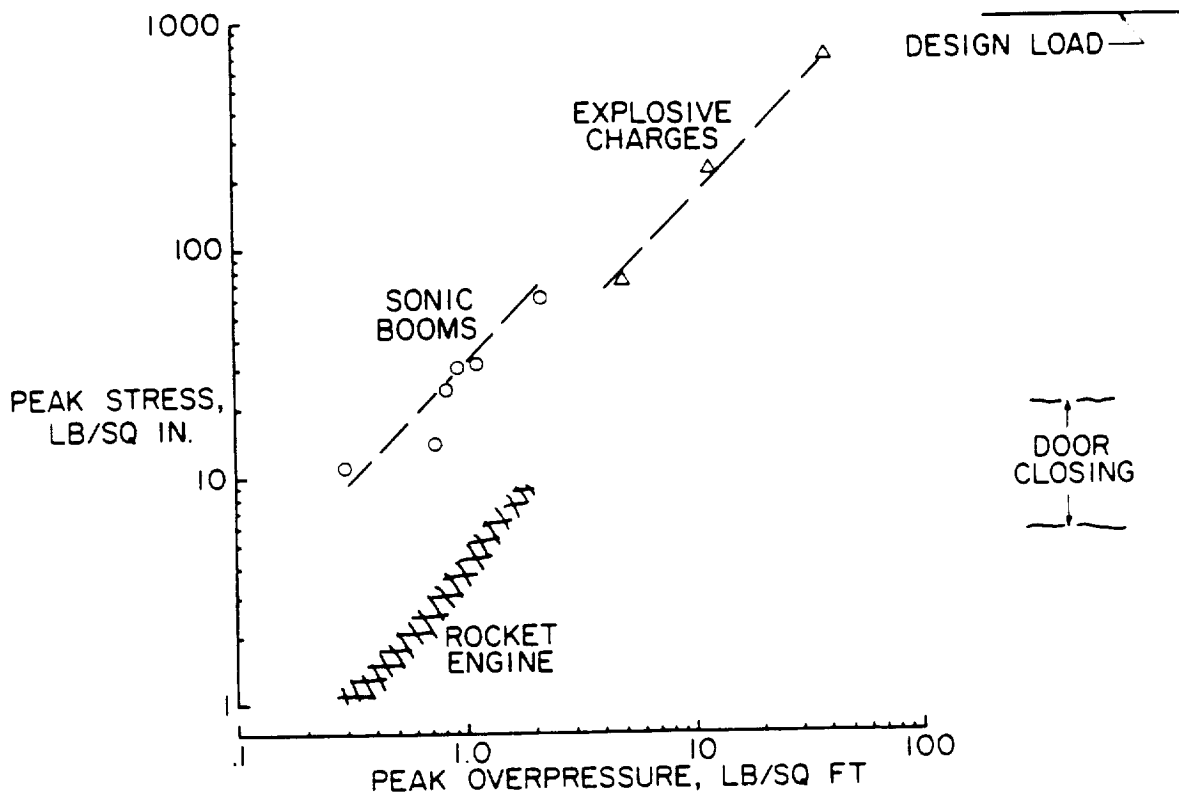
Figure 12. Peak Vertical Stud Stresses as a Function of Peak Overpressure for Various Types of Acoustic Excitation (from Mayes and Edge, 1964).

3-2

3.1 Shock Response Spectrum for Sonic Booms

As discussed in more detail in Appendix A and illustrated by the following sketch, the peak response of a single degree of freedom (SDOF) mass-spring system to a transient excitation, P(t) such as a sonic boom, can be defined by a Shock Response Spectrum. An SDOF model can describe, in simplified form, the basic fundamental vibration response mode of a complex structure. This Shock Response Spectrum is a function of the dimensionless parameter, $f_0 T$ where f_0 is the undamped natural resonance frequency of the SDOF system, and T is the full duration of the (sonic boom) excitation. This Shock Spectrum defines the magnitude of the peak response of the SDOF system at any time, t, after the beginning of the sonic boom.
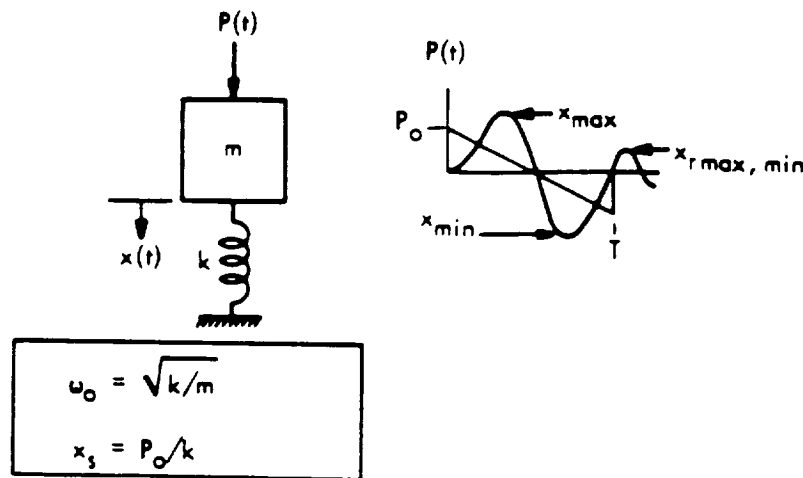
Sketch of Mass-Spring Undamped SDOF System Driven by Sonic Boom N-Wave

This peak response is obtained from a general solution to the equation of motion for the SDOF system illustrated in the sketch with a mass, m, spring constant, k and undamped natural resonance frequency, $f_0 = (1/2\pi)\sqrt{k/m}$. (Note that the system mass, m and excitation, P(t) are defined in terms of values per unit surface area, i.e., surface mass and pressure, respectively. When the acceleration response is expressed in non-dimensional g's, the ratio of acceleration to the acceleration of gravity, g, the surface mass, m is more conveniently specified in terms of surface weight, w = mg.)

This general solution for the response is the combination of the forced response of the system while the excitation (i.e., sonic boom pressure wave) lasts and the transient response of

3-3

the system following the excitation. The envelope of the peak <u>forced</u> response (e.g., peak acceleration) is called the Primary Shock Response Spectrum. The envelope of the peak <u>transient</u> response following the excitation is called the Residual Shock Response Spectrum. As discussed in Appendix A, the amplitude of this Shock Spectrum is conveniently given in one of the following non-dimensional forms.

For the peak displacement response, X_{max}, this form of the Shock Response Spectrum is often referred to as the Dynamic Amplification Factor, (DAF) and is given by:

$$DAF = \frac{X_{max}}{X_s} \quad or \quad \frac{X_{max} \cdot (2\pi f_0)^2 \cdot w}{P_0} \qquad (10)$$

where w = "surface weight" of the (SDOF model) structure with the same units as the pressure, $P(t)$. (The latter has an initial peak value, P_0.)

In this form, the Shock Response Spectrum or DAF is the ratio of the peak dynamic response, X_{max} to the static response, X_s for excitation by a constant or static pressure, P_0 with the same magnitude as the peak pressure of the transient excitation. An example of such a Displacement Shock Response Spectrum is shown in Figure 13 for excitation of an undamped SDOF system by an ideal N-wave.

For the peak acceleration response A_{max}, the corresponding non-dimensional Acceleration Shock Response Spectrum can be expressed in one of the following two forms (the second is the preferred form which will be used throughout this report).

$$\frac{A_{max} \cdot g}{(2\pi f_0)^2 X_s} = \frac{A_{max} \cdot w}{P_0} = \frac{(Peak\ Acceleration,\ g's) \cdot (Surface\ Weight,\ psf)}{(Peak\ Pressure,\ psf)} \qquad (11)$$

where g is the acceleration of gravity, $(9.8\ m/s^2)$.

As shown by the example Acceleration Shock Response Spectrum in Figure 14, this Response Spectrum is partly dependent on damping of the dynamic system, as measured by its Resonance Amplification Factor, Q. It is also dependent upon the non-dimensional system/excitation parameter, $f_0 T$.

The envelope of the maximum values of the combined Primary and Residual Acceleration Shock Response Spectra for the following sonic boom wave shapes are shown in Figure 15 for response of a SDOF system with a Q of 10. In all cases, the spectra are shown as a function of the non-dimensional parameter, $f_0 \cdot T$.
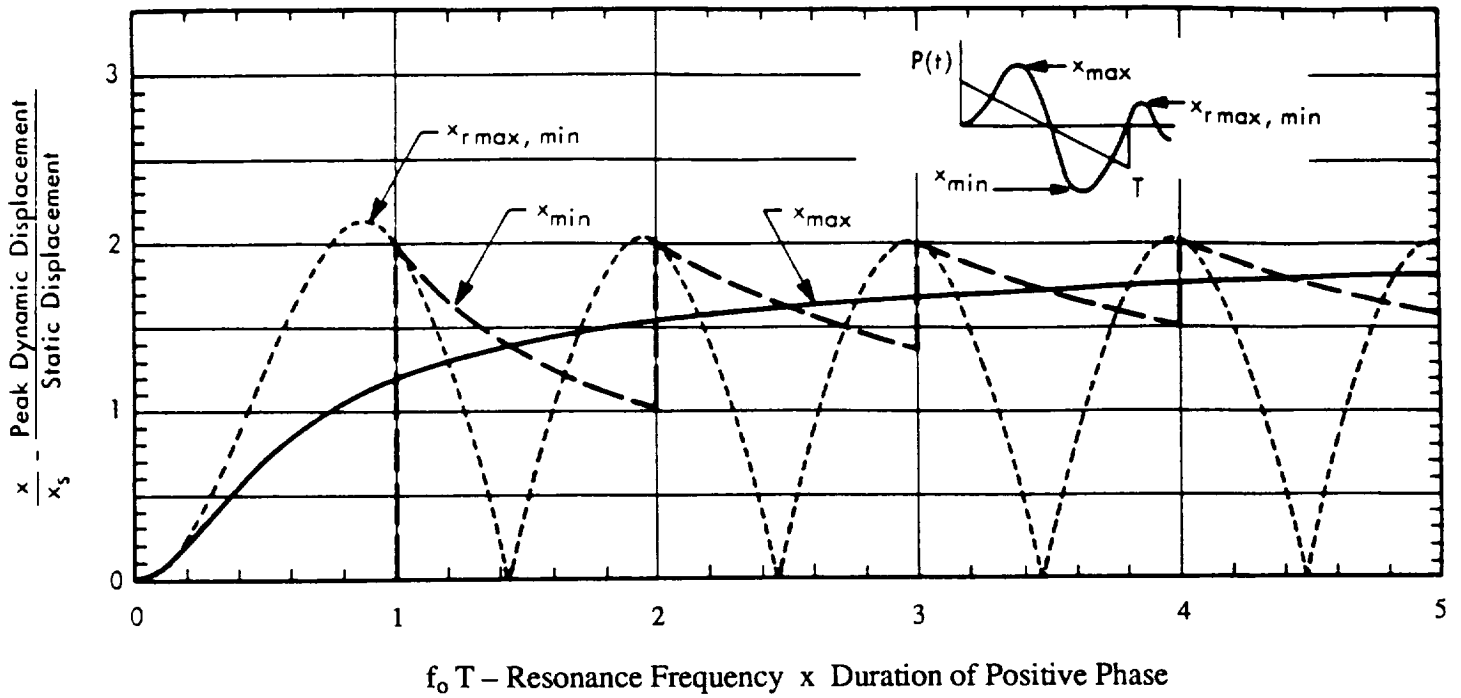
Figure 13. Normalized Displacement Shock Spectrum for Ideal Sonic Boom N-Wave Excitation of Undamped Mass-Spring System (Sutherland, 1968).
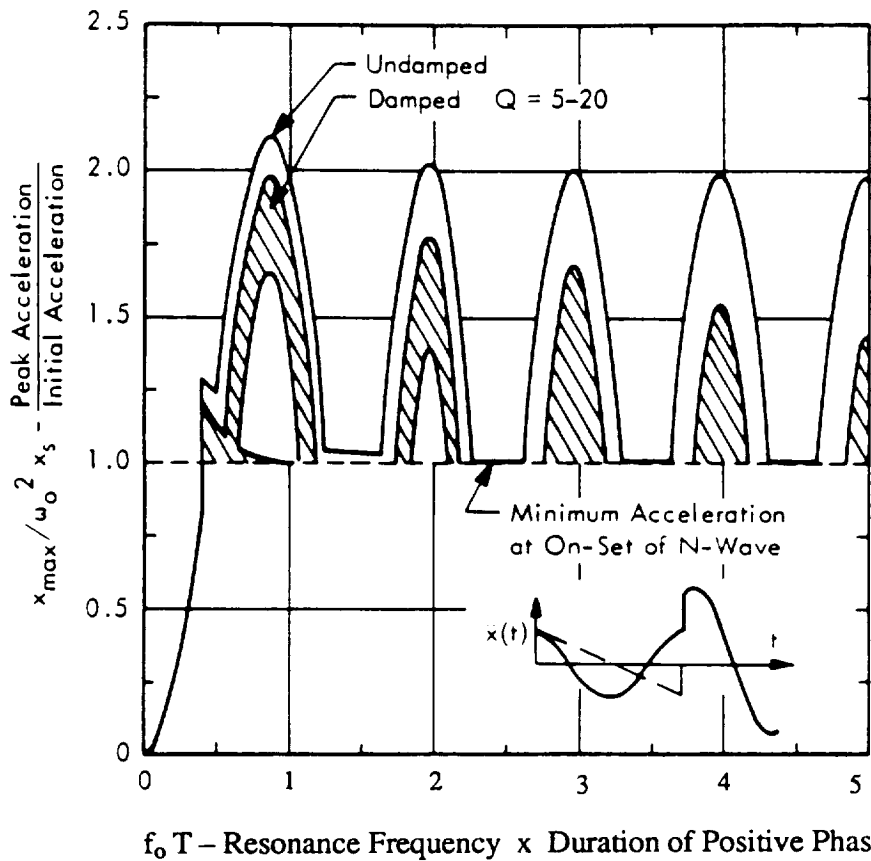
Figure 14. Acceleration Shock Spectrum for Response of Damped and Undamped Mass-Spring System to Ideal Sonic Boom N-Wave Pulse Applied to Mass (Sutherland, 1968).

3-5
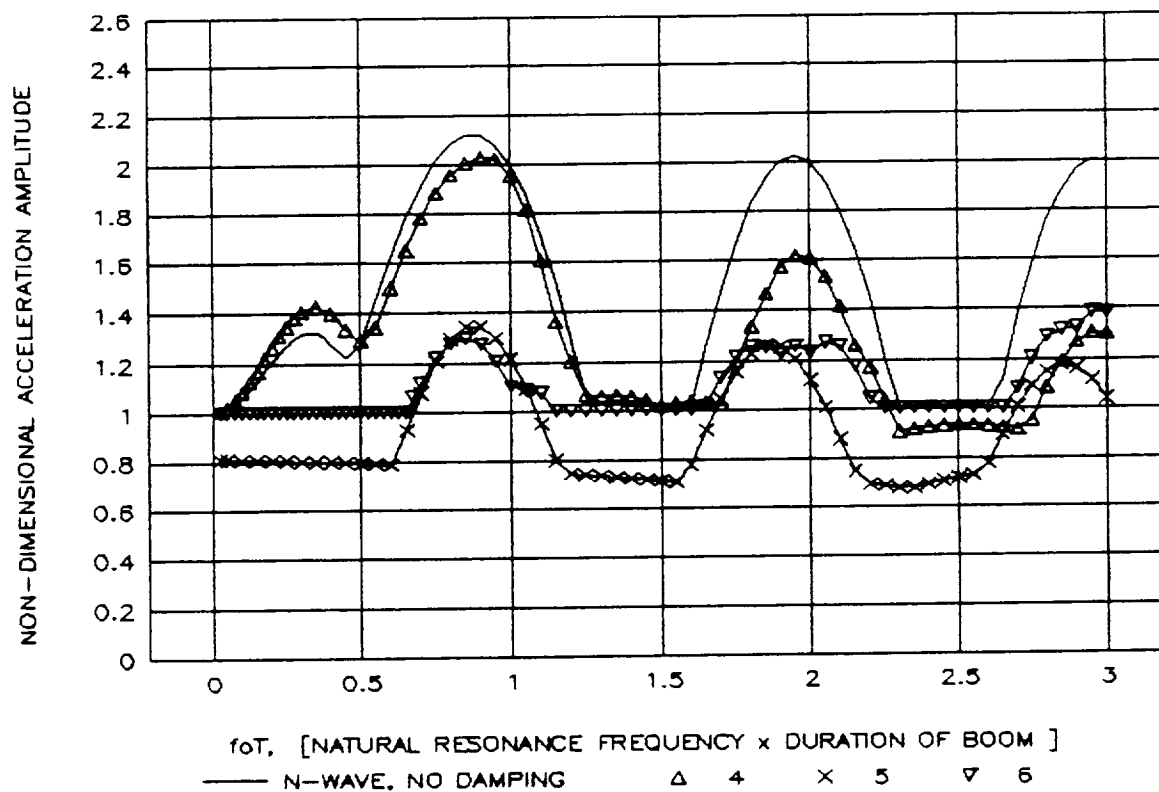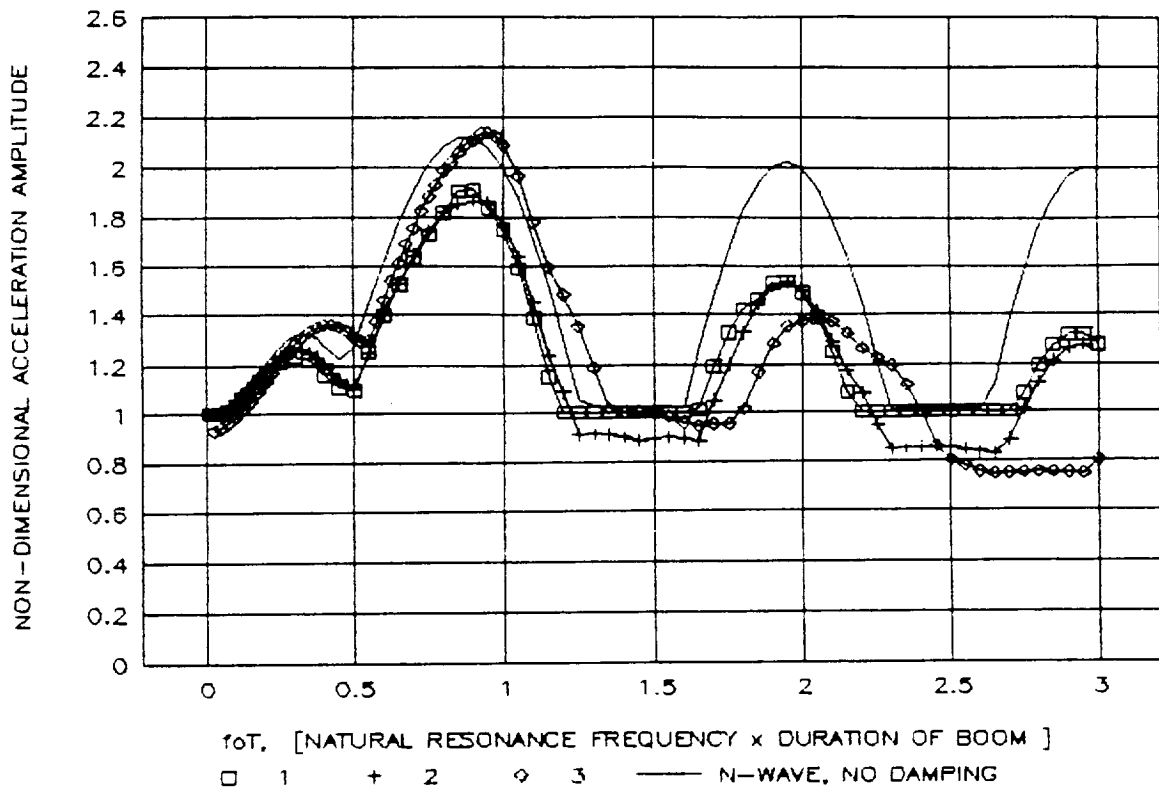
Figure 15. Envelopes of Primary and Residual Acceleration Shock Spectra for Six Different Sonic Boom Wave Shapes Defined in Text. (For SDOF systems with Q=10 except for solid line which is for an undamped system.)

Figure 15a shows the Acceleration Response Spectra for the following three sonic boom wave forms:

Curve 1)   Ideal N-wave sonic boom.

Curve 2)   Reference sonic boom with rise/fall time of 8 ms.

Curve 3)   Symmetric delayed ramp with initial rise to $P_0/2$ in 8 ms followed by a rise to P_0 in 35 more ms and a mirror image pattern at the end of the boom.

Figure 15b shows the spectra for:

Curve 4)   Non-symmetric flat top with initial time of 8 ms, constant pressure of P_0 for 35 more ms and then linear decay and return to zero pressure as for the reference N-wave.

Curve 5)   Ideal N-wave diffracted around one end of a typical residential building with a diffraction time of 50 ms as defined later.

Curve 6)   Racking acceleration response of the same building also explained below.

Also shown by the solid line in each part, for comparison, is the Acceleration Shock Response Spectrum for an undamped system driven by an ideal N-wave. As indicated, this has a maximum value of about 2.2 for $f_0T = 0.88$, and a maximum value of approximately 2 for $f_0T \approx n$ where n = 2,3,4, etc.

Examination of these curves shows that at the first peak in the spectrum, where $f_0T \approx$ 0.9, all of the sonic boom wave forms, including the ideal N-wave, would have nearly the same maximum acceleration response. However, for a value of T = 350 ms, this would correspond to structural resonance frequencies of about 2 to 3 Hz – a range of significance only for very large windows or possibly roofs of large buildings. Such low resonance frequencies are not typical for residential buildings. For higher values of f_0T, as expected, the Acceleration Shock Spectra for damped systems for all of the shaped booms become significantly lower than the value for the ideal N-wave excitation of an undamped system. In particular, the shock spectrum for Curve 3, the symmetric delayed ramp, begins to show a marked deviation from the spectra for the other shapes for $f_0T > 2.5$. However, the resonance frequency, f_0 for T = 350 ms would still be below the range of fundamental resonance frequencies (15-25 Hz) of most residential structures. Evaluation at higher values of f_0 would be desirable. Unfortunately, this could not be reliably carried out with the particular computer program used

to compute these shock spectra numerically according to the method explained in Appendix A. The alternate "equivalent peak acceleration" approach mentioned earlier is used, as explained later, to extend the analysis to cover higher resonance frequencies.

3.1.1 Corrections to Nominal Free Field Sonic Boom Pressure to Account for Angle of Incidence and Diffraction

The analysis so far has assumed that the peak sonic boom pressure, P_0 which loads the structure is the same as the conventional "ground-reflected" value which, by the convention used to define sonic boom pressures, is normally specified as the "free-field" sonic boom pressure. This would be equivalent to assuming that the structural surface under sonic boom loading was set in an infinite rigid reflecting plane for which the measured peak pressure, P_0 is approximately two times the true incident peak pressure. For sonic boom loading on the wall of a finite size building, the effective loading must be modified to account for: (1) the effect of changing the incidence angle from normal to the wall surface, and (2) the effects of diffraction of a sonic boom wave form incident in a direction normal to the building wall. Both effects have been evaluated analytically (ARDE and Associates, 1959).

3.1.2 Angle of Incidence Correction

The angle of incidence effect was also evaluated experimentally during the SST sonic boom tests in the 1960s. An empirical relationship between an effective peak pressure, P_e measured on a building wall and the nominal free-field (i.e., ground reflected) peak pressure P_0 developed from these data can be expressed as (Hershey and Higgins, 1976):

$$P_e/P_0 = 10^{[0.147 \cdot \cos(\theta) - 0.1258]} \tag{12}$$

where θ is the angle, on the ground, between the aircraft flight track and a line normal to the building surface. In the absence of any preferred value for the angle θ, an equal probability for any value corresponds to an average value of P_e/P_0 from Eq. (12) of 0.75 (Sutherland, Brown and Goerner, 1990). It is assumed that this effective peak pressure accounts only for the change in reflection of the initial sonic boom wave front due to the non-normal incidence angle on a given surface. It is further assumed that it does not account for the change in the average sonic boom pressure load on a building wall caused by the effect of diffraction of the sonic boom wave front by the building geometry.

3.1.3 Diffraction Correction

A detailed early study of sonic boom loads on buildings provided a rational approach for evaluation of diffraction effects of sonic booms on buildings (ARDE Associates, 1959). The concept, illustrated in Figure 16, was based on applying well established methods for evaluating blast loads on buildings. For the latter, the incident shock wave front could be considered as a step function. Diffraction was accounted for by multiplying this incident pressure step (taken here as $P_o/2$) by a diffraction correction factor δ. This was equal to 2 at time zero, falling linearly to a value of 1.0 in a "diffraction clearing time," $t_D = 3S/U$ where S is the smaller of the building height or one-half the width and U is the speed of the shock wave front, taken here to be the ambient speed of sound for sonic boom pressures of concern here. As illustrated in Figure 16, the incident sonic boom pressure, assumed to be an ideal N-wave, is treated as the superposition of two ramp-step functions – separated by the duration T with each part multiplied by a corresponding diffraction correction factor. The resulting time history, P(t) of the diffracted average sonic boom pressure on the front wall of the building is the last part of the figure. It can be defined for the three time periods by:

$$0 < t \leq t_D, \qquad P(t) = (P_o/2) \cdot [1 - 2t/T] \cdot [2 - t/t_D] \qquad (13a)$$

$$t_D < t \leq T, \qquad P(t) = (P_o/2) \cdot [1 - 2t/T] \qquad (13b)$$

$$T < t \leq (T + t_D), \qquad P(t) = (P_o/2) \cdot [1 - (t/T - 1)] \cdot [t_D/T] \qquad (13c)$$

This modified time history was used to evaluate the Acceleration Shock Spectrum for Curve 5 in Figure 15 using a value for the clearing time, t_D of 50 ms that could be representative for a two story residential dwelling.

For the case of racking response of a building, a similar approach, illustrated in Figure 17, is used to define the net front-to-back pressure load on a building. In this case, two additional time delays are involved, the delay time L/U for the wave front to travel the length of the building, and a slightly longer "clearing time," 4S/U, for the back pressure load. It should be pointed out that these diffraction models have been well verified for blast waves and are considered good approximations for analysis of diffraction effects for sonic booms (ARDE & Associates, 1959).

FREE-STREAM PRESSURE - p_s

p_s^o

T

(+)

(+)

O

TIME

(−)

$-p_s^o$

(a)

δ FUNCTION

2

1

O

(+)

TIME

$t_D = \dfrac{3S}{U}$

(b)

δ FUNCTION

2

1

O

(+)

TIME

T

t_D

(c)

AVERAGE OUTSIDE FRONT FACE PRESSURE - p_{fo}

2

1

p_{fo}

(+)

(+)

O

TIME

(−)

t_D

−1

T

t_D

(d)
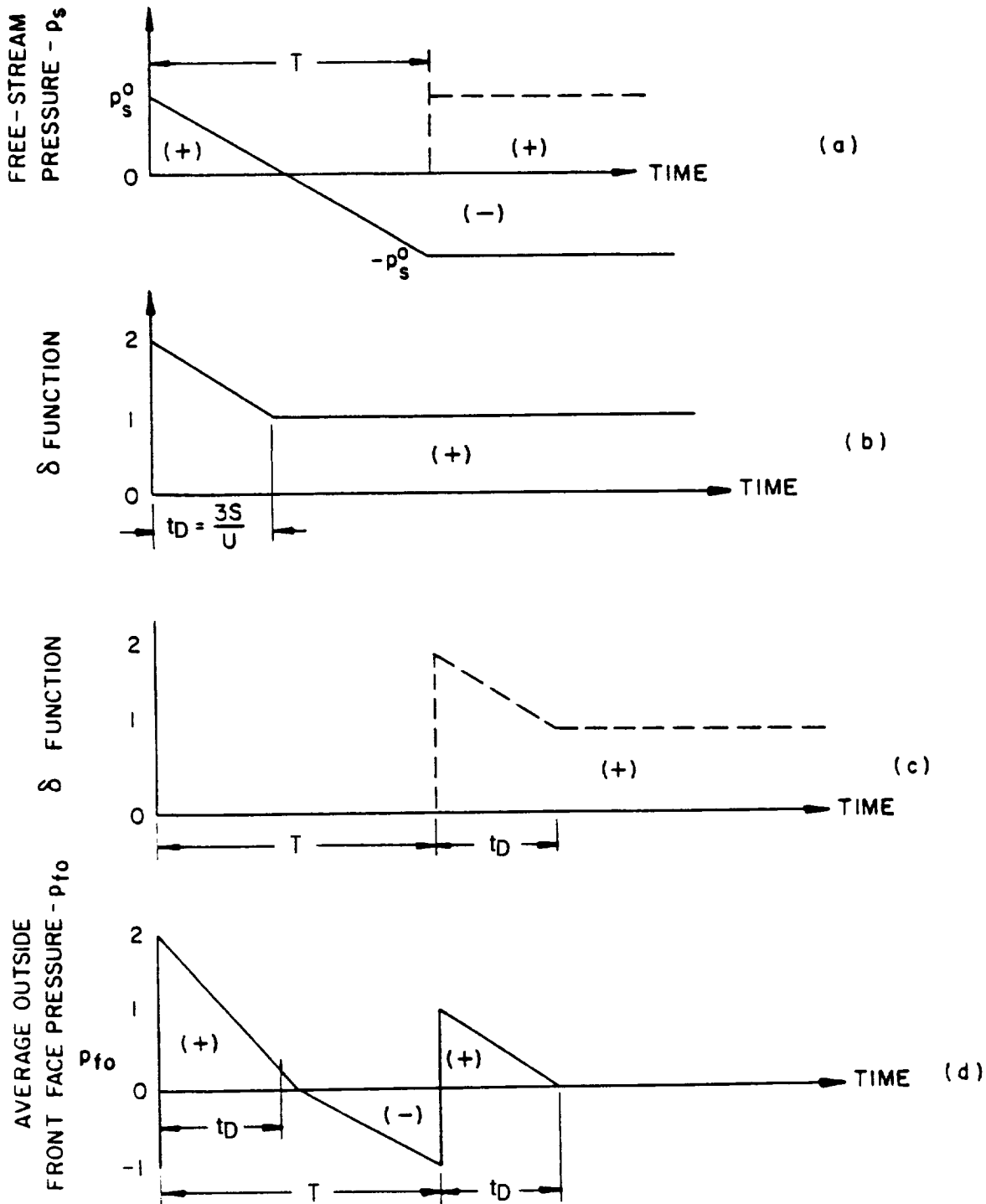
Figure 16. Model for Evaluating Diffraction Effect on Average Pressure on Face of Building Wall Facing Direction of Travel of Sonic Boom. (Note that "Free Stream" pressures, in this figure from ARDE and Associates, 1959, corresponds to one-half the ground reflected pressure, P_0 used in this report.)

3-10
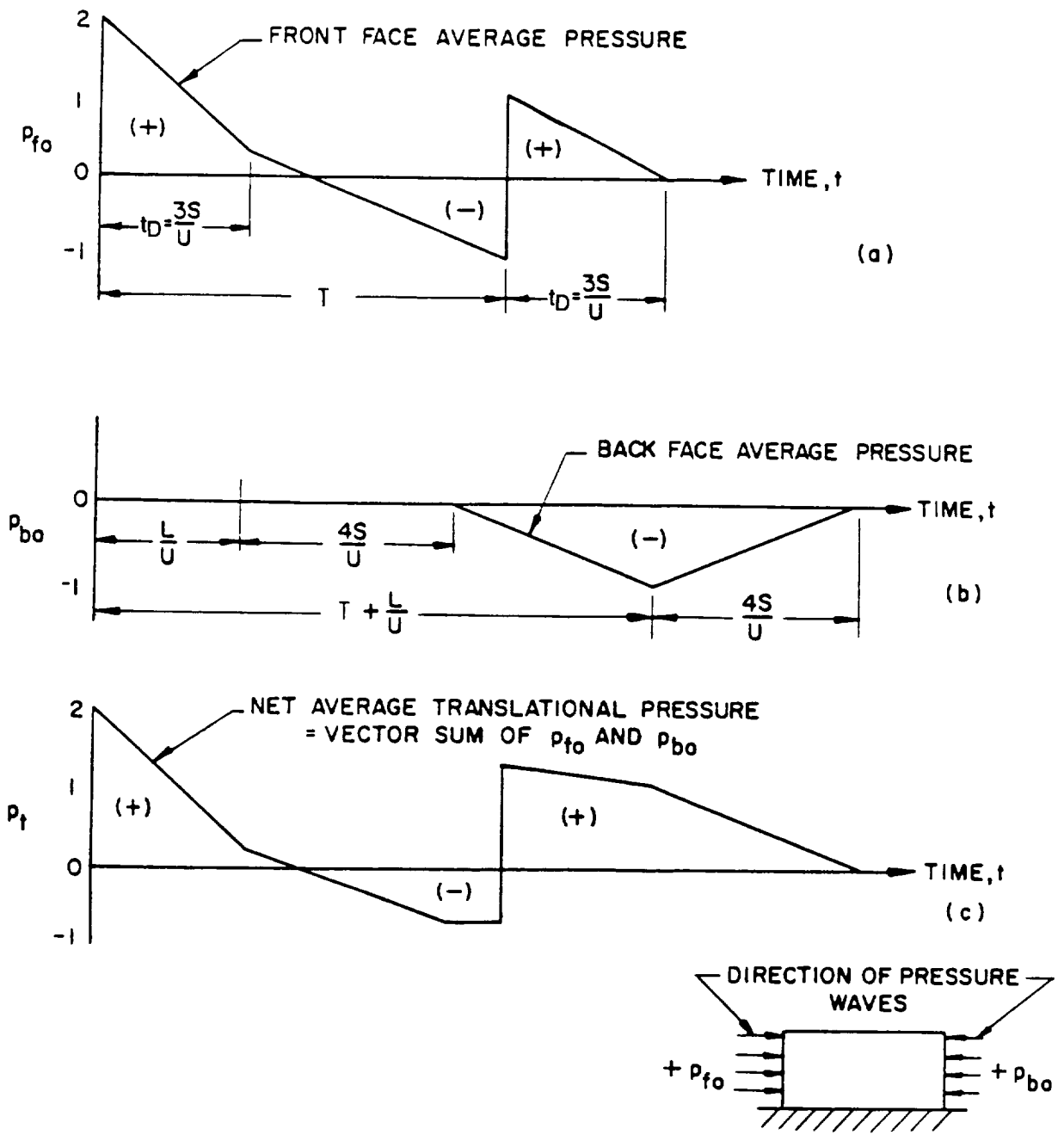
Figure 17. Model for Evaluating Net Translational (Racking) Load on a Closed Building by Accounting for Diffraction and Finite Wave Front Travel Time Between Both Ends of Building. (From ARDE and Associates, 1959.)

3-11

3.1.4 Diffraction Correction for Shaped Sonic Boom Wave Forms

Although the Shock Spectra for the two diffraction cases (Curves 5 and 6 in Fig. 15b) were necessarily based on a pure N-wave, a variation of this technique could also have been applied to the analysis of shaped sonic boom wave forms in the following manner. As illustrated in the following sketch, such a shaped wave form with a finite rise time could be considered as made up of a series of superimposed positive and negative step pulses representing the incident wave form, P(t) at any time t.
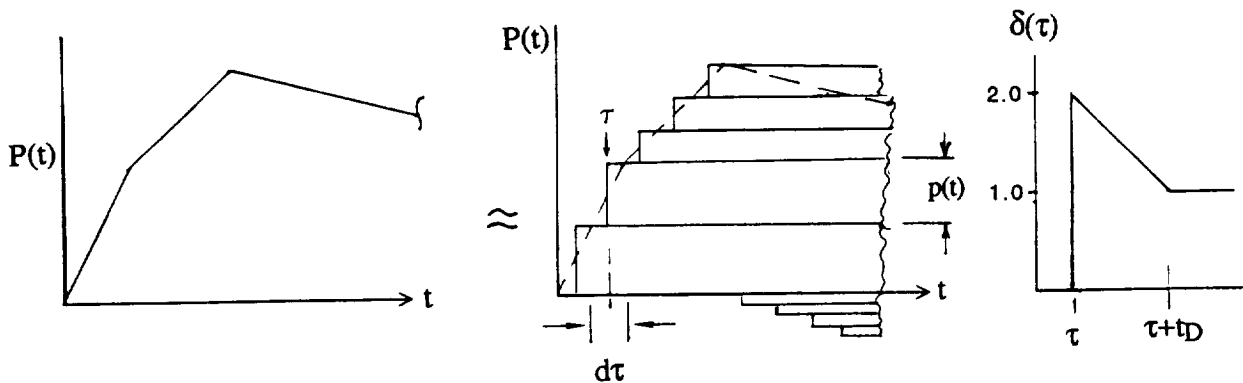
The step pulse with a pressure amplitude, $p(\tau)$ occurring at time $\tau(< t)$ would be multiplied by a corresponding diffraction correction factor $\delta(t-\tau)$. Since the amplitude of each elemental step, $p(\tau)$ at time τ can be determined from product of the slope $[dP(\tau)/d\tau]$ of the incident pressure at this time τ and the time increment, dt, then the time history of the total diffracted pressure load, $P_0(t)$ could be given by a convolution integral:

$$P_0(t) = \int_{\tau=0}^{t} \delta(t-\tau) \frac{dP(\tau)}{d\tau} \cdot d\tau \qquad (14)$$

Once this diffracted, shaped sonic boom load was established, then the same time-domain analysis defined in Appendix A could have been used to establish the new Acceleration Shock Spectrum for the diffracted, shaped sonic boom wave form. One would expect that the results of such an analysis would show the same reduction (of the order of 25%) in the maximum Acceleration Shock Spectrum at the first peak where $f_0T \approx 0.9$ shown in Figure 15 relative to

relative to the other shaped boom wave forms. However, since the effect of diffraction seems to become much less significant for higher values of f_0T, this analysis of diffraction effects for shaped booms was not pursued further.

3.1.5 Shock Spectra – A Summary

In summary, in the absence of diffraction, the Acceleration Shock Response Spectra for various types of sonic boom wave forms differ only slightly from that for an ideal N-wave excitation for an undamped system at values of f_0T less than 1. At higher values of this parameter, the Shock Spectra for the damped systems begin to decrease by as much as 100%, with the delayed, symmetric ramp showing the potential for the greatest reduction. The next section explores the trends in Shock Response Spectrum at higher values of the frequency parameter, f_0T and for different values of damping using a frequency-domain approach.

3.2 Application of Acceleration Exposure to the Prediction of Acceleration Response of Structure to Sonic Booms

The concept of Acceleration Exposure has already been introduced in Section 1.5 as a possible alternate descriptor for assessment of human response to vibration environments. However, as discussed in Section A.3 of Appendix A, another application for this descriptor is to provide an alternate, and computationally convenient, measure of vibration response of a structure to a transient excitation. The key aspects of this application can be summarized as follows. (The reader is referred to Appendix A for the detailed discussion.)

3.2.1 Acceleration Exposure and Equivalent Peak Acceleration

The total "energy" of a transient acceleration signal, $A(t)$ defined as the Acceleration Exposure, with units of $g^2 \cdot second$, which is the integral, over the _time_ duration T of the event, of the square of the acceleration $A(t)$ time history. However, from Parseval's theorem, this Acceleration Exposure, E_A can also be expressed by the integral, over _frequency_ of twice the square of the absolute value of the Fourier Spectrum of $A(t)$. Thus, E_A can be given by:

$$E_A = \int_0^T A^2(t)\,dt = 2 \int_0^\infty |A(f)|^2\,df \qquad (15)$$

This measure, when expressed in decibels as an Acceleration Exposure Level in dB re: $(1\mu g)^2 \cdot s$ has the useful interpretation discussed in Section 1.5. For application to structural vibration, it is useful to define an Equivalent Peak Acceleration which is the initial peak value

of a damped acceleration response of a SDOF system to an impulse and <u>which has the same energy – the same value of E_A – as an actual acceleration response to a sonic boom</u>. Typical experimental data on the acceleration response of buildings to sonic boom often resemble such a simple transient signal. It is shown in Section A.3 of Appendix A that this Equivalent Peak Acceleration, $A(eq)_{pk}$ is very closely approximated by the following simple expression:

$$A(eq)_{pk} = [4\pi f_o \cdot E_A \cdot e^{-\pi/2Q}]^{1/2} \cdot [Q - 1/4Q]^{-1/2} \tag{16}$$

where E_A = the Acceleration Exposure with units $(g)^2 \cdot$ seconds, and

  f_o, Q = the undamped resonance frequency and Resonance Amplification Factor of the SDOF system under consideration.

To apply Eq. (16), it is necessary to obtain an estimate of the Acceleration Exposure of a structural response. This is provided by the second part of Eq. (15) with the use of the absolute value of the Fourier Spectrum, $|A(f)|$ of the acceleration response time history, $A(t)$. This quantity can be derived analytically or experimentally by using one of the following nominally equivalent expressions. For an analytical approach, $|A(f)|$ is given by:

$$|A(f)| = \left[|P(f)|/w \right] \cdot \left| \frac{A(f) \cdot w}{P(f)} \right| \tag{17}$$

where $|P(f)|$ = the absolute value of the Fourier Spectrum of the pressure excitation,

  w = the surface weight of the structure in the same units as the pressure,

and the dimensionless quantity $|A(f) \cdot w/P(f)|$ is the frequency response function for the acceleration response of a structure with a surface weight w to an acoustic field with a Fourier Spectrum, P(f). Note that all that is required here are the absolute values of these quantities – their phase information is ignored so that the time history of the response is not recoverable from these quantities.

To apply the experimental data approach, the Acceleration Exposure for structural response to a sonic boom can also be estimated from the measured response of the structure to an acoustic excitation. Applying this approach, one can express the absolute value of A(f), empirically, by:

$$|A(f)| = \left[|P(f)| /w \right] \cdot M_{SA}(f) \tag{18}$$

where $M_{SA}(f)$ is an experimentally determined, dimensionless vibro-acoustic structural response function, called the Specific Acoustic Mobility, and where $P(f)$ and $A(f)$ are both presumed to be measured in the same filter bandwidth and the surface weight, w is in the same units as the pressure.

It is important to note that Eq. (17) and (18) are nominally the same; that is, the dimensionless Specific Acoustic Mobility, M_{SA} is nominally equivalent to the vibro-acoustic transfer function $|A(f) \cdot w/P(f)|$. They are, in fact, identical if both are evaluated with the same frequency bandwidth resolution.

3.2.2 Theoretical Approach for Computation of Acceleration Exposure

Figure 18 presents the results of applying the first (analytical) approach to compute values for an Equivalent Peak Acceleration, $A(eq)_{pk}$ for the case of a SDOF system with a Q of 4, 10 and 25. This was accomplished with Eq. (16) and (17) where the absolute value of the Fourier Spectrum, $|P(f)|$ for the sonic boom pressure and the frequency response function $|A(f) \cdot w/P(f)|$ for the acceleration response of the structure are specified by Eq. (A6) and (A7) respectively, in Appendix A. It is also shown in this Appendix how closely this Equivalent Peak Acceleration agrees, as expected, with the Acceleration Shock Response Spectrum.

There is one relatively minor but unexpected difference between the Equivalent Peak Acceleration values and the corresponding Shock Spectra. As explained at the end of Appendix A, the former has an extra peak for a low value of f_0T of about 0.3 that is only barely present in the Shock Spectrum. This minor peak shows up in the Primary, Negative response Shock Spectrum as can be seen in Figure 15. (See also Figure A-2 in Appendix A.) However, since the Equivalent Peak Acceleration is based on both the amplitude and duration of an acceleration signal, the lower value of f_0T (i.e., longer duration) causes an increase in the Acceleration Exposure and hence an increase in the Equivalent Peak Acceleration.

The effect of damping on this peak acceleration response to a sonic boom now becomes more apparent. However, it is still important to note that the decrease in the peak acceleration response to a transient sonic boom excitation is not nearly as large as would be obtained for a steady state excitation.

To apply this same approach to other sonic boom wave forms, a simple approximation to the desired result is obtained by adjusting the absolute value of the Fourier Spectrum $|(Pf)|$ to account for the change in the envelope of this quantity for shaped sonic booms. Figure 19

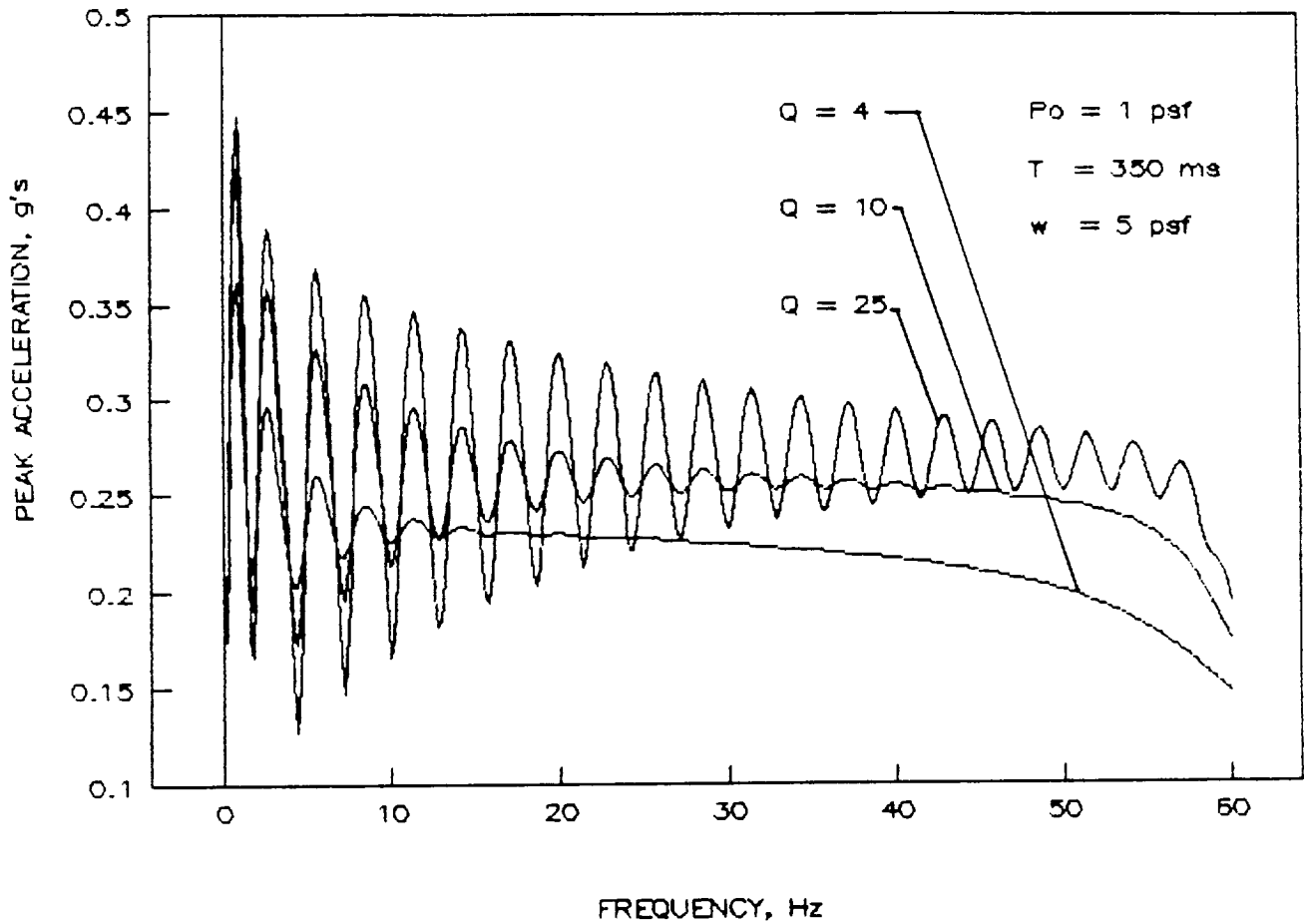Figure 18. Equivalent Peak Acceleration for Excitation of a Damped SDOF System with a Q of 4, 10 and 25 and a Surface Weight of 5 psf by an Ideal Sonic Boom N-Wave with a Duration of 350 ms and Peak Pressure of 1 psf.
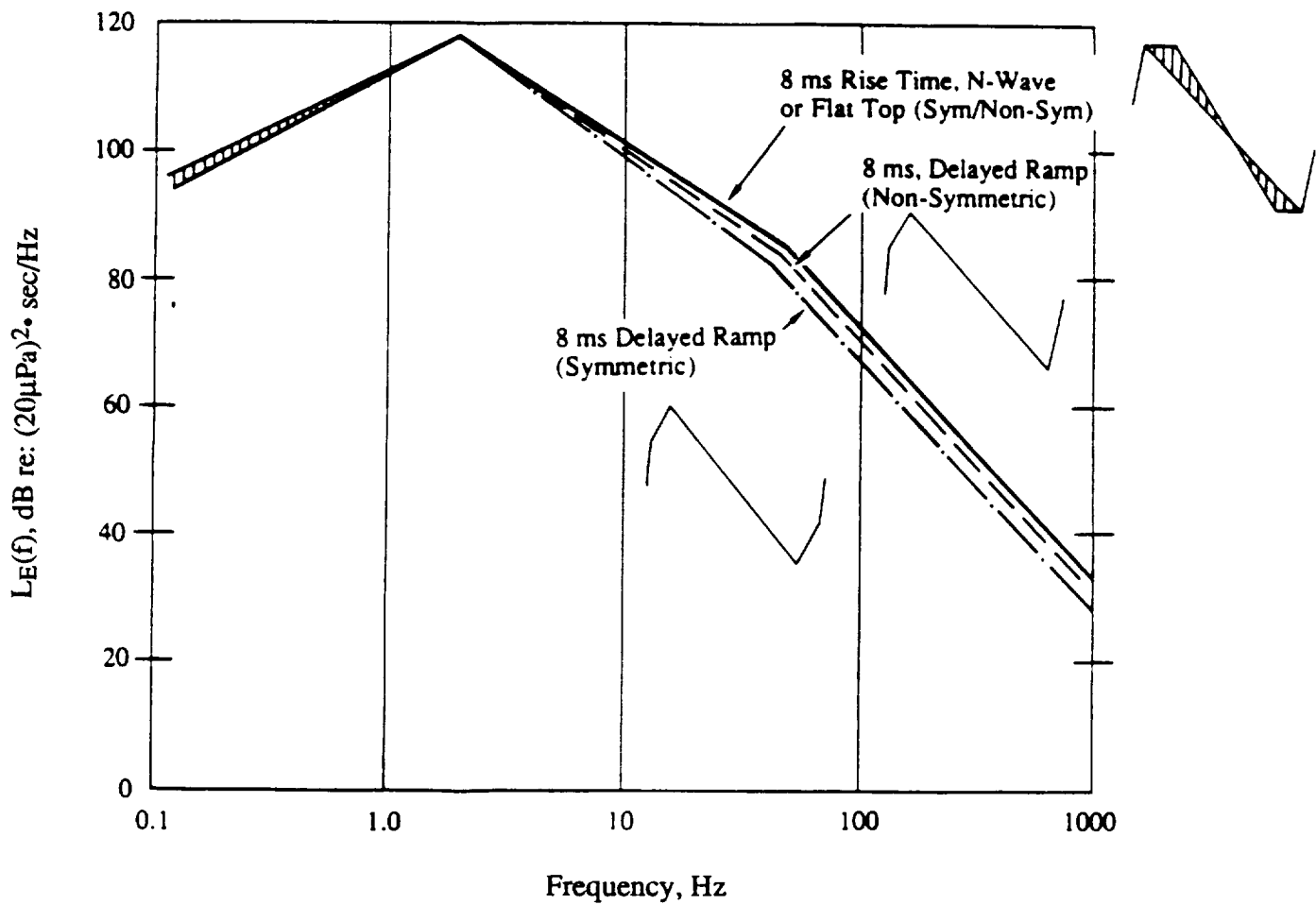
Figure 19. Comparison of Envelopes of Sound Exposure Spectrum Levels for
Various Shaped Boom Wave Forms With a Peak Pressure of 1 psf
and Total Duration of 350 msec (Brown and Sutherland, 1991).

3-17

provides the necessary guidance to allow such adjustments to these estimates, and shows that the envelopes of the Fourier Spectrum for a number of different sonic boom wave forms (Brown and Sutherland, 1991) are not drastically different in the frequency range of primary concern for this study (i.e., below about 50 to 60 Hz). The largest difference is about 3 to 5 dB between the spectrum levels for a reference (8 ms rise time) boom and the levels for a symmetric delayed ramp boom. In the figure, the spectra are shown as the Sound Exposure Spectrum Level, $L_E(f)$, which is equal to $2|P(f)|^2$ expressed in decibels relative to (20 μPa)$^2 \cdot$sec/Hz. (See Brown and Sutherland, 1991, for a more complete discussion of this descriptor.)

To illustrate this approach, the desired squared Fourier Spectrum $|P(f)|^2$ for a reference sonic boom wave form with a peak pressure 1 psf and rise/fall time of 8 ms was closely approximated by multiplying the squared spectra $|P(f)|^2$ for an ideal N-wave by a high-frequency roll-off correction term equal to unity for any frequency f below the rise time cut-off frequency, f_r and equal to $(f_r/f)^2$ for frequencies above this point where f_r is equal to $1/\pi t_r$ and t_r is the rise time. This sort of adjustment is clearly evident in Figure 20 when comparing the spectrum for the ideal N-wave and the reference wave form. The resulting Equivalent Peak Acceleration for excitation of a SDOF system with Q=10 by the Reference Sonic Boom Wave Form is compared in Figure 20 to the corresponding curve from Figure 18 for the ideal N-wave. As expected, the curves are identical until the frequency exceeds the rise time cut-off frequency f_r when the value of $A(eq)_{pk}$ for the reference wave form begins to fall off as $1/f^2$ in addition to the $1/f^2$ roll-off for an ideal N-wave. Note that in both Figures 18 and 20, the gradual roll-off in Equivalent Peak Acceleration at frequencies above about 50 Hz is apparently an artifact of the upper bound (60 Hz) chosen for evaluation of the Acceleration Exposure Spectrum. Had a higher frequency limit been selected, it is not expected that these curves would show this gradual roll-off.

To summarize, a simple theoretical model has been outlined permitting estimates of an equivalent peak acceleration response of a SDOF system to any sonic boom wave shape. A limited application of this approach would indicate that the (equivalent) peak acceleration response, at low (fundamental) frequencies, of typical residential structures to the various shaped sonic boom wave forms illustrated in Figure 19 would not be expected to be more than about 3 to 5 dB lower in response (i.e., reduction in peak acceleration by less than about 30 percent to 45 percent) at typical structural resonance frequencies compared to the response to a reference sonic boom with a nominal 8 ms rise time.
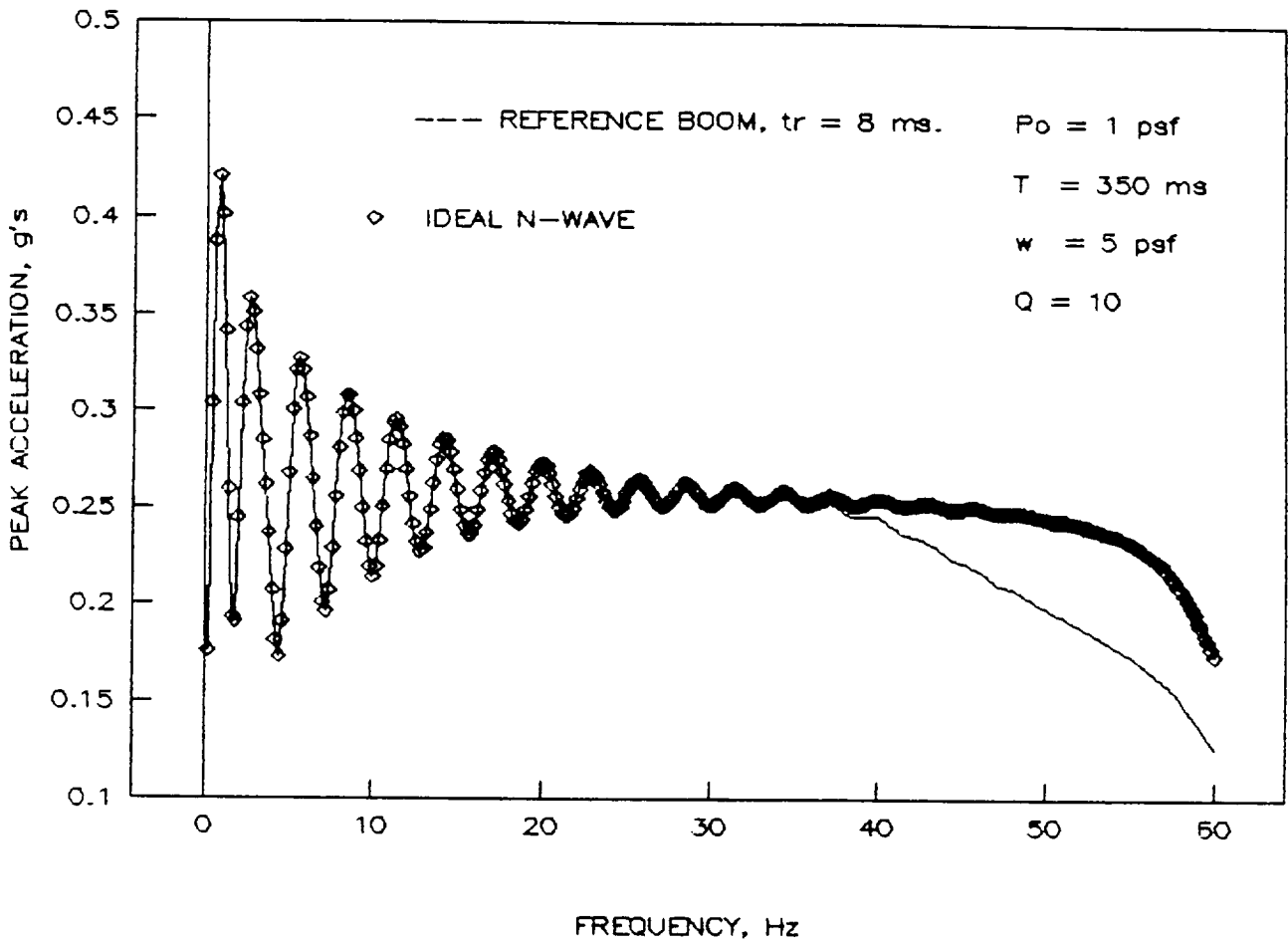
Figure 20. Equivalent Peak Acceleration for Excitation of the Same SDOF System as for Figure 18 with a Q of 10 by a Reference Sonic Boom with a Rise/Fall Time of 8 ms and by an Ideal Sonic Boom N-Wave.

3.2.3 Application of Experimental Data for Computation of Peak Acceleration Response

A number of full scale vibration response tests have been carried out on actual dwellings excited by sonic booms (e.g., see Section 3.3 and Appendix B for a detailed review of one such major program carried out at Edwards Air Force Base in 1966). However, these prior sonic boom tests have seldom included an analysis of the frequency spectrum of the acceleration and pressure signals necessary to define the ratio $|A(f)/P(f)|$. Thus, for this report, data from two different laboratory test programs were considered. These tests provided data on the response of full scale mockups of residential structure to acoustic excitation, thus providing experimental values for the transfer function, i.e., Specific Acoustic Mobility, M_{SA}, required for Eq. (18).

The most recent of these test programs was considered the most potentially useful since the configuration of the test structure is considered more realistic. The test included acceleration measurements of the wall, floor, ceiling and exterior door of a full scale mock-up constructed inside a laboratory at the U.S. Army Construction Engineering Research Laboratory. The mock-up, consisting of three outdoor sides of a typical wood frame residential dwelling, was exposed to simulated blast impulse sounds and to steady-state wide-band noise. Figure 21 presents a summary of data from one series of tests carried out at this facility (Eldred, 1985). The figure shows values of M_{SA} derived from the data as a function of frequency based on the measured acceleration, A(f) and pressure, P(f) signals and estimated values for the surface weight, w to provide values for $M_{SA} \approx |A(f) \cdot w/P(f)|$. In this case, the spectral data were measured as one-third octave bands levels and thus represent only an approximation to the fine structure normally present in the spectral content of A(f) and P(f). An approximation to the average of these measured values for M_{SA} is shown by the heavy line in Figure 21. (Note that the data in Figure 21 are plotted on a relative frequency scale, f/f_0 where f_0 is the estimated fundamental resonance frequency of the surface being measured.) Thus, this measured value for M_{SA} could be applied in Eq. (18), along with computed values for the absolute value, $|P(f)|$ of the Fourier Spectrum for the desired sonic boom wave form and a representative value for the surface weight, w for a residential wall to estimate sonic-boom-induced values for $|A(f)|$. The latter, integrated over frequency, would provide values for the Acceleration Exposure, E_A and hence the Equivalent Peak Acceleration, according to Eq.(16).

The resulting values for $A(eq)_{pk}$ computed in this fashion showed the same variation with frequency as indicated by the values in Figures 18 and 20 but had a magnitude about three times larger. This was attributed to: (1) the fact that the data included the effect of multi-modal
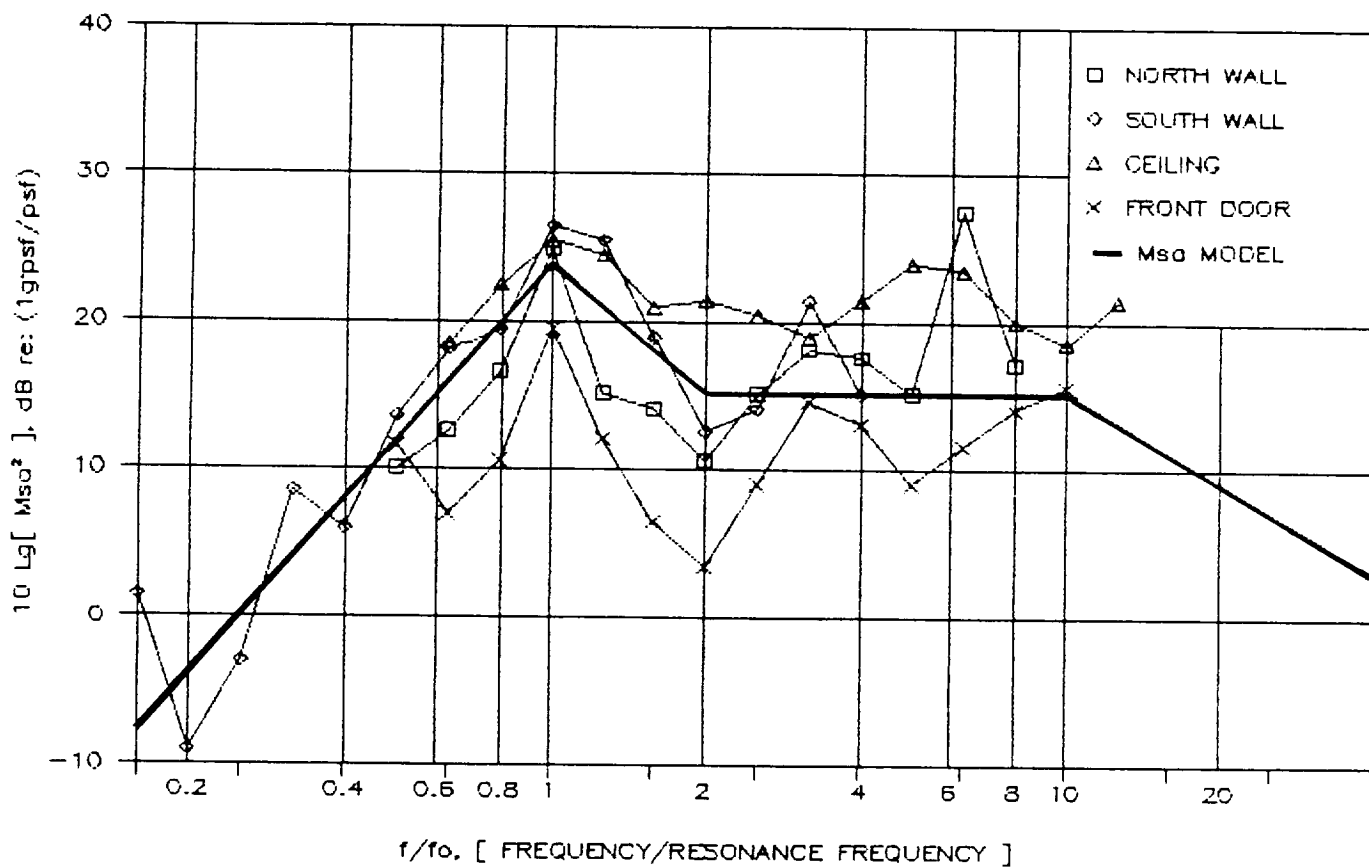
Figure 21. Measured Specific Acoustic Mobility Values from Laboratory Tests of a Full Scale Mock-Up of Three Walls, Floor and Roof of a 13 ft x 19 ft Room in a Typical Wood Frame Dwelling. Excitation by impulse (blast) sounds and steady state wideband random noise. (Data from Eldred, 1985.)

responses of real structure as opposed to the SDOF model employed in Figures 18 and 20 – a valid and expected reason for an increase in $A(eq)_{pk}$; and (2) the lack of adequate frequency bandwidth discrimination in the one-third octave band measurements. For the latter reason, the estimates of $A(eq)_{pk}$ using the simple M_{SA} model in Figure 21 are believed to be excessive since they predict values substantially higher than found in practice based on the actual sonic boom response data reviewed in Appendix B. However, the concept of using measured vibro-acoustic response data, properly analyzed, to measure M_{SA} is still considered valid and worthy of further consideration in the future. It should also be pointed out that the measured values of M_{SA} have face validity under the conditions under which they were obtained so that they can be relied upon to provide valid estimates of the vibro-acoustic responses of similar structures under similar conditions.

The other experimental program from which measured values of M_{SA} could be derived involved structural response measurements of full scale mock-ups of a large section (e.g., 8 ft x 10 ft) of a single wall (or roof) located in one side of a large reverberation chamber. The results, summarized in Figure 22, covering a wider range of structures than in Figure 21, are generally similar to the latter.

Finally, some of the key parameters employed in this approach to utilize experimental data on vibro-acoustic response of structure are summarized in Table 1. This presents measured values of the fundamental resonance frequency, f_0 for a variety of structural elements, average maximum values for M_{SA} at this frequency, and calculated values for the surface weight, w for these structures.

3.3   Structural Response to Sonic Booms from Edwards Air Force Base Test

Data from one major test program involving structural vibration response measurements of two residential-type buildings carried out at Edwards Air Force Base in 1966 are reviewed in Appendix B. The general test layout and definition of the accelerometer measurement locations are shown in Figure 23. The data from this test program provide one of the more complete data sets for validation of any method to predict structural vibration response to sonic boom. The analysis of the data consisted of computing a regression coefficient for an assumed linear relationship between the peak acceleration, A_{pk} reported, and the measured "free field" (ground reflected) peak sonic boom pressure, P_0. A typical result of this process is shown in Figure 24, taken from Appendix B. In all cases, the computed regression line was assumed to have a zero intercept to obtain a "transfer function" in the form of the ratio, A_{pk}/P_0 in g's per psf. A listing of these derived "transfer functions" is given in Table B-1 in Appendix B broken down

3-22
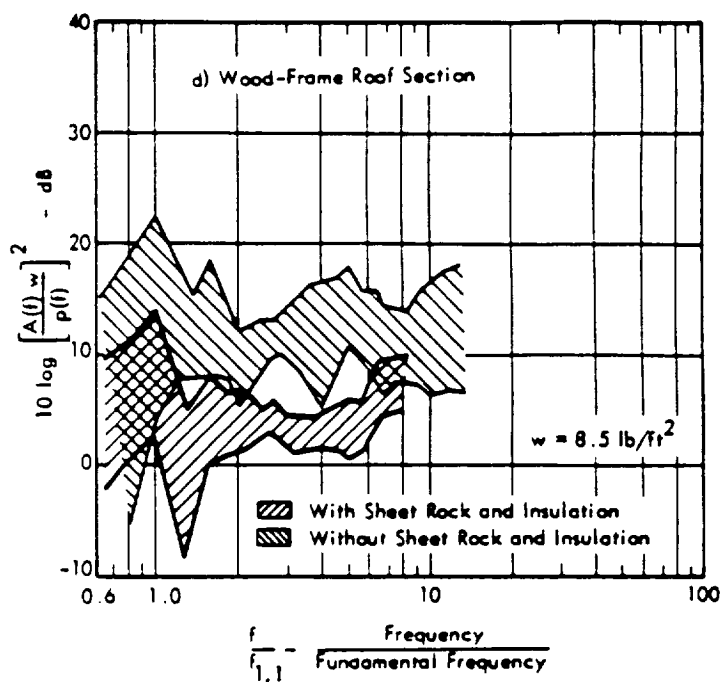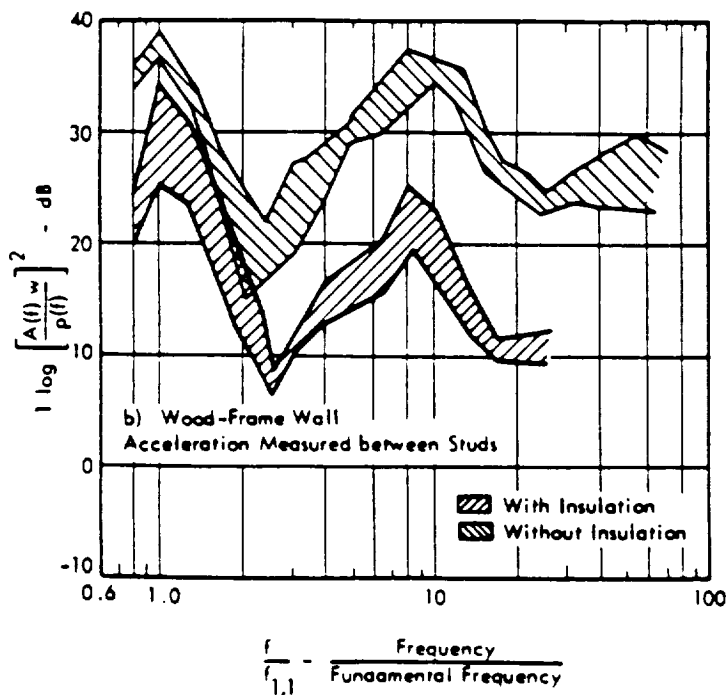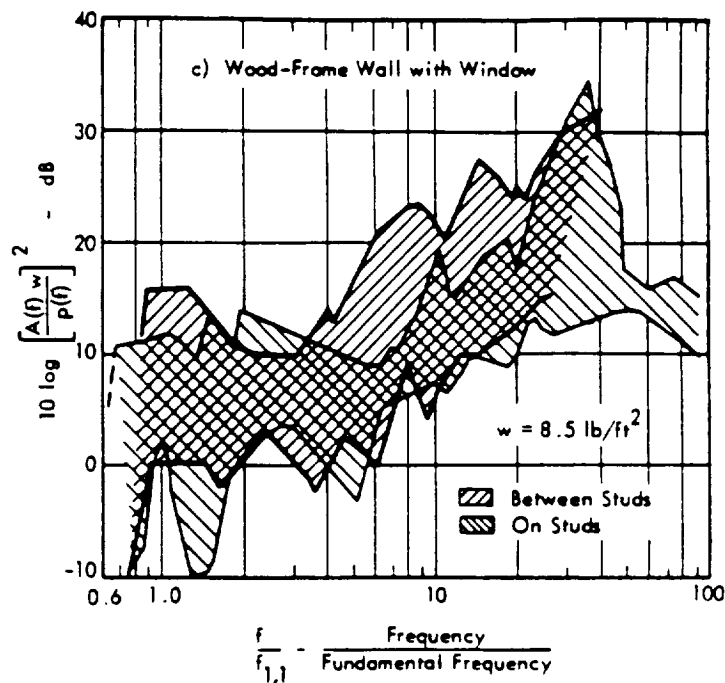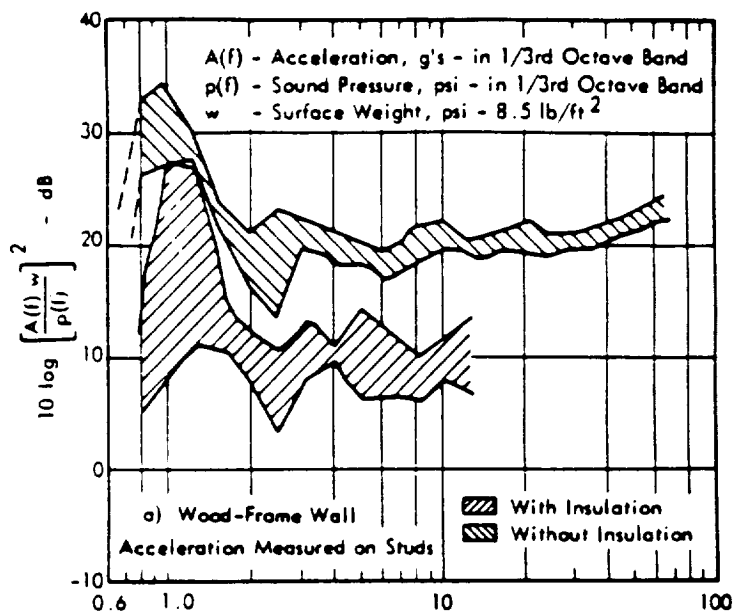
Figure 22. Measured Specific Acoustic Mobility Values from Laboratory Tests of Full Scale Mock-Ups of Three Types of Walls (8 ft x 10 ft) and a Roof Section (10 ft x 14 ft) Excited by Wideband Random Noise in a Large Reverberation Chamber. (Data from Sutherland, Chan and Andriulli, 1968.)

3-23

Table 1

Values for Average Surface Weights, w, Average Specific Acoustic Mobility, $\overline{M_{SA}}$ and Resonance Frequency f_0 for Various Building Elements (from Sutherland, 1990)

Type of Structure		Insulated	w lb/ft^2	Average[h] $M_{SA}\pm$Std. Dev.	$f_0 \pm$ Std. Dev. Hz
Metal Industrial Walls[a]					
		No	1.6 - 2	5.5 ± 100%	14 ± 24%
		Yes	2-4	3.5 ± 100%	14 ± 24%
Plaster Ceiling (3/4")		-	9.7	17 ± 40%	14 ± 10%
Wood Frame Building Walls/Roofs					
No	Between Studs/Joists[a]	No	5.0	33.0 ± 40%	17 ±34%
Window	Between Studs/Joists[a]	Yes	5.0	15.0 ± 40%	17 ±34%
|	On Studs/Joists[a]	No	5.0	10.0 ± 40%	17 ±34%
|	On Studs/Joists[a]	Yes	5.0	4.5 ± 40%	17 ±34%
with	Between Studs[a]	No	5.0	4.5 ± 40%	17 ±34%
Window	Between Studs[b,c]	Yes	5.0	4.5 ± 40%	17 ±34%
in Wall	On Studs[a]	-	5.0	2.0 ± 40%	17 ±34%
Walls/Ceilings with Plaster Interior		-	9.75	10.0 ± 40%	16 ± 29%
Windows[d]		-	(f)	13 ± 85%	(g)
Masonry Walls[a,c]					
Brick		-	67	5.6 ± 40%	12 ± 45%
Concrete Block		-	67	5.6 ± 40%	25 ± 30%
Stone		-	110	5.6 ± 40%	24 ± 20%

[a] Sutherland, 1968
[b] Estimated
[c] Eldred, 1985
[d] Langley Research Center, 1976
[e] Sutherland, Brown and Goerner, 1990
[f] Surface weight of typical window glass: 1/8" - 1.7 lb/ft^2
   3/16" - 2.6 lb/ft^2
   1/4" - 3.4 lb/ft^2
[g] $f_0 = [1 + (a/b)^2]\,(h/a^2)\,10^5$ Hz, where a, b= sides, h = thickness (all dimensions in inches)
[h] Average value at resonance frequency of structure

(a) Test Geometry
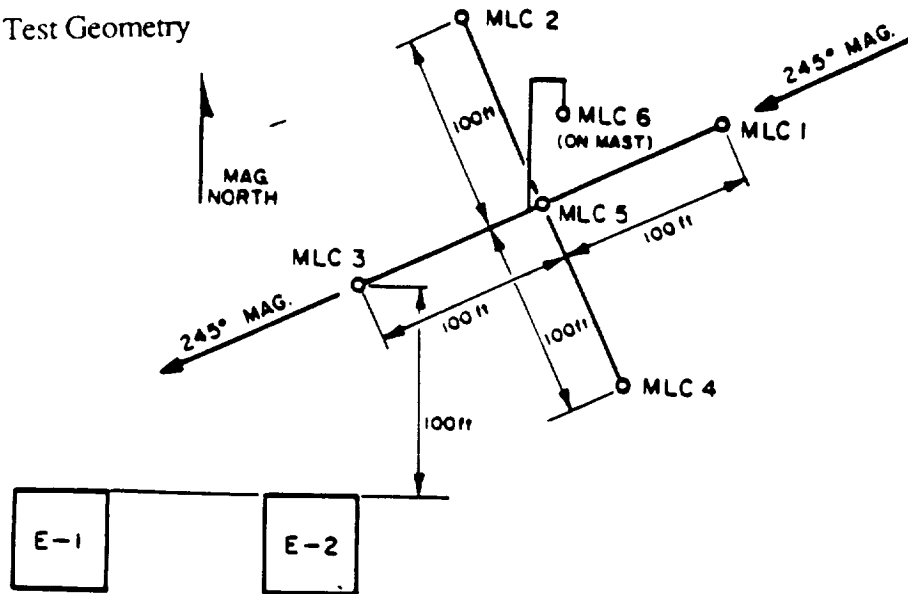
(b) Accelerometer Channels and Location

INSTRUMENTATION LOCATION, STRUCTURE E-1 FLOOR PLAN

INSTRUMENTATION LOCATION, STRUCTURE E-2 FLOOR PLAN
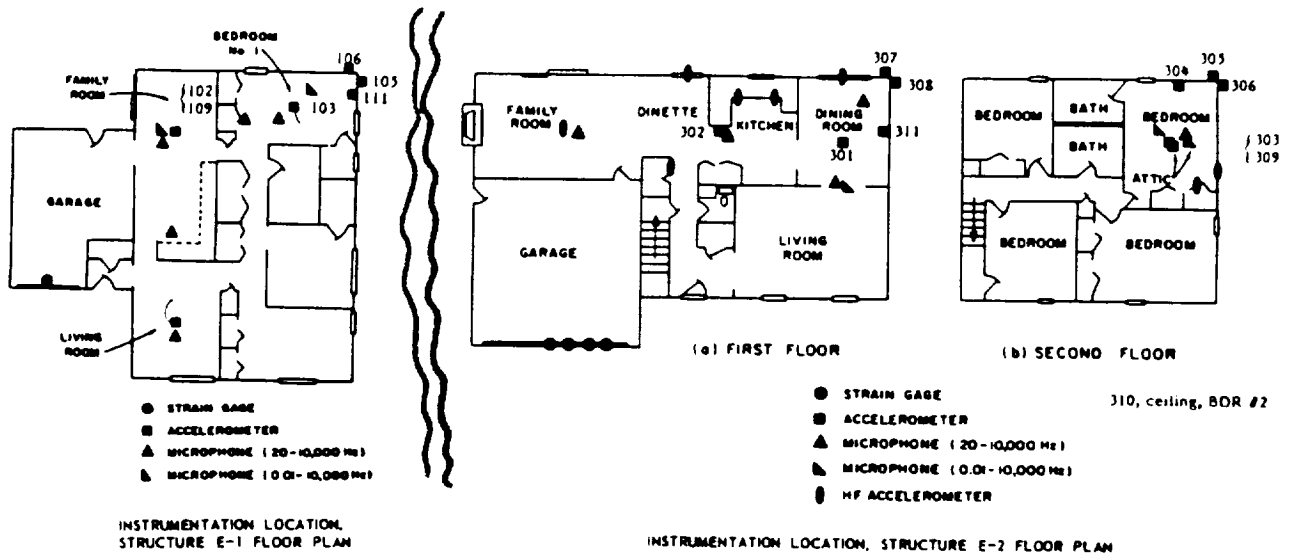
| Element | Wall | | Floor | Ceiling | Roof Line | | Kitchen |
	East	North			East	North	
House #1	111		101,102 103	109,110	105	106	
House #2	311	304	301,303	309,310	306,308	305,307	302

Figure 23. Test Geometry (a), and Accelerometer Positions and Data Channel Location (b) for Edwards AFB Sonic Boom Tests (Phase I) (from Stanford, 1967).
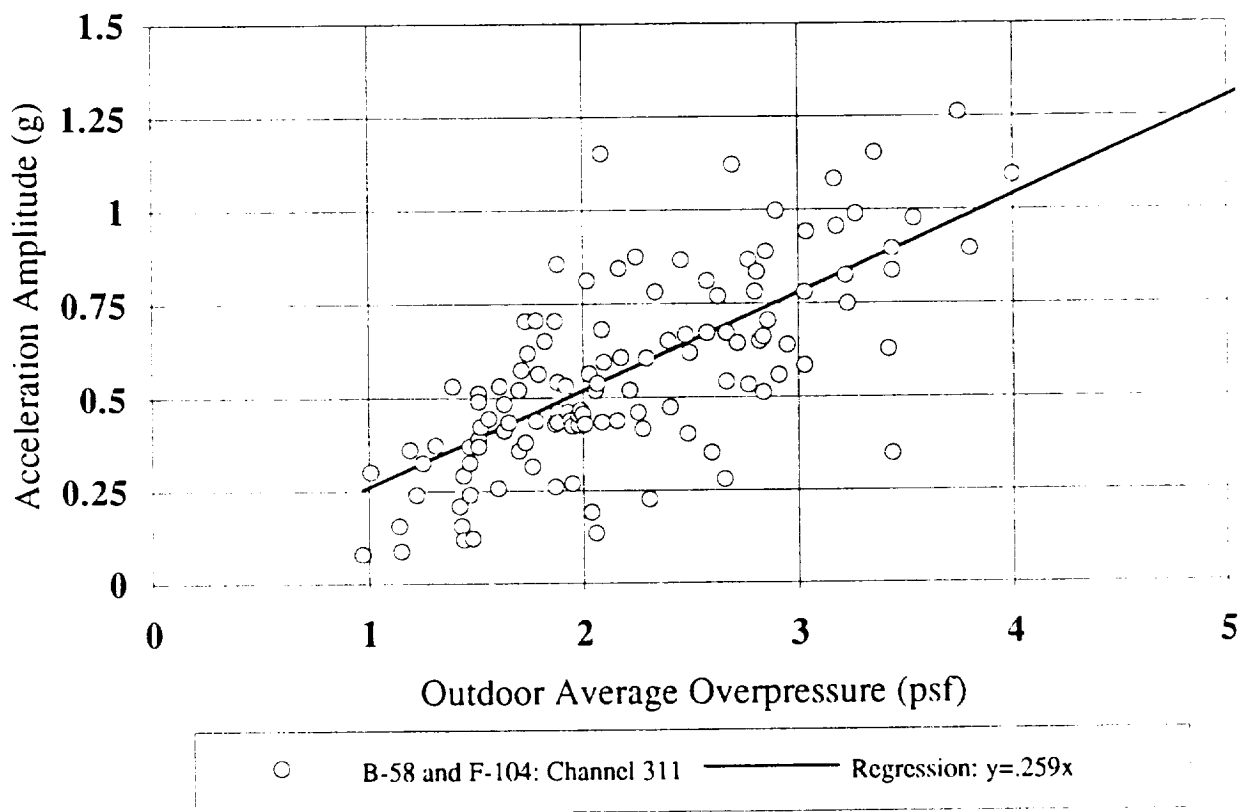
Figure 24. B-58 and F-104 Sonic Boom Induced Horizontal Acceleration Response of the East Dining Room Wall of House E-2 (Stanford, 1967).

by type of structural element (e.g., floor, roof line, ceiling, wall, etc.) measured in the two buildings.

A word about the source of these "transfer functions" is in order here. The data used to develop the transfer functions were taken from Tables II and IV of Annex G, Part II of the preliminary report of the subject tests (Stanford, 1967). These presented values for peak positive and negative acceleration read from oscillograph records of the test data. A detailed analysis was reported (Stanford, 1967) of the relationship between displacement response and peak sonic boom pressure from these tests and from a second phase of tests on the same structures (Blume, 1967). In addition, the relationship between peak acceleration and peak overpressure was shown for just two walls and a window in the first test report. However, no thorough evaluation of the correlation between acceleration and peak pressure for these tests could be located. Establishing this relationship was paramount to achieving the objectives of this report and hence required the extensive analysis presented in Appendix B.

A detailed summary of the values for the ratio, A_{pk}/P_0 is repeated here in Table 2. Here, the values are grouped conveniently to enable an assessment of differences in response due to aircraft type, structural element, and for racking and wall responses, orientation of the responding (vertical) surface relative to the direction of the supersonic aircraft flight path. In addition to the average value of A_{pk}/P_0 derived from the zero-intercept regression line through the data, the standard error of this regression coefficient is also given as a percentage of the mean value. Although there was considerable scatter in the data, the large number of measurements provided a surprisingly small standard error for the data. The average value over all of the elements was about 6 percent indicating the values of A_{pk}/P_0 measured in this program can be considered very reliable for the conditions encountered.

No distinction was made between data for small or large amounts of lateral offset of the flight track relative to the location of the test structures since it was found that the relationship between peak acceleration and peak pressure was not very sensitive to this distinction.

However, examination of the data in Table 2 suggests an interesting trend relative to estimates of residential structural response under the flight track of an HSCT.

An aircraft-type effect is apparent in the data in Table 2, primarily for responses by ceilings, floors and one of the three walls evaluated. This is presumed to be due to the difference in the duration T of the sonic boom signatures for the two different aircraft and

Table 2

Summary of Regression Coefficients for Structural Response
from Edwards AFB Tests (data from Stanford, 1967)

A/C	Channel	Structural Element	House No.	A_{pk}/P_o g/psf	Std. Error of A_{pk}/P_o	B58-F104 Delta[1] re: %	SE[2] —
B58	310	Attic - BDR 2	2	0.109	2.9%		
F104	310	Attic - BDR 2	2	0.143	5.1%	-27.1%	-0.85
B58	309	Attic - BDR 1	2	0.082	5.6%		
F104	309	Attic - BDR 1	2	0.104	6.3%	-23.2%	-0.37
B58	110	Ceiling	1	0.139	7.0%		
F104	110	Ceiling	1	0.246	8.5%	-55.6%	-1.38
B58	109	Ceiling	1	0.099	5.0%		
F104	109	Ceiling	1	0.180	5.4%	-57.6%	-1.54
Average				0.138			
Standard Deviation				0.050			
XB70	101	Floor	1	0.086	12.0%		
B58	101	Floor	1	0.069	3.0%		
B58	102	Floor	1	0.043	2.8%		
B58	103	Floor	1	0.052	2.6%		
Average for B58 - Floor, one story				0.055	2.8%		
F104	101	Floor	1	0.090	3.9%		
F104	102	Floor	1	0.062	3.4%		
F104	103	Floor	1	0.058	3.0%		
Average for F104 - Floor, one story				0.070	3.4%	-24.4%	-0.49
B58	301	Floor	2	0.048	2.7%		
B58	303	Floor	2	0.041	2.9%		
Average for B58 - Floor, two story				0.044	2.8%		
F104	301	Floor	2	0.049	3.9%		
F104	303	Floor	2	0.060	10.0%		
Average for F104 - Floor, two story				0.055	6.9%	-21.2%	-0.22
Overall Average for Floors				0.060			
Standard Deviation				0.015			
B58	302	Kitchen Counter	2	0.053	10.6%		
F104	302	Kitchen Counter	2	0.048	3.4%	10.9%	0.08
B58	107	Patio	1	0.012	5.0%		
F104	107	Patio	1	0.014	8.6%	-13.5%	-0.03
Average				0.013			

---

[1] Difference between B58 and F104 values in percent of average for both aircraft for a given element.

[2] Difference between B58 and F104 values relative to Average Standard Error for both aircraft for a given element.

[3] Response in direction approximately 25° relative to flight track.

Table 2 (Continued)

A/C	Channel	Structural Element	House No.	A_{pk}/P_0 g/psf	Std. Error of A_{pk}/P_0	B58-F104 Delta[1] re: SE[2] %	B58-F104 Delta[1] re: SE[2] —
B58	105	Racking - east [3]	1	0.044	5.0%		
F104	105	Racking - east	1	0.048	6.1%	-8.0%	-0.07
Average - Racking - east, one story				0.046			
B58	308	Rack - east - floor	2	0.065	4.4%		
F104	308	Rack - east - floor	2	0.070	7.6%	-6.9%	-0.08
B58	306	Rack - east - roof	2	0.080	16.0%		
F104	306	Rack - east - roof	2	0.069	12.4%	15.6%	0.08
Average - Racking - east, two story				0.071			
Average - Racking east, one and two story				0.058			
B58	106	Racking - north [4]	1	0.053	3.9%		
F104	106	Racking - north	1	0.053	5.7%	-1.7%	-0.02
Average - Racking north, one story				0.053			
B58	307	Rack - north - floor	2	0.060	6.6%		
F104	307	Rack - north - floor	2	0.072	10.4%	-18.6%	-0.14
B58	305	Rack - north - roof	2	0.049	4.6%		
F104	305	Rack - north - roof	2	0.049	5.9%	1.0%	0.01
Average - Racking north, two story				0.058			
Average - Racking north, one and two story				0.055			
Average - Racking north/east, one and two story				0.057			
B58	111	Wall - east [3]	1	0.111	4.2%		
F104	111	Wall - east	1	0.193	6.1%	-54.2%	-1.59
Average				0.152			
B58	311	Wall - east	2	0.248	3.1%		
F104	311	Wall - east	2	0.248	5.8%	-0.2%	-0.01
Average				0.248			
Average wall - east				0.200			
Standard Deviation				0.056			
B58	304	Wall - north [4]	2	0.170	10.4%		
F104	304	Wall - north	2	0.204	6.0%		-0.41
Average Wall - north				0.187			
Standard Deviation				0.017	6.04% = Average Standard Error		

---

[1] Difference between B58 and F104 values in percent of average for both aircraft for a given element.

[2] Difference between B58 and F104 values relative to Average Standard Error for both aircraft for a given element.

[3] Response in direction approximately 25° relative to flight track.

[4] Response in direction approximately 65° relative to flight track.

hence in the key response-dependent parameter, $f_0 T$ for a given structural element. For the principal aircraft employed for this test, the average sonic boom durations were 164 ms for the B-58 aircraft and 79 ms for the F-104 aircraft. Only two or three A_{pk}/P_0 data points were available for most of the structural elements from the three XB70 flights (T ≈ 0.267 sec.) compared to the 30 to 90 data points per element from the two principal aircraft. Thus, no attempt has been made to evaluate these XB70 data in any detail. However, the following trend in the average relative value of A_{pk}/P_0 over all structural elements was noted when the limited XB70 data was considered.

Aircraft	Average T (sec.)	Relative $A_{pk}/P_0 \pm$ S.D.
F104	0.079	1.0
B58	0.164	0.88 ± 0.20
XB70	0.267	0.75 ± 0.18

It is not safe to assume that the particular sample of structural types that were monitored for this program are representative for all similar structures (i.e., one and two story wood frame dwellings). Nevertheless, the above figures would extrapolate to a trend in the relative acceleration response, for the same peak overpressure, of about 64 percent of that for sonic booms from F-104 aircraft for similarly shaped sonic booms with a duration of 350 ms. However, it must be emphasized that this trend could only be considered potentially valid for the particular sample of structures measured for this program. It is also important to point out that while the above trend was observed at nearly all of the measurement positions in both houses, the average normalized response of the center of the dining room in House No. 2, induced by two XB-70 flights, increased by 32 percent relative to the value for the F-104 flights for the same measurement position. Recalling the discussion about the Acceleration Shock Response Spectra or the Equivalent Peak Acceleration, it can be stated that for values of the parameter, $f_0 T$ above 1, that on the average, as $f_0 T$ increases (e.g., as T increases for a given structure with a constant f_0), the overall envelope of peak acceleration responses will tend to decrease slightly. Thus the above trend is not inconsistent with theoretical expectations, but for any one structural element, the peak acceleration response will fluctuate up and down as T increases in the manner indicated by the oscillations in the shock response or peak acceleration spectra shown earlier (e.g., Figure 15 or 18).

Further evaluation of this potentially important influence of sonic boom duration on maximum acceleration response was desirable but progress was hampered by lack of detail on the dynamic response characteristics of the test structures. However, it was possible to make a

limited comparison between some of the measured results and predicted values for the acceleration response. This was possible only for those elements for which an adequate time history record was available to allow estimates of the resonance frequency, f_0 and sonic boom duration, T. The results are summarized in Table 3 in terms of "measured" and predicted values for the dimensionless peak acceleration, $A_{pk} \cdot w/P_0$. Predicted responses were based on the computed Acceleration Shock Response Spectra for a reference sonic boom with a rise/fall time of 8 ms and for a SDOF system with a Q of 10 or 20 to bracket expected values. This spectrum was considered a reasonable approximation for the average nominal wave form actually encountered in the Edwards AFB tests. (Perturbations to the nominal wave form caused by the atmosphere are not expected to be significant for structural response.)

As indicated at the lower right side of the table, the ratio between measured and estimated values for the peak acceleration response was close to 1.0 only for the walls. The ratio was about 1.7 for ceilings, which is believed to be due to the more complex structural response patterns for ceilings not accounted for by the simple SDOF model. For floors and roof lines (corresponding to racking responses), not surprisingly, the ratio between measured and predicted acceleration response is substantially less than 1.0.

This comparison between measured and predicted values of A_{pk}/P_0 was only expected to show reasonable agreement for response of diaphragm surfaces, such as walls or roofs, which can be represented by the simple mass-spring SDOF model illustrated earlier at the beginning of Section 3.1. However, the Edwards AFB test data also provided unique information on the other more complex types of structural responses, such as racking and floor or ceiling vibration, which are indirectly coupled by the building frame vibration (Carden and Mayes, 1970). Thus the measured data for these cases provide an invaluable source for empirical prediction.

While the Shock Response Spectrum prediction was expected to be in reasonable agreement with measurements only for walls, the prediction model gives no consideration to:

* expected reductions in response by as much as 100 percent due to the effect of angle of incidence and diffraction, as discussed earlier in Sections 3.1.1 to 3.1.4.

* potential increases in response by as much as 100 percent due to multi-modal effects (Sutherland, Brown and Goerner, 1990).

For the other types of structure not directly exposed to the sonic boom wave front, a structure-to-structure coupling correction is expected to apply. Thus an empirically corrected model for

Table 3

Comparison of Measured and Predicted Values
for Normalized Peak Acceleration from Edwards AFB Phase I Test
(Data from Stanford, 1967)

A/C	Channel	Element	No. of Tests	Apk/Po g/psf	St. Err. of Coeff.	f_o Hz	T sec	f_oT -	w psf	Apk·w/Po Measr'd -	Apk·w/Po Pred'ctd Q=10	Apk·w/Po Pred'ctd Q=20
B58	109	Ceiling	86	0.099	0.005	16 *	0.164	2.6	9.8	0.97	0.83	0.90
B58	110	Ceiling	63	0.139	0.010	16 *	0.164	2.6	9.8	1.36	0.83	0.90
F104	109	Ceiling	32	0.180	0.010	16 *	0.079	1.3	9.8	1.75	0.91	1.00
F104	110	Ceiling	24	0.246	0.021	16 *	0.079	1.3	9.8	2.40	0.91	1.00
B58	309	Ceiling Joist	91	0.082	0.005	38	0.160	6.0	2.8	0.23	0.81	1.04
B58	101	Floor	82	0.069	0.002	21	0.196	4.1	5.0	0.34	0.99	1.25
B58	102	Floor	91	0.043	0.001	20	0.196	4.0	5.0	0.22	1.03	1.30
B58	103	Floor	91	0.052	0.001	18	0.196	3.6	5.0	0.26	0.78	0.85
B58	303	Floor	69	0.041	0.001	24	0.160	3.8	5.0	0.20	0.92	1.07
B58	105	Roof Line(1)	91	0.044	0.002	14	0.170	2.4	8.5	0.38	0.85	0.91
F104	105	Roof Line	33	0.048	0.003	14	0.080	1.1	8.5	0.41	1.45	1.57
B58	111	Wall	79	0.111	0.005	17	0.150	2.6	4.8	0.53	0.83	0.89
B58	311	Wall	91	0.248	0.008	25	0.180	4.5	4.8	1.19	0.57	0.66
F104	111	Wall	82	0.193	0.012	17	0.079	1.3	4.8	0.93	0.91	0.97
F104	311	Wall	76	0.248	0.014	25	0.079	2.0	4.8	1.19	1.50	1.72

Average of $\dfrac{P_{bk} \cdot w/P_o \text{ (measured)}}{A_{pk} \cdot w/P_o \text{ (predicted)}}$

	Q=10	Q=20
Ceiling	1.84	1.69
Floor	0.28	0.24
Roof Line	0.34	0.32
Walls	1.13	1.01

*   Estimated
(1)   Racking mode in east-west direction

3-32

structural response to sonic boom, based on these limited data, is suggested which would have the form:

$$A_{pk}(eff) \cdot w/P_0 = K \cdot [A_{pk} \cdot w/P_0] \qquad (19)$$

where $A_{pk}(eff)$ is an effective (or measured) value for the peak acceleration response, and K is a structural-element-dependent correction factor to be estimated by the ratio between the measured and predicted values of $[A_{pk} \cdot w/P_0]$. (No angle of incidence correction is included.)

Based on the results in Table 3, it is proposed that first order estimates of structural responses to sonic booms, assuming normal incidence, can be made with the following semi-empirical models.

WALLS — Use Acceleration Shock Spectra for a SDOF system with a Q of 20 to predict the dimensionless peak acceleration, $A_{pk} \cdot w/P_0$, where w is the average surface weight of the wall and P_0 is the peak *ground reflected* sonic boom pressure. (In this case, the "correction factor," K is assumed to be unity.)

FLOORS — Apply the same process but multiply the resulting value by an empirical correction factor, K = 0.25.

RACKING VIBRATION MODES — Again apply the same process, using for the surface weight, w, an average for the entire roof structure, and a correction factor, K = 0.35.

CEILINGS — Again, apply the same model as for walls using the average surface weight for the ceiling structure and a correction factor of 1.7.

In lieu of Acceleration Shock Spectra, one may choose to compute an Equivalent Peak Acceleration, $A(eq)_{pk} \cdot w/P_0$ and an Acceleration Exposure Level, applying the concepts outlined in Section 3.2. In all cases, the same correction factors identified above would be applied to the magnitude of the acceleration. To estimate the Acceleration Exposure Level for such cases, one would add a correction, $20 \cdot Lg(K)$ to the Acceleration Exposure Level computed in the manner specified in Section 3.2 or Appendix A.

It must be emphasized that the simple procedure just outlined is only intended to provide the basis for preliminary estimates of structural response. A more detailed evaluation should consider the first order effects of sonic boom duration more carefully, as well as effects

of diffraction on the response spectra for shaped sonic booms along the lines outlined earlier. It is expected, however, that a proper evaluation of either the Acceleration Shock Spectra or an Equivalent Peak Acceleration for any desired wave form, including the effects of diffraction, would show similar trends.

3.4 Preliminary Estimates of Structural Vibration Levels from Sonic Booms of a High-Speed Civil Transport in Typical Residential Buildings

To illustrate the potential application of these simple concepts, consider the following example. Assume a sonic boom wave form consisting of a reference sonic boom with a rise/fall time of 8 ms and a duration, T of 350 ms. (The structural response for other wave shapes, such as illustrated in Figure 19, can be estimated to a first approximation by accounting for differences in the envelope of the Sound Exposure Spectrum for alternate wave shapes.) Further, for convenience, let the peak (ground reflected) overpressure, P_0 be assumed to be 1 psf. (The response for other peak pressures can be estimated by multiplying the estimated response for 1 psf by the desired peak pressure since the structural response is expected to be linearly related to this pressure, all other things being equal.) For this example, estimate the peak acceleration response of the exterior wall and floor of a residential building, each element having an average surface weight, w of 5 psf. The resonance frequency of these structural elements will be assumed to be 17 Hz (see Table 1) and 20 Hz, respectively. The Resonance Amplification Factor, Q of each will be assumed to be 10. For convenience for this example, the acceleration response is specified in terms of the Equivalent Peak Acceleration since the necessary values are illustrated graphically in Figure 20. However, the results could also have been found using an Acceleration Shock Response Spectrum plot or calculation (see Appendix A) covering the required range for $f_0 T$.

From Figure 20, one can find the following values for the Equivalent Peak Acceleration, $A(eq)_{pk}$. where it is assumed that the value applies for a unit value of the empirical correction factor, K specified by Eq. (19). This is equivalent to reading the ordinate of Figure 20 as $A(eq)_{pk}$ divided by K.

Structural Element	f_0 Hz	T sec	$f_0 T$ –	$A(eq)_{pk}/K$ g	K –	$A(eq)_{pk}$ g
Wall	17	0.35	5.95	0.278	1	0.278
Floor	20	0.35	7.0	0.273	0.25	0.068

By applying Eq. A17 and A12 in Appendix A, it can be shown that the Acceleration Exposure Level, L_{AE} for these two cases is given by:

Wall,　L_{AE} = 96.3　dB re:$(1\mu g)^2 \cdot s$

Floor,　L_{AE} = 83.4　dB re:$(1\mu g)^2 \cdot s$

These estimates of the vibration environment in terms of an Acceleration Exposure Level for a single sonic boom can now be compared to the criteria defined in Section 1 for the perception of whole-body or tactile vibration and in Section 2 for the detection of rattle.

4.0 COMPARISON OF HUMAN RESPONSE CRITERIA TO ESTIMATED STRUCTURAL VIBRATION ENVIRONMENT

4.1 Comparison to Composite Whole-Body/Tactile Vibration Criteria

A composite criteria for the perception of whole-body or tactile vibration was defined, for purposes of this report by Eq. (1). When expressed in terms of g's, the peak acceleration values, $A_{pk}(f)$ above which the average person would be expected to perceive the vibration can be given as a function of frequency, f by:

$$A_{pk}(f) = \begin{cases} 0.001\,g & f < 4\,\text{Hz} \\ 0.001 \cdot (f/4) & 4 \leq f < 40\,\text{Hz} \\ 0.01 & 40 \leq f < 200\,\text{Hz} \\ 0.01 \cdot (f/200)^{3.3} & f \geq 200\,\text{Hz} \end{cases} \qquad (20)$$

These vibration perception criteria and the preceding example estimates of vibration environment compare as follows:

Structural Element	f_o Hz	$A(eq)_{pk}$, g's Estimated Environment	$A(eq)_{pk}$, g's Perception Criteria	Estimated Env. Criteria
Wall	17	0.278	0.0043	65
Floor	20	0.068	0.005	14

Allowing for uncertainty in all parts of this comparison, on the basis of peak acceleration, there would appear to be no question that the structural vibration would be readily perceived by the average person in a normal quiescent environment. The ratio of the estimated environment to the criterion levels varies from 14 to 65 – or a range of 23 to 36 dB on a decibel scale.

Consider the other possible form of a vibration perception criteria: Acceleration Exposure Level, AEL. Although exact values for a criterion in terms of this descriptor are less certain, it is suggested in Section 1.5 that the threshold for acceptability for vibration is expected to fall within a range of Acceleration Exposure Levels of 75 to 95 dB re: $(1\mu g)^2 \cdot \text{sec}$. The preceding environmental estimates of the AEL were 96 and 83 dB, respectively, for the wall and floor vibration. In this case, the estimated environment lies in the upper part of the

criterion range. For the worst case, the floor and wall Acceleration Exposure Levels would be 8 to 21 dB above the most stringent criterion level (i.e., AEL = 75 dB). If the average of the range of criterion levels were used (i.e., AEL = 85 dB), then the estimated environment would be from 2 dB below the criterion level for the floor to 11 dB above the criterion level for the wall. The point here is that <u>if one attempts to factor in duration effects on human response to a transient vibration, the potential impact of sonic boom-induced structural vibration (ignoring rattle) is potentially much less severe</u>.

4.2   Comparison to Rattle Vibration Criteria

In Section 2.3.2, it is suggested that a threshold for the onset of wall vibration-induced rattle of hanging mirrors, pictures, etc., is a peak acceleration of 0.045 ± 0.021 g in the frequency range of low-order wall resonance frequencies – 15 to 150 Hz. The estimated peak wall vibration environment was 0.278 g – well above this rattle threshold. While the occurrence of rattle can be, and frequently is, completely mitigated by simple means such as the use of felt pads located at potential impact points for hanging pictures, etc., it seems clear that if hanging objects are located near the middle of a typical outside wall and do not employ such measures, transient rattle triggered by the sonic boom-induced structural vibration would very likely occur. The significance of this frustratingly minor, and readily abated, source of annoyance is that it may very well be a major source of community annoyance response to the impulsive sound of sonic booms, as suggested by the data in Figure 9.

5.0 SUMMARY

A review of vibration perception criteria and methods for predicting structural vibration response to sonic booms has indicated the following:

- Estimates of potential structural vibration of typical residential dwellings induced by a 1 psf, 350 ms reference sonic boom with a rise/fall time of 8 ms indicate levels 23 to 36 dB above composite perception criteria for whole-body and tactile vibration.

- When compared on the basis of a new descriptor – Acceleration Exposure Level – a measure which can account for the effect of duration of the vibration environment – the predicted environment lies in the upper range of acceptable vibration defined in terms of this descriptor. The predicted environment is estimated to be from -2 to 11 dB above average acceptable acceleration exposure levels. However, further research on human response to transient vibration is suggested.

- Changes in the estimated vibration environment levels due to the use of shaped sonic booms with the same peak pressure, such as delayed ramps, and flat-top wave forms, are expected to reduce the vibration, at most, by less than 3 to 5 dB, and then only at higher structural resonance frequencies above their normal range.

- An appendix presents a basic review of a classical Shock Response Spectrum method for evaluation of response to sonic booms, and defines methods for computation of the new Acceleration Exposure descriptor and a related quantity, an (energy) Equivalent Peak Acceleration. It is shown that these are readily computed from the absolute value of the Fourier Spectrum of the sonic boom signal and either analytically or experimentally determined absolute values for the steady-state frequency response characteristics of the structure to acoustic excitation.

- Another appendix provides a detailed review of the relationship between peak acceleration and peak sonic boom pressure as observed from one of the largest sonic boom structural response programs ever conducted (Phase I of the Edwards AFB sonic boom tests in 1966). A detailed analysis of the data provided the basis for empirical corrections to simple SDOF structural response models to account for the more complex vibration response patterns of internal building structure.

Finally, it is important to point out that many simplifying assumptions have been made in this report for the sake of providing a simple means of making a preliminary assessment of structural vibration from HSCT operation over populated areas. However, the degree of uncertainty in these results is considered comparable to the inherent variation in acceleration response of a given structure for the same nominal peak sonic boom pressure. This point is made clear upon examination of the regression plots of the Edwards AFB test data in Appendix B. The degree of scatter in the data is particularly striking considering the fact that the flight track of the aircraft was nearly always the same although aircraft Mach number and altitude did vary somewhat from test to test. In any event, detailed considerations of the exact pressure loading time history (i.e., diffraction, wave front angle effects, etc.) on external structural surfaces, multi-modal response behavior and the complex interaction between these external surfaces and internal structure, such as floors, were not included in this report. These refinements, along with possible consideration of statistical models for structural and human response and consideration of possible infrasound effects may deserve some consideration if the observations contained herein still leave unresolved concerns about human response to structural vibration induced by HSCT operations over inhabited land.

REFERENCES

ARDE Associates (1959), "Response of Structure to Aircraft Generated Shock Waves," WADC Technical Report 58-169, April 1959.

Benveniste, J.E., and Cheng, D.H. (1967), "Dynamic Effects of Sonic Booms on a Beam Loosely Bound to its Supports," AIAA Paper 67-14 before AIAA 5th Aerospace Sciences Meeting, New York, January 1967.

Blume, J.A., et al. (1967), "Response of Structure to Sonic Booms Produced by XB-70, B-58 and F-104 Aircraft," John A. Blume and Associates, Final Report to National Sonic Boom Evaluation Office, NSBEO-2-67, October 1967.

Bolt, Beranek & Newman (1974), "Impact Noise Testing and Rating," Report COM-75-10133 by Bolt, Beranek & Newman, Inc., for National Bureau of Standards, January 1974.

Borsky, P.N. (1965), "Community Reactions to Sonic Booms in the Oklahoma City Area," National Opinion Research Center, AMRL-TR-65-37, Report I and II, 1965.

Brown, D., and Sutherland, L.C. (1991), "Sonic Boom (Human Response and Atmospheric Effects) Outdoor-to-Indoor Response to Minimized Sonic Booms," NASA High-Speed Research Workshop, NASA–Langley Research Center, Williamsburg, Virginia, May 15-16, 1991.

Carden, H.D., and Mayes, W.H. (1970), "Measured Vibration Response Characteristics of Four Residential Structures Excited by Mechanical and Acoustical Loadings," NASA TN-D-5776, NASA–Langley Research Center, April 1970.

Cawthorne, J.M., et al. (1978), "Human Reponse to Aircraft-Noise-Induced Building Vibration," NASA Conference Publication 2052, Part II, 479-491, May 1978.

CHABA (1977), "Guidelines for Preparing Environmental Impact Statements on Noise," Working Group 69, on Evaluation of Enviromental Impact of Noise, of the Committee on Hearing, Bioacoustics, and Biomechanics, National Research Council, 1977.

Clarkson, B.L., and Mayes, W.H. (1972), "Sonic-Boom Induced Building Structure Responses Including Damage," J. Acoust. Soc. Am., 51: 742-757.

Clevenson, S.A. (1978), "Experimental Determination of the Rattle of Simple Models," NASA TM 78756, NASA–Langley Research Center, July 1978.

Clevenson, S.A., et al. (1978), "Effect of Vibration Duration on Human Discomfort," NASA TP-1283, September 1978.

Crandall S.H., and Kurzweill, L. (1968), "On the Rattling of Windows by Sonic Booms," J. Acoust. Soc. Am., 464-472, 1968.

Eldred, K.McK. (1985), "Noise and Vibration Characteristics of the CERL Low-Frequency Blast Pressure Facility Test House," KEE Report 85-29 for U.S. Army Construction Engineering Research Laboratory, November 1985.

REFERENCES (Continued)

Findley, D.S., Huckel, V., and Hubbard, H. (1975), "Vibration Responses of Test Structure No. 2 During the Edwards Air Force Base Phase of the National Sonic Boom Program", NASA TM X-72704, NASA–Langley Research Center, 1975 (see also NASA TM X-72706).

Freund, J.E. (1971), *Mathematical Statistics*, Second Edition, Prentice Hall, Inc., New Jersey, 1971.

Freynik, H.S. (1963), "The Non-Linear Response of Windows to Random Noise," NASA TN–D–2025, 1963.

Goldman, D.E. (1957), "Effects of Vibration on Man," *Handbook of Noise Control*, Harris, C.M. (Ed.), McGraw-Hill Book Co., New York, 1957.

Goldman, D.E., and von Gierke, H.E. (1961), "Effects of Shock and Vibration on Man," Chapter 44, *Shock and Vibration Handbook*, Harris, C.M., and Crede, C.E., (Eds.), McGraw-Hill Book Co., New York, 1961.

Hershey, R.L., and Higgins, T.H. (1976), "Statistical Model of Sonic Boom Structural Damage," FAA-RD-76-87, July 1976.

Hubbard, H.H. (1982), "Noise-Induced House Vibrations and Human Perception," *Noise Control Engr.*, *19*, 49-55, Sept.-Oct. 1982.

Hubbard, H.H., and Mayes, W.H. (1967), "Sonic Boom Effects on People and Structures," in *Sonic Boom Effects*, Seebass, A.R. (Ed.), NASA SP-147, NASA–Langley Research Center, 65-76, 1967.

International Organization for Standardization (1977), "Guide to the Evaluation of Human Exposure to Vibration and Shock in Buildings (1 Hz to 80 Hz)," Amendment to ISO Standard 2631-1974, April 1977.

International Organization for Standardization (1979), "Guide to the Evaluation of the Response of Occupants of Fixed Structures, Especially Buildings and Off-Shore Structures, to Low-Frequency Horizontal Motion," April 1979.

International Organization for Standardization (1985), "Evaluation of Human Exposure to Whole-Body Vibration – Part 1: General Requirements," ISO 2631-1:1985.

International Organization for Standardization (1989), "Evaluation of Human Exposure to Whole-Body Vibration – Part 2: Continuous and Shock-Induced Vibration in Buildings (1 to 80 Hz)," ISO 2631-2:1989.

Langley Research Center (1976), "Concorde Noise-Induced Building Vibrations for Sully Plantation, Chantilly, Virginia," NASA Technical Memorandum TM X-73919, June 1976.

Mayes, W.H., and Edge, P.M. (1964), "Response of Ground Buildings to Sonic Booms," American Society for Testing and Materials, Symposium on Effect of Sonic Blast on Buildings, Chicago, June 25, 1964.

Nakamura, S., and Tokita, Y. (1981), "Frequency Characteristics of Subjective Responses to Low-Frequency Sound," Proc. INTER-NOISE 81, 735-742, 1981.

Richards, E. (1983), "Vibration and Noise Relationships – Some Simple Rules for the Machinery Design Engineer," *J. Noise Control Eng.*, *20* (2) 46-60, 1983.

Schomer, P., and Neathammer, R.D. (1985), "The Role of Vibration and Rattle in Human Response to Helicopter Noise," USA-CERL Technical Report N-85/14, 1985.

Schomer, P.D., and Averbuch, A. (1989), "Indoor Human Response to Blast Sounds that Generate Rattle," *J. Acoust. Soc. Am.*, *86*, 665-673, 1989.

Siskind, D.E., *et al.* (1980), "Structure Response and Damage Produced by Airblast from Surface Mining," Bureau of Mines Report of Investigations RI 8485, 1980.

Siskind, D.E. *et al.* (1980a), "Structure Response and Damage Produced by Airblast From Surface Mining," Bureau of Mines Report of Investigations, RI 8485, 1980.

Stanford Research Institute (1967), "Sonic Boom Experiments at Edwards Air Force Base," Interim Report for National Sonic Boom Evaluation Office, NSBEO-1-67, July 1967.

Stephens, D.G., and Mayes, W.H. (1979), "Aircraft Noise-Induced Building Vibrations," ASTM Special Publication 692, 1979.

Stephens, D.G., *et al.* (1982), "Guide to the Evaluation of Human Response to Noise From Large Wind Turbines," NASA TM-83288, March 1982.

Sutherland, L.C. (Ed.) (1968), "Sonic and Vibration Environments for Ground Facilities – A Design Manual," Wyle Research Report WR 68-2, 1968.

Sutherland, L.C. (1978), "Indoor Noise Environments Due to Outside Noise Sources," *Noise Control Engineering*, *11*, 124-137, 1978.

Sutherland, L.C. (1990), "Assessment of Potential Structural Damage from Low-Altitude Subsonic Aircraft," Wyle Research Report WR 89-16(R) for Martin Marietta Energy Systems, Inc., June 1990.

Sutherland, L.C., Brown, R., and Goerner, D. (1990), "Evaluation of Potential Damage to Unconventional Structure by Sonic Booms," Wyle Research Report for Tyndall AFB, HSD-TR-90-021, June 1990.

Sutherland, L.C., Chan, G., and Andriulli, J. (1968), "Experimental Tests on the Response of Industrial and Residential Structure to Acoustic Excitation," Appendix A to Wyle Research Report WR 68-2, March 1968.

Tokita, Y., and Nakamura, S. (1981), "Frequency Weighting Characteristics for Evaluation of Low-Frequency Sounds," Proc. INTER-NOISE 81, The Netherlands, 739-742, October 1981, and Personnal Communication, Y. Tokita, Kobayasi Institute of Physical Research, 3-20-41 Higashi-motomachi, Kokubunji, 185 Tokyo, Japan.

REFERENCES (Continued)

Verillo, R.T. (1962), "Investigation of Some Parameters of the Cutaneous Threshold for Vibration," *J. Acoust.Soc. Am.*, *34*, 1768-1773, 1962.

von Gierke, H.E. (1964), "Biodynamic Response of the Human Body," *Appl. Mech. Rev.*, *17*, 951-958, December 1964.

Wiss, J.F., and Parmelee, R.A. (1974), "Human Perception of Transient Vibration," *J.Struct. Div. ASCE*, *100*(ST4) Proc. Paper 10495, 773-787, April 1974.

Young, J.R. (1975), "Measurement of the Psychological Annoyance of Simulated Explosion Sequences," Stanford Research Institute Final Report for Dept. of the Army, Construction Engineering Research Laboratory, January 1975.

OTHER REFERENCES NOT INCLUDED IN TEXT

Broner, N. (1978), "The Effects of Low-Frequency Noise on People – A Review," *J. Sound and Vib.*, *58*, 483-500, 1978.

Brown, R., and Sutherland, L.C. (1976), "Selection of an Audible Automobile Back-Up Pedestrian Warning Device – Development and Evaluation," Wyle Research Report WR 76-12, for U.S. Dept. of Transportation, July 1976.

Chaumette, A. (1972), "Effect of Sonic Booms on Buildings – Report of the Final Synthesis," Centre Scientifique et Technique du Batiment, Paris, March 1971, Royal Aircraft Establish-ment Library Translation 1633, 1972.

Crocker, M.J., and Sutherland, L.C. (1968), "Instrumentation Requirements for Measurement of Sonic Boom and Blast Waves – a Theoretical Study," *J. Sound and Vib.*, *7*, 351-370, 1968.

Kelley, N.D. (1987), "A Proposed Metric for Assessing the Potential of Community Annoyance from Wind Turbine Low-Frequency Emissions," Paper before Windpower Conference and Exposition, San Francisco, Oct. 5-8, 1987.

Langley Research Center (1978), "Noise-Induced Building Vibrations Caused by Concorde and Conventional Aircraft Operations at Dulles and Kennedy International Airports," Final Report, NASA TM-78769, 1978.

Nussbaum, D.S., and Reinis, S. (1985), "Some Individual Differences in Human Responses to Infrasound," Institute of Aerospace Studies, University of Toronto, UTIAS Report No. 282, January 1985.

Plotkin K., and Sutherland, L.C. (1987), "Sonic Boom Considerations for High-Speed Civil Transport Aircraft," Wyle Research Report WR 87-4, June 1987.

Reddin, W. (1991), Riverside County Planning Dept., Personal communication with L.C. Sutherland.

Siskind, D.E., *et al.* (1976), "Noise and Vibrations in Residential Structures from Quarry Production Blasting," Bureau of Mines Report of Investigations, RI 8168, 1976.

Siskind, D.E., *et al.* (1980b), "Structure Response and Damage Produced by Ground Vibration from Surface Mine Blasting," Bureau of Mines Report of Investigations RI 8507, 1980.

Sutherland, L.C. (1982), "Low-Frequency Response of Structures," Wyle Research Report WR 82-18, May 1982.

Sutherland, L.C., Sharp, B., and Mantey, R.A. (1983), "Preliminary Evaluation of Low-Frequency Noise and Vibration Reduction Retrofit Concepts for Wood Frame Structures," Wyle Research Report WR 83-26, June 1983.

Wiggins, J.H., Jr. (1969), *Effects of Sonic Boom,* J.H. Wiggins and Co., Palos Verdes Estates, California, 1969.

APPENDIX A

Models for Vibro-Acoustic Response of Buildings to Sonic Boom

A.1 Introduction

Vibro-acoustic response of structures to transient excitation from a sonic boom can be determined, analytically, by several methods (Sutherland, 1968). Only two methods, one well known and one new, are identified here.

A.2 Shock Response Spectrum Method

The peak response of a single-degree-of-freedom (SDOF) system to a transient excitation can be defined by a Shock Response Spectrum which is a function of the dimensionless parameter, f_oT, where f_o is the undamped natural resonance frequency, f_o, and T is the full duration of the excitation. This Shock Response is the envelope of the general solution for the response at any time t of the linear dynamic system. Consider, for example, an SDOF model of the outside wall of a building with a surface mass, m (Kg/m^2), driven by a sonic boom with a peak pressure, P_o, and duration T. The displacement response, $X(t)$, during the time the excitation is present is the <u>forced response</u> which is given by the Duhamel integral:

$$X(t) = \int_{\tau=0}^{t} h(t-\tau) \, P(\tau) \, d\tau \tag{A1}$$

where $\quad h(t) \quad = \quad$ displacement response to the excitation at time t

$\qquad\qquad = \quad (1/2\pi \, f_d \, m) \cdot \exp(-\delta \, 2\pi \, f_o \, t) \cdot \sin(2\pi \, f_d \, t)$

$\qquad f_d \quad = \quad f_o\sqrt{1-\delta^2}$, the damped resonance frequency, and

$\qquad \delta \quad = \quad 1/2Q$, the critical damping ratio, where Q is the resonance amplification factor

$\qquad P(\tau) \quad = \quad$ the excitation force (i.e., the effective sonic boom load) at time τ (e.g., equal to $P_o(1 - 2\tau/T)$ for an ideal N-wave sonic boom with a full-duration T and peak overpressure P_o).

The resulting integration indicated by Eq. (A1) is straightforward but very tedious for anything but the simplest (e.g., undamped) cases and is best evaluated by numerical integration. For

computational purposes, it is convenient to define three non-dimensional response parameters, displacement, velocity, and acceleration, as follows.

Displacement response, $X(t)$ becomes $X^*(t) = X(t) (2\pi f_0)^2 m/P_0$

Velocity Response, $V(t)$ becomes $V^*(t) = V(t) (2\pi f_0) m/P_0$

Acceleration Response, $A(t)$ becomes $A^*(t) = A(t) w/P_0$, with $A(t)$ in units of g,

and where m is the surface mass and w is the surface weight of the structure.

To determine the <u>forced</u> acceleration response, $A(t)$ from Eq. (A1), it is necessary to first solve for $X(t)$ and then compute the second derivative, numerically, to obtain $A(t)$. When the above non-dimensional forms are used, and time, t, is also expressed in non-dimensional form as the ratio, t/T, then the required second derivative is given by:

$$A(t) \cdot w/P_0 = \frac{d^2 [X(t) (2\pi f_0)^2 \cdot w/P_0]}{(2\pi f_0 T)^2 \, d [t/T]^2} \tag{A2a}$$

where the d^2 terms represent the second-order differences between sequential numerical values of the non-dimensional displacement and time variables, respectively. The velocity response is found in the same way using only the first-order differences so that, in non-dimensional form:

$$V^*(t) = \frac{d [X(t)]}{(2\pi f_0 T) \, d [t/T]} \tag{A2b}$$

Following the excitation, the residual response of the SDOF system is found from the general transient solution for free vibration of a SDOF system. The free vibration displacement response can be expressed in non-dimensional form as:

$$X^*(t/T) = \frac{e^{-\delta\mu(\beta-1)}}{\sqrt{1-\delta^2}} \left[X^*(T) \cos [\mu_d(\beta-1) - \theta] + V^*(T) \sin([\mu_d(\beta-1)]) \right] \tag{A3}$$

where μ = $(2\pi f_0 T)$ and f_0 is the undamped resonance frequency.

μ_d = $(2\pi f_d T)$ and f_d is the damped resonance frequency.

β = t/T, the non-dimensional time which is ≥ 1 for this free response period.

$X^*(T)$, $V^*(T)$ are the non-dimensional <u>forced</u> displacement and velocity responses of the system at the end of the excitation (at β = t/T = 1). These become the necessary and sufficient initial conditions for the free vibration, and

θ = $\tan^{-1} \left[\delta/\sqrt{1-\delta^2} \right]$

Again, numerical analysis can be conveniently used to compute the free vibration acceleration response using Eq (A2a) taking care to insure that an accurate value for the initial velocity, V*(T), is obtained. This was done by using a simple extrapolation method (a two-term Taylor's expansion) to extrapolate V*(T) from the last value computed for V*(t) for the forced vibration period at time T–dt to the value at time T where dt is the time interval between sequential computed values of the response.

Figure A-1a shows the result of applying this process to compute the time history of the displacement, velocity, and acceleration responses to an ideal N-wave for an undamped system with a value for f_0T of 0.875 for which the peak response is a maximum. The symbols represent the numerically computed values and the solid lines are from closed-form solutions for Eq. (A1) and (A3) for an undamped system, thus demonstrating the validity of the computational process. Figure A-1b shows the numerically computed responses for the same system but with damping corresponding to a typical Q of 10. The rapid decay in the peak responses following the first peak is very apparent. However, as has already been suggested in the main body of the text, the total energy of this decaying vibration pattern is suggested as a more realistic and meaningful measure of the total response. That is, while the peak acceleration response of damped systems can only increase by a factor of less than two for, say, a ten-fold increase in Q. However, as shown in Section A.3, the total energy of the decaying vibration will increase approximately in direct proportion to the increase in Q.

The Shock Response Spectrum, computed by the numerical analysis process described here, provides a simple way to summarize the pattern of peak responses for a range of values of the system parameter, f_0T, and for various values of damping parameter, Q.

Figure A-2 shows the Acceleration Shock Response Spectrum for excitation of a damped SDOF system with a Q of 10 by an ideal sonic boom N-wave of duration T. The plot defines the Primary (i.e., $t \leq T$) and Residual ($t \geq T$) Shock Response Spectra by the envelopes of the absolute value of their Positive and Negative peak accelerations, expressed in terms of the non-dimensional acceleration amplitude $A_{pk} \cdot w/P_0$. This response spectrum is a function of the non-dimensional product, $f_0 \cdot T$, and when this parameter is equal to approximately 0.88, the Acceleration Shock Spectrum has a maximum value of about 2.2 for undamped systems and a maximum value ranging from 1.65 to 1.95 for damped systems with Q's ranging from 5 to 20. At higher values of f_0T, the upper bound of the Shock Spectrum for the damped system decreases slowly as the dimensionless product, f_0T, increases. This decrease in the maximum envelope of the shock response spectrum is proportional to $\exp(-\delta \cdot 2\pi f_0T)$ so that it

(a) Response to Ideal N-Wave of Undamped System
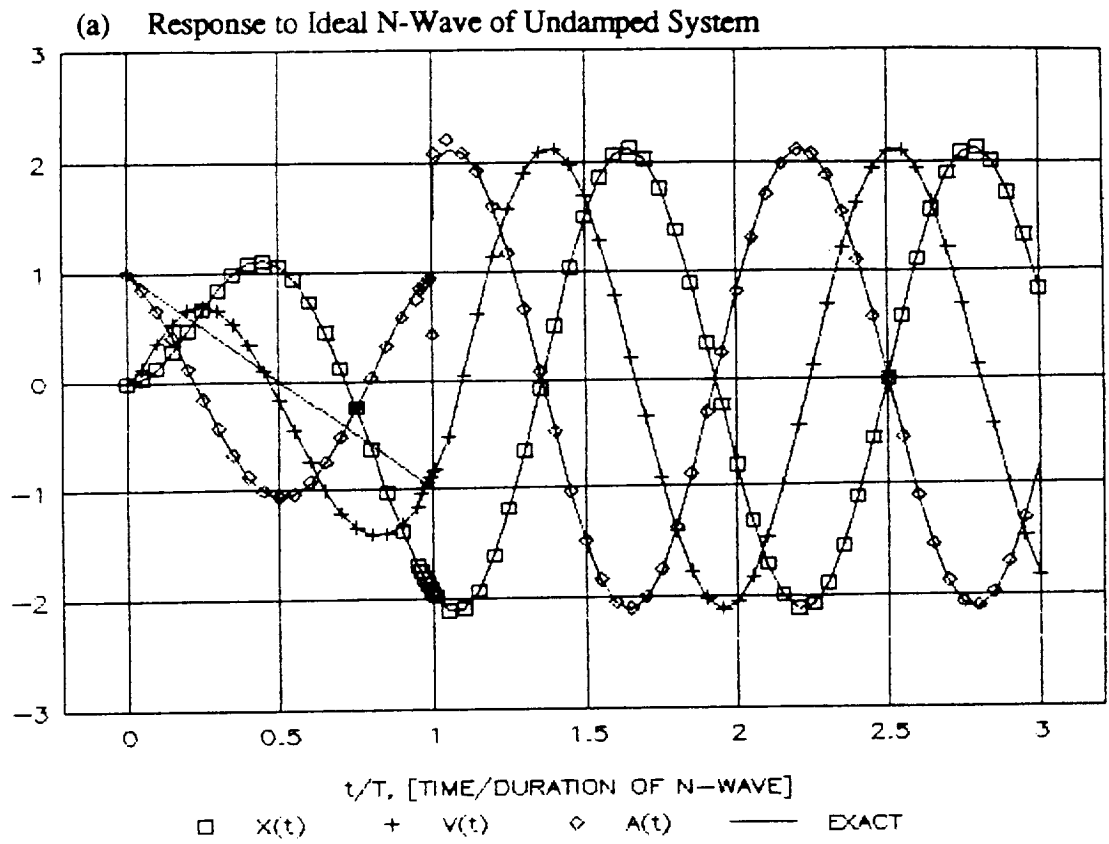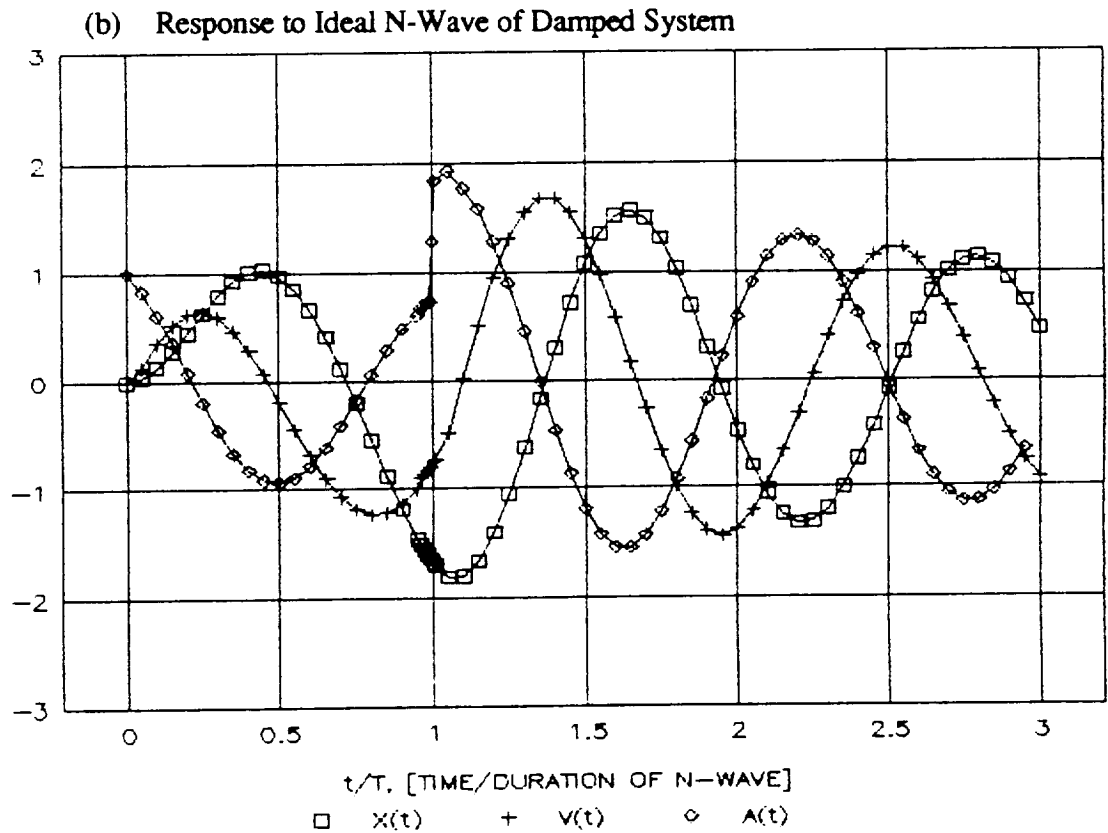
(b) Response to Ideal N-Wave of Damped System

Figure A-1.   Time History of Response of SDOF System with an Undamped Natural Frequency f_0 to Ideal N-Wave with Duration T for the Case with $f_0T = 0.875$ for (a) Undamped SDOF System, and (b) Damped SDOF System with Q = 10.
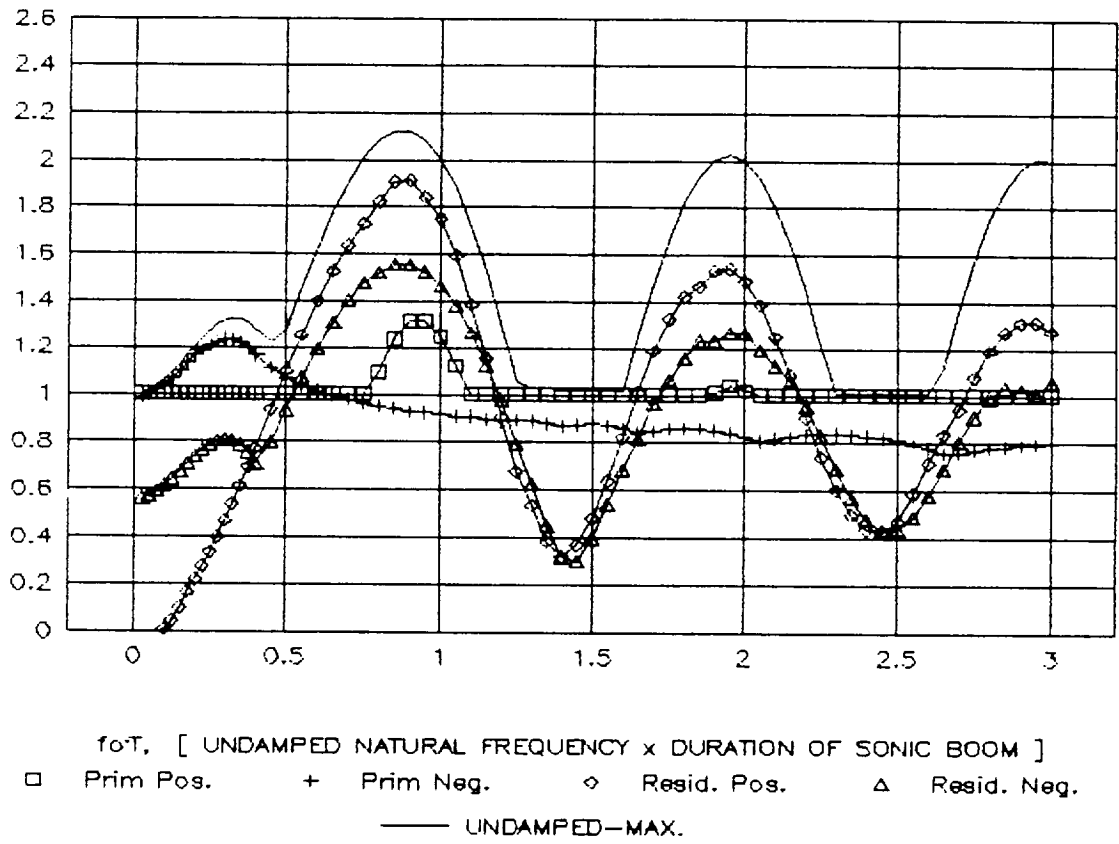
Figure A-2.   Acceleration Shock Response Spectrum for N-Wave (Damped System with Q = 10). The solid line is the maximum envelope of the Primary and Residual Shock Spectrum for an undamped system.

decreases, exponentially, as f_0T increases. Also shown in Figure A-2, for comparison, is the maximum value of the Acceleration Shock Response Spectrum for an undamped system driven by an ideal N-wave. As indicated, this has a maximum value of about 2.2 for $f_0T = 0.875$ and a maximum value of 2 for $f_0T \approx n$, where n = 2, 3, 4, etc.

This same process has been applied to the evaluation of the response time histories and Acceleration Shock Response Spectra for several other sonic boom wave forms. Figure A-3 shows the response time histories for a value of $f_0T = 0.875$ (part a) and the Acceleration Shock Response Spectrum (part b) for a reference sonic boom with a rise time of 8 ms and total duration, T of 350 ms. For convenience, the time histories and Shock Spectrum are presented in non-dimensional form in terms of a relative time scale, t/T, and the dimensionless frequency, f_0T, respectively. In all cases, the results are calculated for response of a damped SDOF system with a Q of 10.

Figure A-4 presents the same results for a symmetric delayed-ramp sonic wave form with a two-part rise/fall phase with an initial/final change in pressure by 1/2 P_0 in 8 ms and the remaining change to a full value of P_0 in an additional 35 ms for a total rise/fall time of 43 ms. Figure A-5 presents the same results for an unsymmetrical flat-top wave form with a rise time of 8 ms to a pressure of P_0 and remaining at that pressure for an additional 35 ms before decreasing to -P_0 at a time of 8 ms before the final decay to zero pressure.

In the main body of the text, the envelope of these response spectra are summarized along with two examples of the acceleration shock response spectrum, obtained in a similar manner, for diffracted sonic boom pressure loads on finite-size buildings.

Two points are very clear upon examination of these figures:

1. The time histories and acceleration shock spectra for all of the shaped sonic boom wave forms (Figures A-3 through A-5) are very similar and differ very little from the corresponding values for the response to an ideal N-wave.

2. For values of f_0T greater than 0.5, corresponding to values for f_0 greater than 1.4 Hz for T = 0.35 sec., the upper bound of the Positive Residual Shock Spectrum dominates the peak acceleration response. Almost all structures of concern for sonic boom vibration response will have resonance frequencies well above this frequency. As the parameter f_0T increases, the envelope of the maximum value of the residual Shock Response Spectrum falls off approximately as $\exp[-\pi f_0T/Q]$.

A-6

(a)   Response Time Histories

t/T. [TIME/DURATION OF N—WAVE]

□ X(t)   +   V(t)   ◇   A(t)

(b)   Acceleration Shock Response Spectrum

foT, [UNDAMPED NATURAL FREQUENCY x DURATION OF SONIC BOOM]

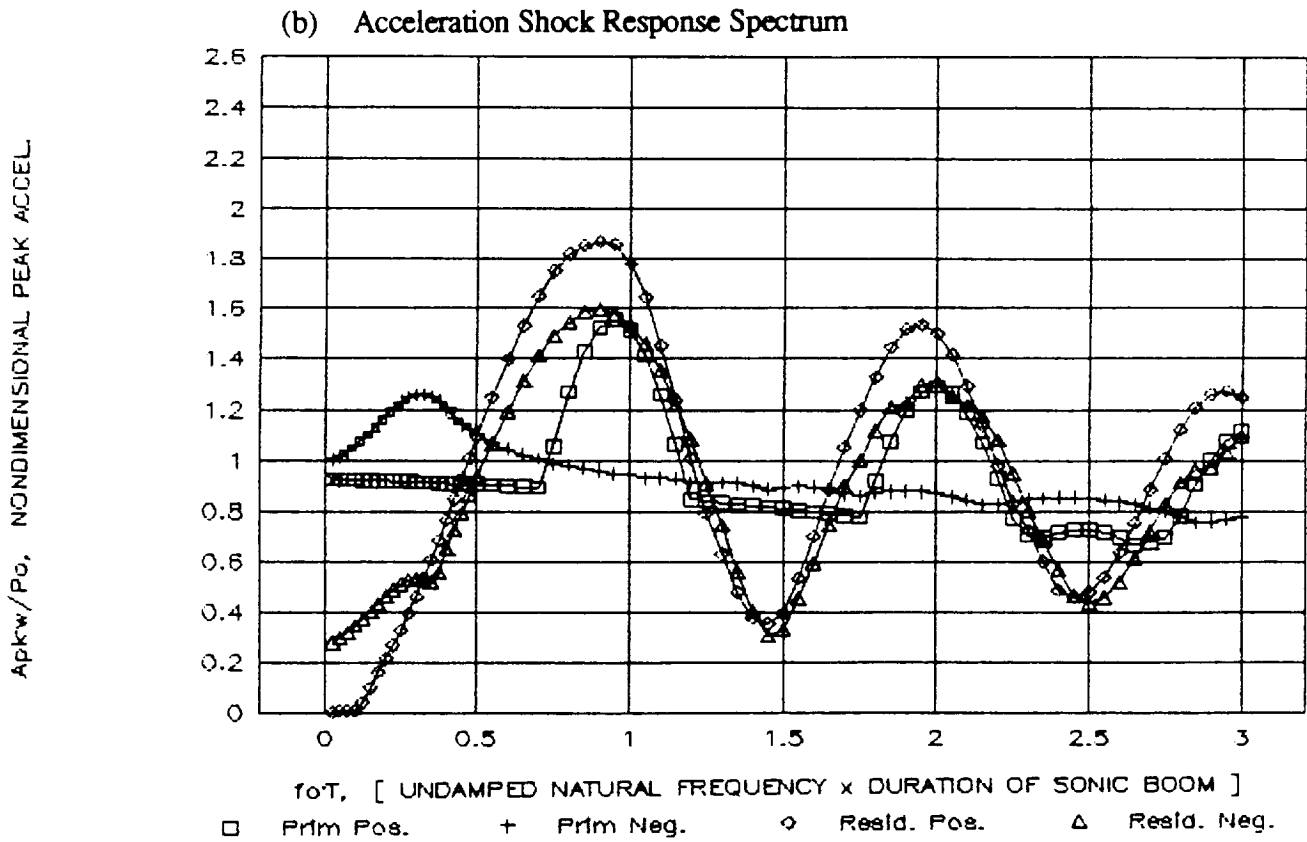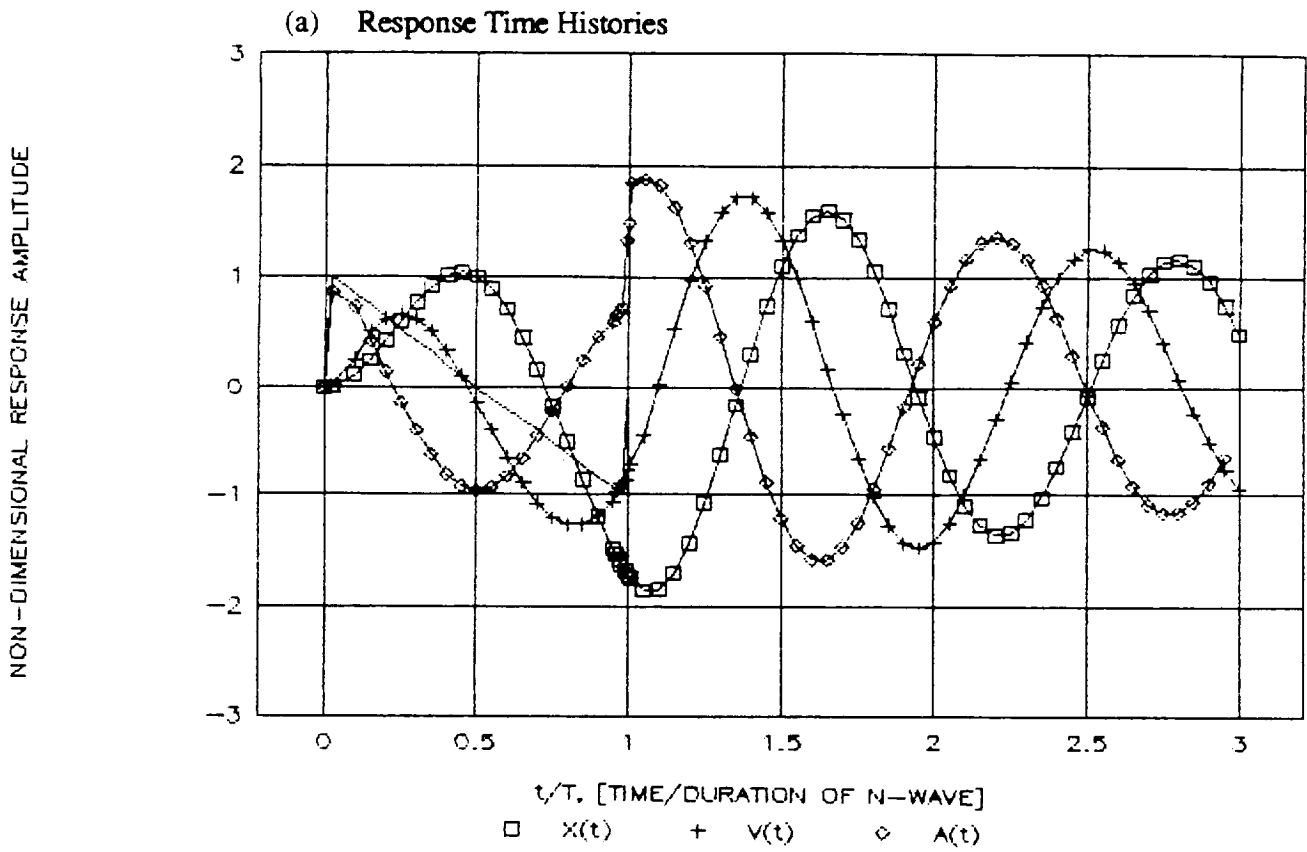□ Prim Pos.   +   Prim Neg.   ◇ Resid. Pos.   △ Resid. Neg.

Figure A-3.   Response Time Histories and Acceleration Shock Spectrum for Reference
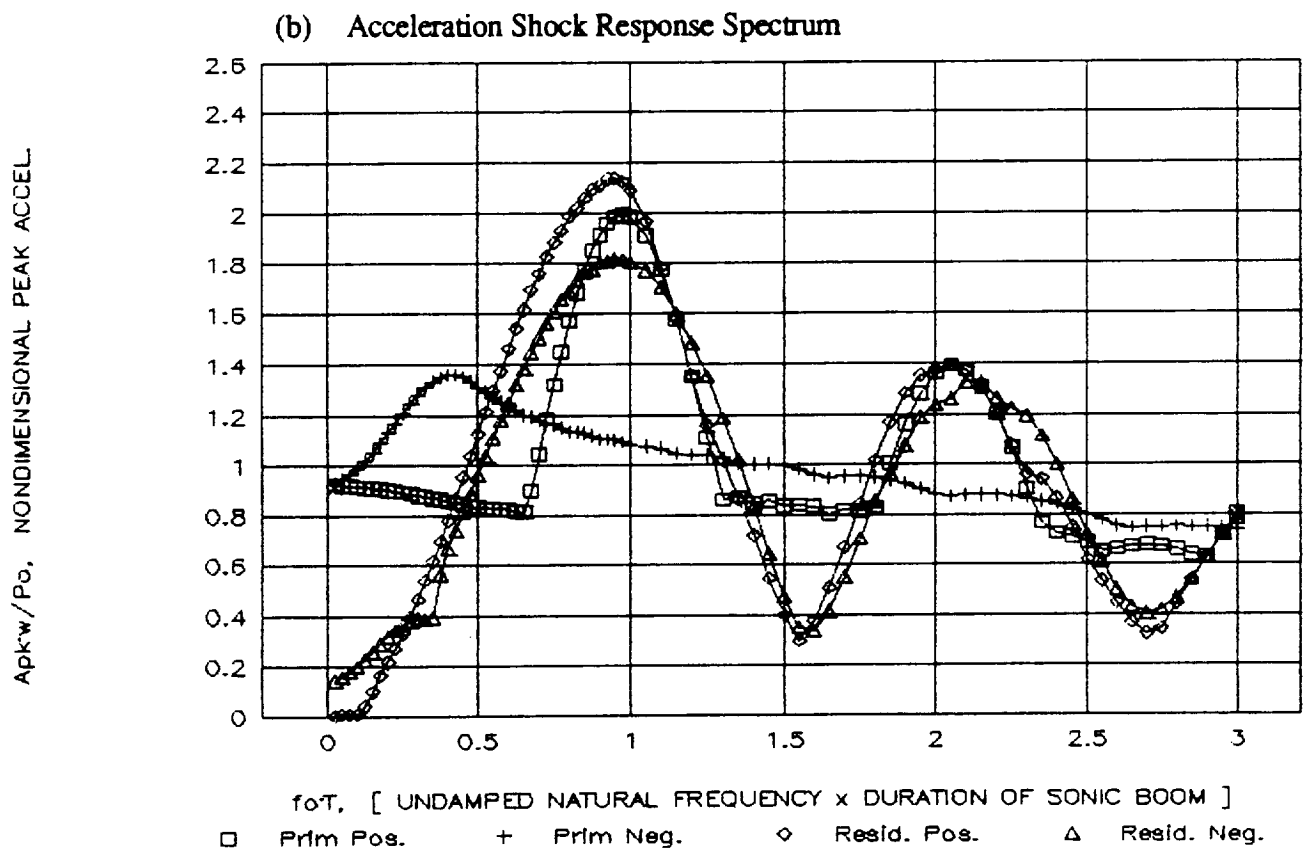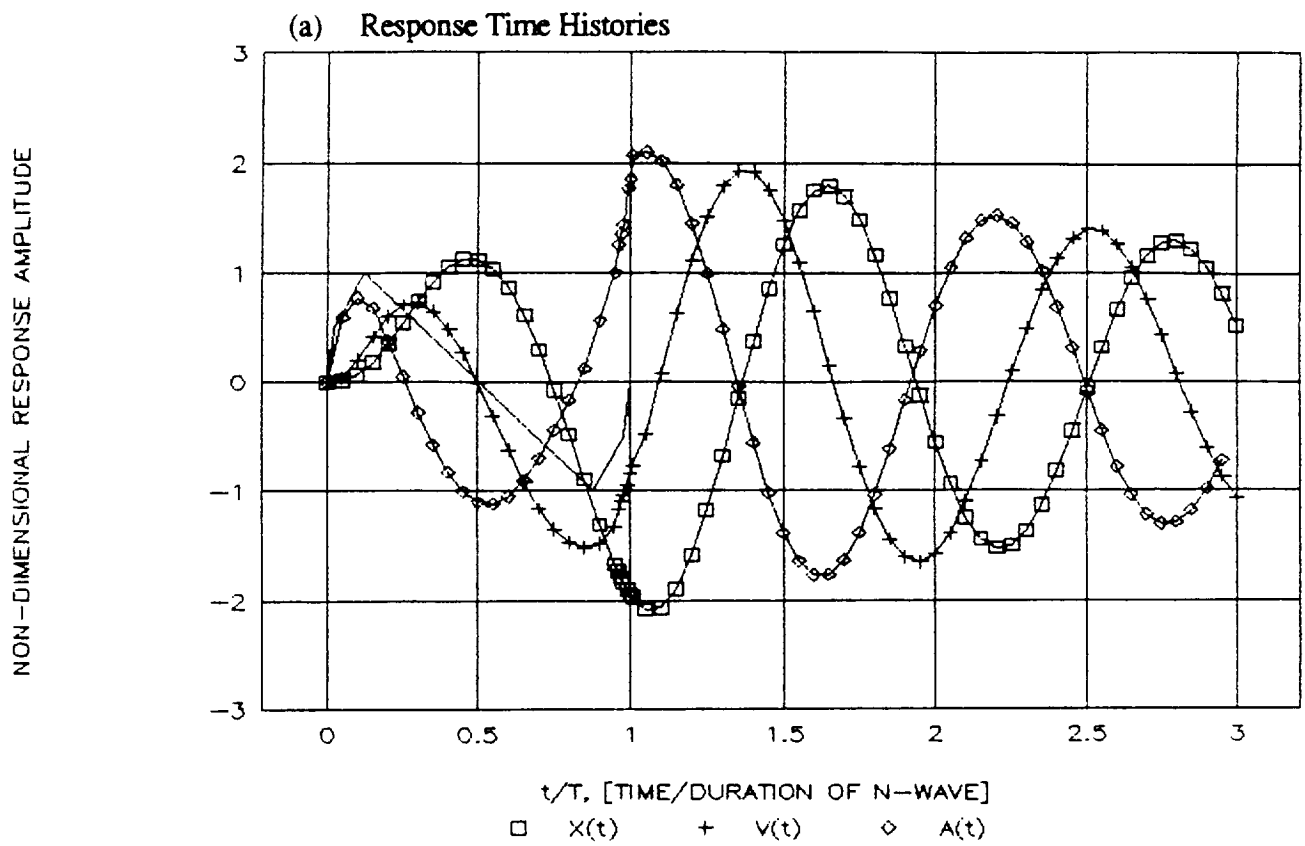Sonic Boom Waveform with Rise Time of 8 ms and Duration of 350 ms
(Q = 10)

(a) Response Time Histories

t/T, [TIME/DURATION OF N—WAVE]

□ X(t)   + V(t)   ◇ A(t)

(b) Acceleration Shock Response Spectrum

foT, [UNDAMPED NATURAL FREQUENCY x DURATION OF SONIC BOOM]

□ Prim Pos.   + Prim Neg.   ◇ Resid. Pos.   △ Resid. Neg.

Figure A-4. Response Time Histories and Acceleration Shock Response Spectra for Symmetric Delayed Ramp with 8 ms Rise Time to 1/2 P_0 and Rise, Within 35 ms to P_0– Mirror Image at End (Q = 10).
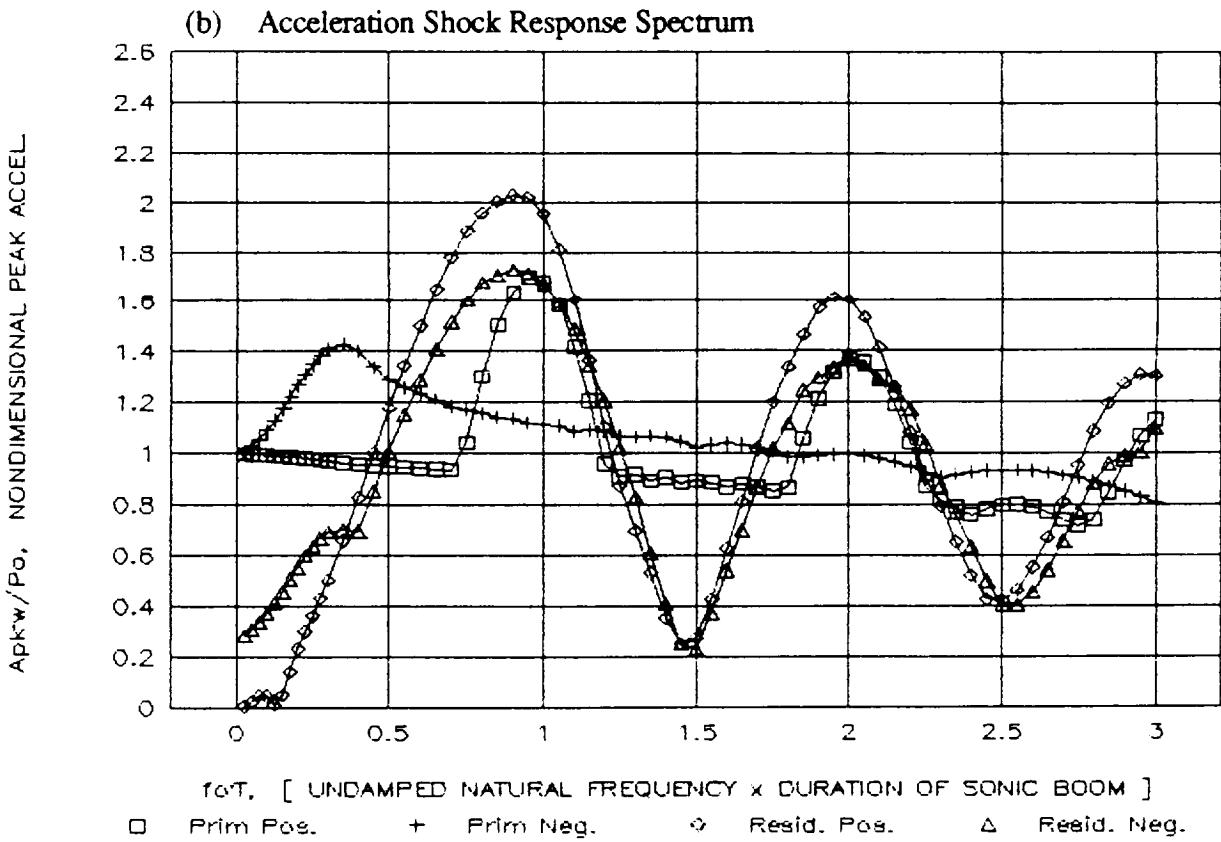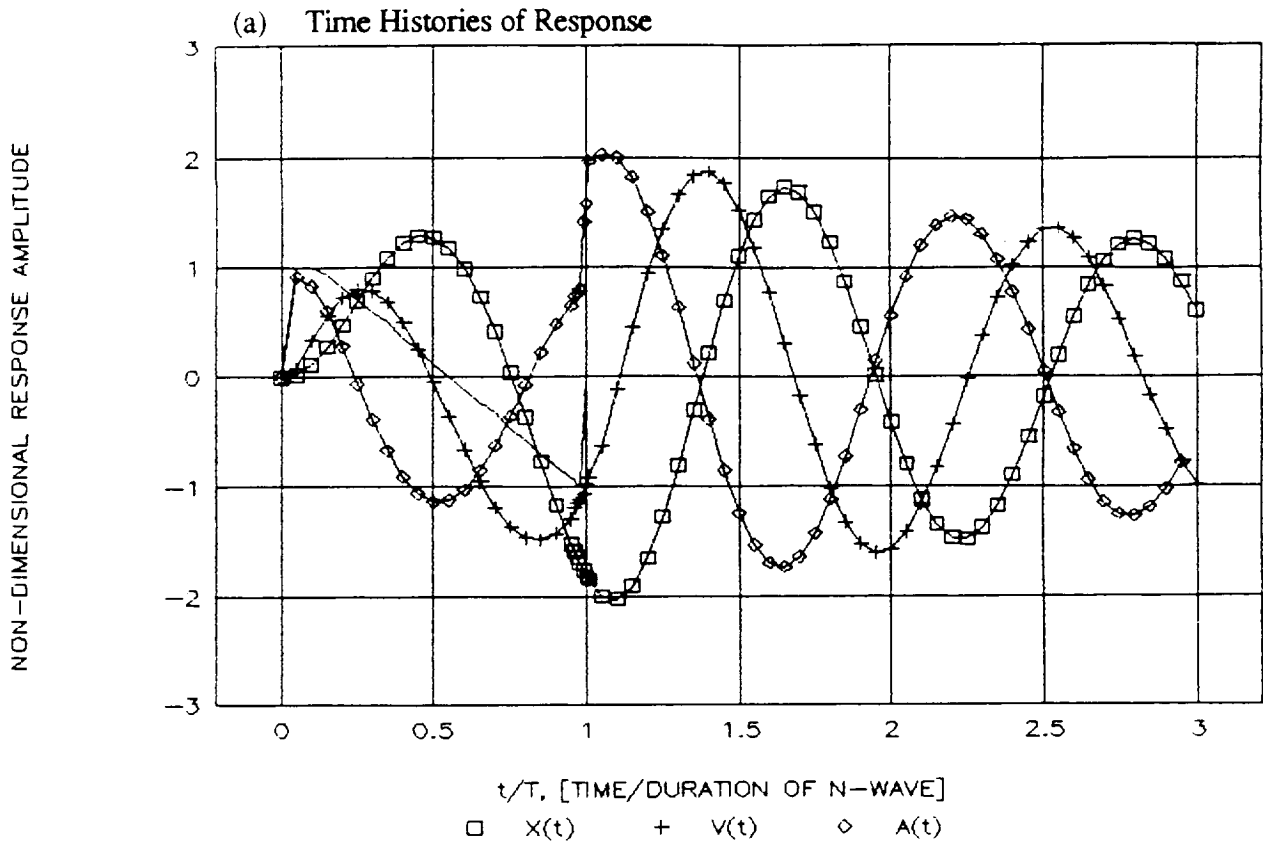
A-8

Figure A-5.   Response Time Histories and Acceleration Shock Response Spectrum for an Unsymmetric Flat Top with a Rise/Fall Time of 8 ms and an Initial Flat Top for a Period from 8 to 43 ms. (Q = 10)

For undamped systems, there is a simple way to estimate this Residual Shock Response Spectrum with the use of the Fourier Spectrum (Rubin, 1961). It can be shown that $(2\pi f_0)$ times the absolute value of the Fourier Spectrum $|P(f)|$ of the acoustic excitation, $P(t)$, divided by its peak value, P_0, is the same as the magnitude of the non-dimensional Residual Acceleration Shock Spectrum, $A_r(f_0) \cdot w/P_0$, or (Sutherland, 1968):

$$A_r(f_0) \cdot w/P_0 = (2\pi f) \cdot |P(f)|/P_0 \qquad \text{(A4a)}$$

where

$$|P(f)| = \left| \int_T^O P(t) \exp(-2\pi ft) \, dt \right| \qquad \text{(A4b)}$$

is the absolute value of the Fourier Spectrum of $P(t)$ and $A_r(f_0) \cdot w/P_0$ is the non-dimensional peak residual acceleration response equivalent to the form $A^*(t)$ used earlier except that it is valid only for the peak response of an undamped SDOF system with an undamped natural frequency of f_0. However, from a comparison of the Residual Shock Spectrum in Figure A-2 for the damped and undamped system, it is apparent that an **ENVELOPE** of the latter is a reasonable but conservative approximation to the peak response of the damped system if one can accept a degree of conservatism (or uncertainty) in the peak acceleration response of as much as 100 percent.

While this may seem excessive, this simplified analysis has not considered the effects of modal response or diffraction. The former modal response effect can cause an **increase** in peak modal response of a real structure, beyond that estimated by a simple SDOF model, by a factor of about 2 (Sutherland, Brown, and Goerner, 1990). The diffraction effect, on the other hand, is shown in the main body of the text of this report to cause a **decrease** in peak acceleration response by as much as about 100 percent. Thus it is not unreasonable to use the simple expression given by Eq. (A4) as one way to estimate the approximate peak response of a structure to alternate sonic boom wave forms.

Consider, now, other ways to apply the Fourier Spectrum of a sonic boom wave form to assess the potential structural response in more detail. *The following analysis is carried out for response to only an ideal sonic boom, partly for the sake of simplicity, but also due to the fact that, as shown already, the difference in peak structural response at typical (low) resonance frequencies of interest is not vastly different from that expected for shaped sonic booms. However, the analysis methods presented are readily applicable to any desired wave shape.*

A.3 Fourier Spectrum of Acceleration Response, Acceleration Exposure Level, and Equivalent Peak Acceleration

The Fourier Spectrum A(f) of the acceleration response time history, A(t), can be expressed, correctly, as the complex product of the Fourier Spectrum of the effective Pressure excitation, P(f), and an analytically or experimentally determined, complex Frequency Response Function, R(f), which specifies the response of the structure to a sinusoidal excitation. Using steady-state acoustic response data for a structure, we can also express the absolute value of A(f), empirically, by:

$$|A(f)| = |P(f)| \cdot M_{SA}(f)/w \qquad (A5)$$

where $|P(f)|$ is the absolute value, of the Fourier Spectrum of the pressure excitation,

   $M_{SA}(f)$ is an experimentally determined vibro-acoustic structural response function, called the Specific Acoustic Mobility, and

   w is the surface weight of the structure (in the same units as the acoustic pressure).

Consider, now, these two different ways to utilize the Fourier Spectrum, P(f), of the excitation. The end objective, in both cases, will be to define two quantities;: (1) the Acceleration Exposure Level of the response – a measure of its total vibration energy, and (2) an equivalent peak acceleration of a damped sinusoidal acceleration signal with the same energy as the actual acceleration response signal. The "energy" measure is consistent with the concept suggested in Section 2 of this report that vibration energy or Acceleration Exposure may be a more powerful descriptor for comparison of a sonic-boom-induced vibration environment with human response criteria. The second "equivalent peak" acceleration could also be used for a simpler comparison with existing criteria for both human response and for the onset of rattle.

Acceleration Exposure for a, SDOF System Response to a Sonic Boom

For purposes of this analysis, let the sonic boom be assumed to be an ideal N-wave with a peak pressure, P_0, a duration, T, and a pressure time history, $P(t) = P_0(1-2t/T)$. Inserting this into Eq. (A4a), it can be shown that $|P(f)|$ is given by:

$$|P(f)| = \left[\frac{P_oT}{(\omega T)^2} \right] \cdot \left\{ [2(1-\cos\omega T) - \omega T\sin\omega T]^2 + [2\sin\omega T - \omega T(1+\cos\omega T)]^2 \right\}^{1/2} \quad (A6)$$

where $\omega = 2\pi f$, the angular frequency, in radians per sec.

The absolute value of the Frequency Response Function, R(f), for an SDOF system driven by a such an excitation can be expressed, in non-dimensional form, as:

$$|R(f)| = \left| \frac{A(f) \cdot w}{P(f)} \right| = |(f/f_o)| \cdot \left\{ [1-(f/f_o)^2]^2 + [f/f_oQ]^2 \right\}^{-1/2} \quad (A7)$$

Note that the Frequency Response Function, R(f), is the same non-dimensional Specific Acoustic Mobility defined by Eq. (A5). Thus, combining Eq.(A6) and (A7) with (A5), and taking advantage of the fact that the absolute value of the ratio of two complex quantities is the same as the ratio of their absolute values, it can be shown that the absolute value of the Fourier Spectrum, $|A(f)|$ of the acceleration response is given by:

$$|A(f)| = |P(f)/w| \cdot \left| \frac{A(f) \cdot w}{P(f)} \right| \quad , \quad \text{or} \quad (A8a)$$

$$|A(f)| = [P_o \cdot T/(2\pi f_o T)^2 w)] \cdot [(a^2+b^2)/(c^2+d^2)]^{1/2} \quad (A8b)$$

where a and b are the two (real and imaginary) parts of $|P(f)|$ inside the brackets on the right side of Eq. (A6) and c and d are the corresponding parts in the denominator of $|R(f)|$ in Eq. (A7).

Consider, now, how this absolute value of the Fourier Spectrum of the acceleration can be used to define: (1) an Acceleration Exposure (or Exposure Level, when expressed in decibels), and (2) a quantity that will be called an Equivalent (equal energy) Peak Acceleration, $A(eq)_{pk}$. A more complete development of the former relationship has been given elsewhere for the Sound Exposure Level of a sonic boom signal (Sutherland, 1991).

The total "energy" of a transient acceleration signal is defined as the Acceleration Exposure with an abbreviation AE, a letter symbol E_A, and units of $g^2 \cdot sec$. It is the integral, over the duration T of the event, of the square of the acceleration A(t) time history or,

$$E_A = \int_O^T A^2(t)\, dt \quad (A9)$$

However, from Parseval's theorem, this Acceleration Exposure, AE, can also be expressed by the integral, over <u>frequency</u> of the square of the absolute value of the Fourier Spectrum. Taking advantage of the even symmetry of this spectrum, this can be given as:

$$E_A = 2 \int_O^\infty |A(f)|^2 \, df = \int_O^\infty E_A(f) \, df \qquad (A10)$$

where $E_A(f)$ = the Acceleration Exposure Spectral Density, with units $(g)^2 \cdot sec/Hz$ and equal to $2 \cdot |A(f)|^2$

and $|A(f)|$ is given by Eq. (A8).

When expressed in decibels, the Acceleration Exposure Spectral Density is called the Acceleration Exposure Spectrum Level with an abbreviation AESL, letter symbol $L_{AE}(f)$ and units, decibels. It is defined as:

$$L_{AE}(f) = 10 \cdot Lg \, [E_A(f)/E_{Ao}(f)], \quad dB \qquad (A11)$$

where $E_{Ao}(f)$ is the reference Acceleration Exposure Spectral Density equal to $A_o^2 \cdot t_o/\Delta f$ where $A_o = 1 \, \mu g$, $t_o = 1$ sec., and $\Delta f = 1$ Hz or $E_{Ao}(f) = [1\mu g]^2 \cdot sec/Hz$. Figure A-6 presents two examples of such Acceleration Exposure Spectrum Levels for the response of an SDOF model of a structure with an effective surface weight of 5 psf, to an ideal sonic boom N-wave with peak (ground reflected) pressure of 1 psf. The two cases shown are for a SDOF system with a Q of 10 and values for f_o of 10 Hz and 20 Hz.

The corresponding overall Acceleration Exposure Level, with an abbreviation AEL and letter symbol L_{AE}, is the value of AE, expressed in decibels re: $(1\mu g)^2 \cdot s$ by

$$L_{AE} = 10 \cdot Lg \, [E_A/E_{Ao}], \quad dB \qquad (A12)$$

where $E_{Ao}(f)$ is a reference AEL equal to $[1\mu g]^2 \cdot sec.$

<u>Equivalent Peak Acceleration</u>

The concept of an Equivalent Peak Acceleration is derived from the peak acceleration of a damped SDOF system with a natural (undamped) resonance frequency of f_o, to an impulse excitation of vanishingly small duration. The acceleration response, A(t), of such a system can be defined by:

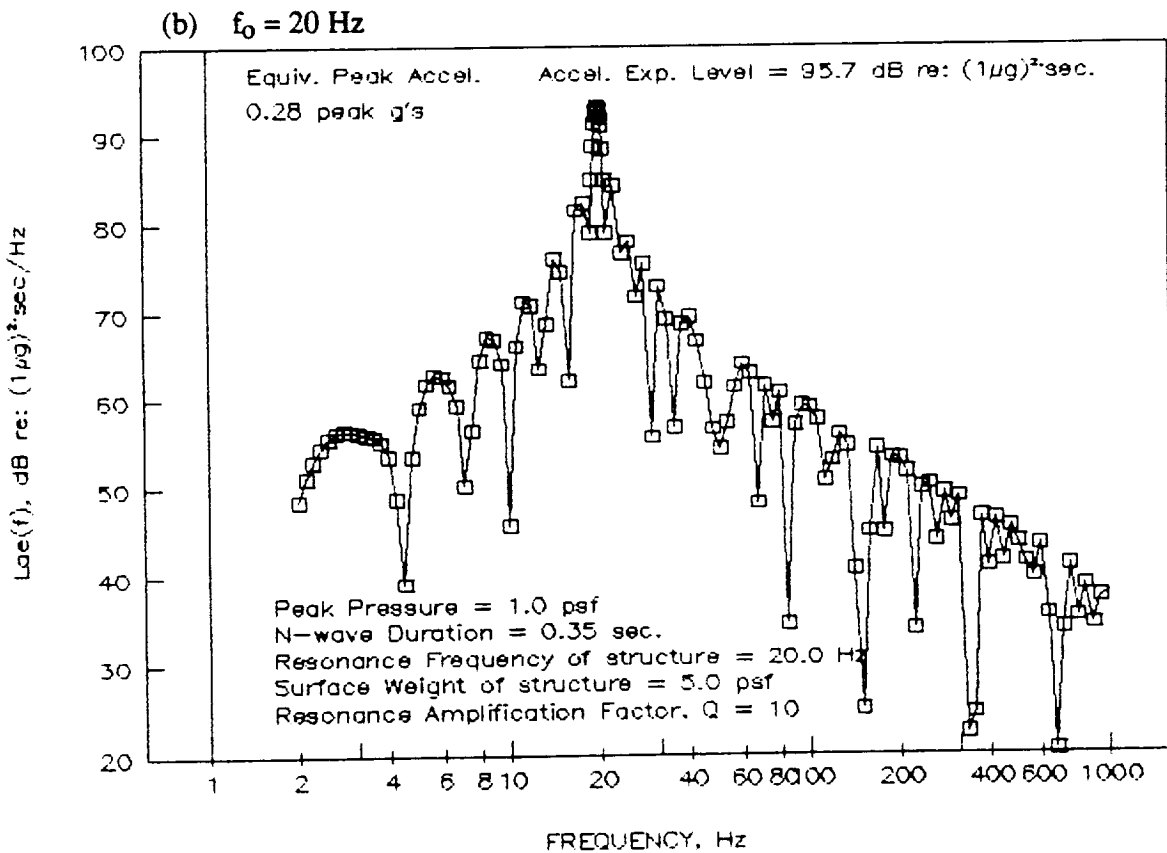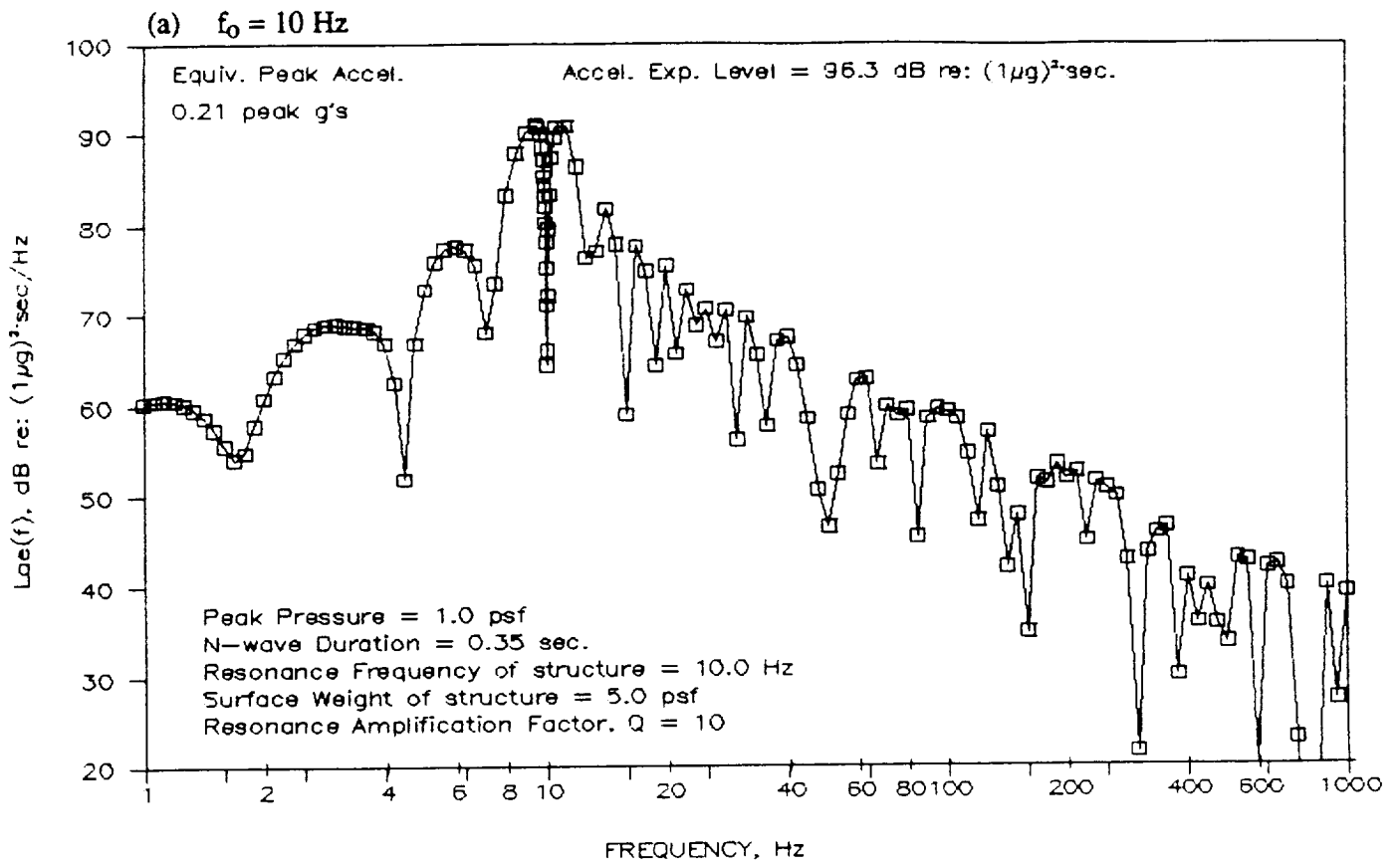$$A(t) = A_o \cdot e^{(-2\pi\delta f_o t)} \, \sin(2\pi f_d t) \qquad (A13)$$

Figure A-6. Acceleration Exposure Spectrum Level for Response of SDOF System with Q = 10 and Resonance Frequencies of (a) 10 Hz, and (b) 20 Hz, to Ideal N-Wave with Peak Pressure of 1 psf.

where δ = 1/2Q, the critical damping constant

f_d = the damped resonance frequency = $f_0 \cdot \sqrt{1-\delta^2}$

and A_o = the acceleration amplitude of this damped sinusoidal response as illustrated in the sketch below.
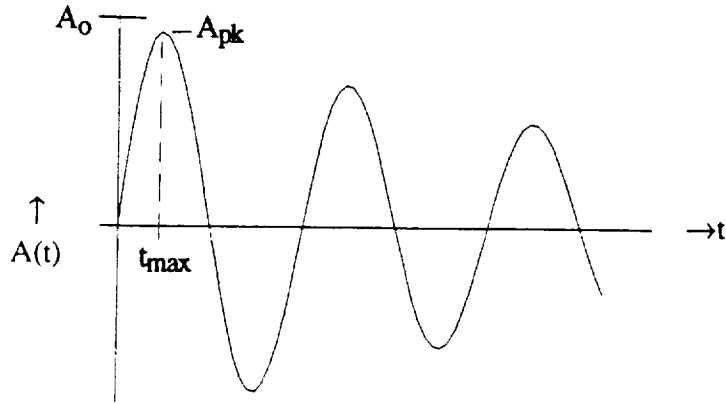
Decaying Sinusoidal Acceleration and Equivalent Peak Acceleration, A_{pk}

The actual initial peak acceleration, A_{pk} of this damped sinusoid is less than the acceleration amplitude, A_o due to the effect of damping between time 0 and the time of the first peak. Differentiating Eq. (A13), it can be shown that the time, t_{max} when this first peak occurs is given by:

$$t_{max} = [\ 1/(2\pi f_d)\ ]\ tan^{-1}\ [\sqrt{1-\delta^2}/\ \delta] \tag{A14}$$

and the corresponding value of the actual first peak acceleration, A_{pk} is given, to a close approximation, by:

$$A_{pk} \simeq A_o\ e^{-\pi/4Q} \tag{A15}$$

Applying Eq. (A9), it can be shown that the Acceleration Exposure, AE, of this damped acceleration signal (not unlike many of the actual responses to sonic booms), is given by:

$$E_A \simeq [\ A_o^2/(4\pi f_o)]\cdot[\ Q-1/4Q] \tag{A16}$$

A-15

Note that for a given acceleration amplitude, A_o, the Acceleration Exposure is inversely proportional to the undamped resonance frequency, f_o and directly proportional to the Resonance Amplification Factor, Q.

Thus, given the Acceleration Exposure, AE, for any other transient structural response, such as from a sonic boom, an Equivalent Peak Acceleration, $A(eq)_{pk}$, can be defined as the value of the initial peak acceleration, A_{pk} response of an SDOF system to an impulse for which the Acceleration Exposure, AE, is the same as for the actual acceleration signal. Thus, from Eq. (A15) and (A16), to a close approximation, this Equivalent Peak Acceleration, $A(eq)_{pk}$ can be shown to be equal to:

$$A(eq)_{pk} \simeq [4\pi f_o \cdot E_A \cdot e^{-\pi/2Q}]^{1/2} \cdot [Q - 1/4Q]^{-1/2} \qquad (A17)$$

Clearly, this expression could be applied to define the Equivalent Peak Acceleration for any transient acceleration response, A(t), in terms of the Acceleration Exposure, E_A, which can be determined by the integral, over frequency, of the absolute value of its Fourier Spectrum, $|A(f)|$ as defined by Eq. (A10).

Equivalent Peak Acceleration for Response of SDOF System to Sonic Boom

As a simple example of this concept, consider the case defined by Eq. (A8b) for the response to an ideal N-wave. By numerical integration of $|A(f)|^2$ according to Eq. (A10), and applying Eq. (A12), values for the Acceleration Exposure Level, AEL, were obtained for an SDOF system with a Q of 10 and effective surface weight of 5 psf for varying values for the undamped natural resonance frequency, f_o, when driven by an N-wave with a duration, T. The result is shown in Figure A-7 for an N-wave sonic boom with a peak pressure, P_o of 1 psf. The abscissa is the same non-dimensional product of frequency times duration of the sonic boom as used before.

From the corresponding values of the Acceleration Exposure, E_A, by applying Eq. (A17), the resulting values for the Equivalent Peak Acceleration, $A(eq)_{pk}$, could also be obtained for this case, again as a function of the product, f_oT. This result is compared in Figure A-8 with the envelope of the peak acceleration response that is predicted from the envelope of the Primary and Residual Shock Response Spectrum for the same case. (For convenience, the acceleration amplitude has been converted back to the non-dimensional form equal to $A_{pk} \cdot w/P_o$. With one exception, the two models predict approximately the same trend in peak response as a function of f_oT. The exception, significant in practical cases only for very low resonance frequencies, is the curve for the Equivalent Peak Acceleration, $A(eq)_{pk}$, shows
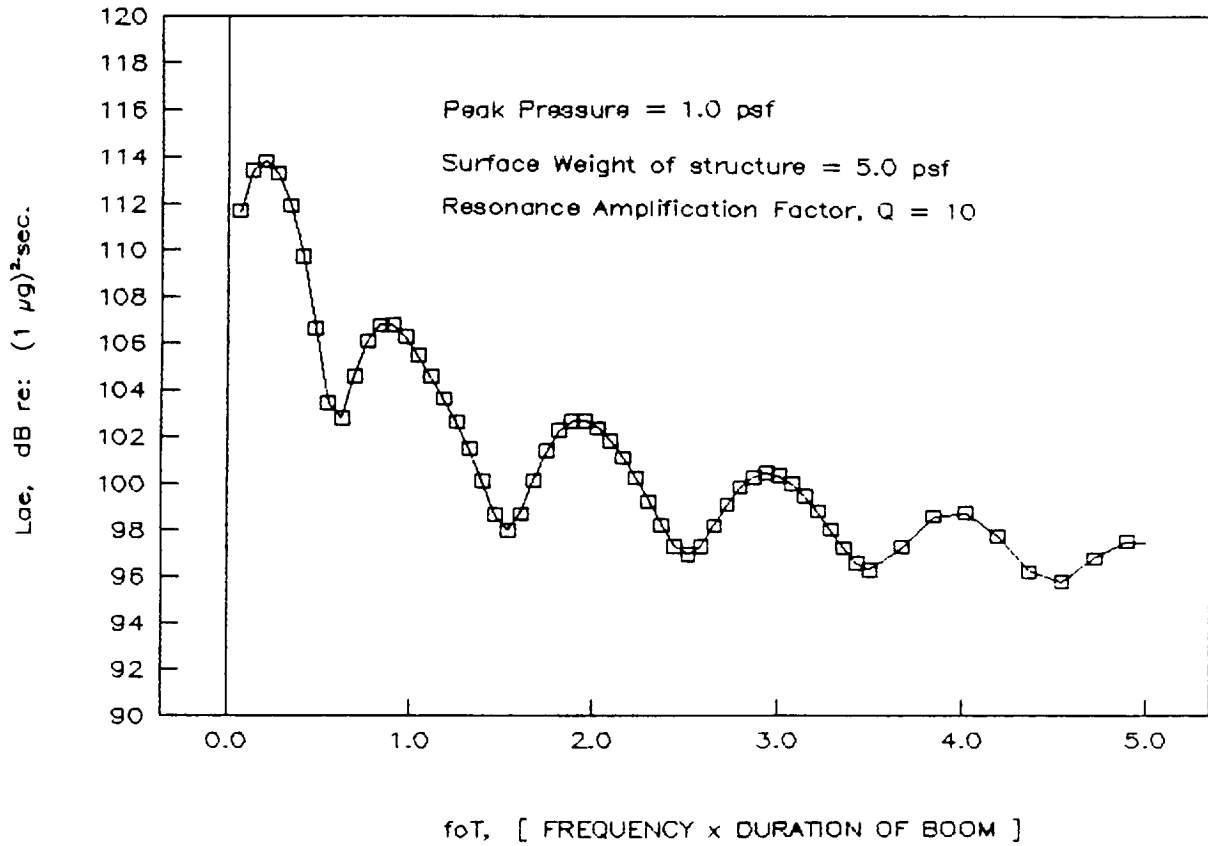
Figure A-7. Acceleration Exposure Level as a Function of F_0T for Response of Damped SDOF System with Q = 10, Surface Weight of 5 psf, to an Ideal N-Wave with a Peak Pressure of 1 psf.
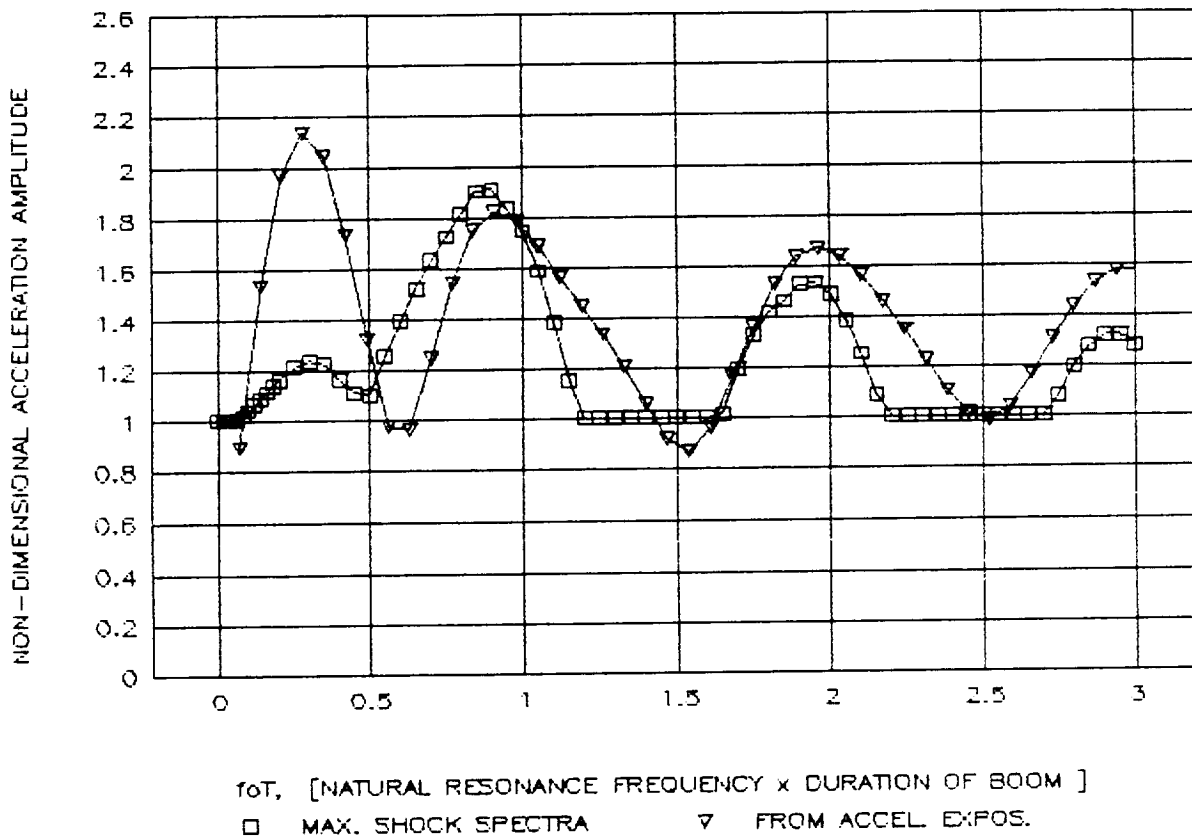
Figure A-8.   Comparison of Values for the Peak Acceleration Response of a SDOF System
to an N-Wave Predicted by the Envelope of the Shock Response Spectrum and
the Equivalent Peak Acceleration from the Acceleration Exposure.

a new maximum value for f_oT equal to about 0.3. This can be explained by a closer examination of the relationship between $A(eq)_{pk}$ and the parameters, f_oT and Q.

Examination of Eq. (A8b), (A10), and (A17) shows that $A(eq)_{pk}$ will be inversely proportional to the product $(f_oT{\cdot}Q)$. It was shown in Figure A-2 that the Primary Negative Shock Spectrum has an interim maximum value of about 1.2 for f_oT equal to about 0.3. Thus, while the actual peak acceleration is higher for f_oT of about 0.88, the Equivalent Peak Acceleration is actually greater at the lower value of f_oT since the lower frequency damped acceleration response will actually have a greater <u>Acceleration Exposure</u> than the response at f_oT of 0.88 and hence will have a greater $A(eq)_{pk}$.

The concepts developed in this appendix are applied in the main body of the report for a more detailed evaluation of structural response to a sonic boom. This includes the application of experimental data on vibro-acoustic response of structure to steady-state sound to define, empirically, absolute values for the dimensionless frequency response function, $|A(f){\cdot}w \,/\, P(f)|$ and hence be able to predict the peak transient response to sonic booms with the use of Eq. (A8a).

APPENDIX B

Evaluation of Edwards AFB Sonic Boom
Structural Response Test Data

During the Phase I sonic boom tests at Edwards AFB (Stanford, 1967, and Blum,e 1967), 22 accelerometers were mounted in in various locations in two houses (E-1, one-story, and E-2, two-story). For the 94 B-58 missions and 35 F-104 missions, peak amplitudes of acceleration for nearly every mission were tabulated along with other mission parameters and data from various types of vibration and acoustic pressure transducers. Some time histories of acceleration were also reported. This appendix is a summary of the B-58 and F-104 acceleration time history and acceleration data from these tests in support of this report. XB-70 data (but not time histories) was omitted from analysis since acceleration data from only three XB-70 missions were available.

Figures B-1 through B-3 are time histories of acceleration. They show the effect of different aircraft signatures on the acceleration response of various elements of the houses. Figure B-1 shows the responses of the dining room east wall of House E-2. Figure B-2 shows the racking response of the northeast corner of House E-1. Figure B-3 shows the response of the bedroom east wall of House E-1.

Figures B-4 and B-5 show the responses of the various elements of Houses E-1 and E-2, respectively, due to two B-58 sonic booms.

Figure B-6 shows the small change in acceleration response of the east bedroom wall of House E-1 for various B-58 missions.

Table B-1 is a summary of the linear regression analyses on the B-58 and F-104 peak acceleration versus peak pressure data. The data in the table are grouped by structural element. Also in the table are the resonance frequencies of some of the elements as derived from the time histories of Figures B-1 through B-6. From the architectural drawings of the Houses (Blume, 1967, and Stanford, 1967), estimates of surface weight were computed and presented in Table B-1.

Linear regression analyses with the y-intercept points forced to zero were applied to all the channels of data. These analyses yielded computed slopes for all the data channels. In order to determine if a statistical significance or similarity exists between the computed slopes, the "t" test (Freund, 1971) was applied.

It was determined, with a 95 percent level of confidence, that only three of the 22 channels of B-58 and F-104 data were statistically similar. Figures B-7 through B-9 are plots of acceleration amplitude versus outdoor average overpressure for those three channels of data with an accompanying linear regression line. Note that Figures B-7 and B-8 were both racking responses in the east–west direction and were the uppermost roof line of both houses. The House E-2 dining room wall response to sonic booms of both aircraft was also statistically similar as seen in Figure B-9.

Figure B-10 through B-15 are also plots of acceleration amplitude versus outdoor average peak overpressure but represent the other structural elements, such as floors and ceilings, whose data sets for each aircraft were statistically *different*. The accompanying linear regression lines with y-intercept points forced to zero are also shown in the figures.

Table B-1

Summary of Acceleration Amplitude Data from Edwards AFB Sonic Boom Test (data from Blume, 1967 and Stanford, 1967)

House	Data Channel	Element	Room	Aircraft	R^2	Slope (g/psf)	Standard Error of the Slope	Misn	Approx. f0 (Hz)	Boom Dur. (T,sec)	f0 x T	Surface Area (ft^2)	Approx. Surface Weight (lb/ft^2)
E-1	101	Floor	Living Rm	B58	-0.031	0.069	0.002	18B	20.7	0.196	4.06	198	5
E-1	103	Floor	Bedroom #1	B58	0.374	0.052	0.001	18B	18.3	0.196	3.58	140	5
E-1	102	Floor	Family Rm	B58	0.528	0.043	0.001	18B	20.2	0.196	3.97	268	5
E-1	102	Floor	Family Rm	F104	0.657	0.062	0.002						
E-1	101	Floor	Living Rm	F104	0.431	0.090	0.004						
E-1	103	Floor	Bedroom #1	F104	0.737	0.058	0.002						
E-2	301	Floor	Dining Rm	B58	0.125	0.048	0.001						
E-2	303	Floor	Bedroom #1	B58	0.350	0.041	0.001	80RB	23.7	0.16	3.79	146	5
E-2	301	Floor	Dining Rm	F104	0.640	0.049	0.002						
E-2	303	Floor	Bedroom #1	F104	-0.234	0.060	0.006						
				Average =	0.358	0.057	0.002				3.85		
				Std Dev.=	0.301	0.015	0.001				0.18		
E-1	107	Patio	Outside, concrete	B58	0.316	0.012	0.001						
E-1	107	Patio	Outside, concrete	F104	0.269	0.014	0.001						
				Average =	0.293	0.013	0.001						
				Std Dev.=	0.024	0.001	0.000						
E-1	105	Roof Line	E. Wall, NE corner	B58	0.363	0.044	0.002	15-2	14.7	0.17	2.50		
E-1	106	Roof Line	N. Wall, NE corner	B58	0.320	0.053	0.002						
E-1	106	Roof Line	N. Wall, NE corner	F104	0.358	0.053	0.003						
E-1	105	Roof Line	E. Wall, NE corner	F104	0.466	0.048	0.003	15-3	12.8	0.08	1.02		
				Average =	0.377	0.049	0.003				1.76		
				Std Dev.=	0.054	0.004	0.000				0.74		
E-2	302	Under Counter Edge	Kitchen	B58	-0.006	0.053	0.006						
E-2	302	Under Counter Edge	Kitchen	F104	0.650	0.048	0.002						
				Average =	0.322	0.050	0.004						
				Std Dev.=	0.328	0.003	0.002						

Regression Analysis (y-intercept = 0)

Table B-1 (Continued)

### Summary of Acceleration Amplitude Data from Edwards AFB Sonic Boom Test (data from Blume, 1967 and Stanford, 1967)

House	Data Channel	Element	Room	Aircraft	Regression Analysis (y-intercept = 0) R^2	Slope (g/psf)	Standard Error of the Slope	Misn	Approx. f0 (Hz)	Boom Dur. (T,sec)	f0 x T	Surface Area (ft^2)	Approx. Surface Weight (lb/ft^2)
E-2	308	2nd Floor Line	E. Wall, NE corner	B58	0.269	0.065	0.003						
E-2	307	2nd Floor Line	N. Wall, NE corner	B58	0.057	0.060	0.004						
E-2	308	2nd Floor Line	E. Wall, NE corner	F104	0.307	0.070	0.005						
E-2	307	2nd Floor Line	N. Wall, NE corner	F104	0.166	0.072	0.008						
				Average =	0.200	0.067	0.005						
				Std Dev.=	0.097	0.005	0.002						
E-2	306	2nd Roof Line	E. Wall, NE corner	B58	0.031	0.080	0.013						
E-2	305	2nd Roof Line	N. Wall, NE corner	B58	0.102	0.049	0.002						
E-2	305	2nd Roof Line	N. Wall, NE corner	F104	0.364	0.049	0.003						
E-2	306	2nd Roof Line	E. Wall, NE corner	F104	-0.072	0.069	0.008						
				Average =	0.358	0.057	0.002						
				Std Dev.=	0.301	0.014	0.001						
E-1	109	Ceiling	Family Rm	B58	0.245	0.099	0.005						
E-1	110	Ceiling	Bedroom #1	B58	0.181	0.139	0.010						
E-1	109	Ceiling	Family Rm	F104	0.345	0.180	0.010						
E-1	110	Ceiling	Bedroom #1	F104	0.219	0.246	0.021						
				Average =	0.248	0.166	0.011						
				Std Dev.=	0.061	0.054	0.006						
E-2	310	Ceil. Joist	Bedroom #2 Attic	B58	0.578	0.109	0.003	80RB	37.8	0.16	6.04	146	2.8
E-2	309	Ceil. Joist	Bedroom #1 Attic	B58	0.246	0.082	0.005						
E-2	309	Ceil. Joist	Bedroom #1 Attic	F104	0.334	0.104	0.006						
E-2	310	Ceil. Joist	Bedroom #2 Attic	F104	0.446	0.143	0.007						
				Average =	0.401	0.110	0.005						
				Std Dev.=	0.124	0.022	0.002						

Table B-1 (Continued)

Summary of Acceleration Amplitude Data from Edwards AFB Sonic Boom Test (data from Blume, 1967 and Stanford, 1967)

Regression Analysis (y-intercept = 0)

House	Data Channel	Element	Room	Aircraft	R^2	Slope (g/psf)	Standard Error of the Slope	Misn	Approx. f0 (Hz)	Boom Dur. (T,sec)	f0 x T	Surface Area (ft^2)	Approx. Surface Weight (lb/ft^2)
E-1	111	Wall (east)	Bedroom #1	B58	0.345	0.111	0.005	73A	17.5	0.15	2.63	77	4.8
								86B	17.5	0.16	2.81	77	4.8
								87B	17.9	0.16	2.86	77	4.8
								80B	17.9	0.16	2.86	77	4.8
								80B	15.4	0.196	3.02	77	4.8
								18B	16.9	0.08	1.35	77	4.8
E-1	111	Wall (east)	Bedroom #1	F104	0.007	0.193	0.012	37B	25.7	0.18	4.63	102	4.8
E-2	311	Wall (east)	Dining Rm	B58	0.556	0.248	0.008	16-1	24	0.16	3.85	102	4.8
E-2	304	Wall (north)	Bedroom #1	B58	0.032	0.170	0.018	80RB					
E-2	311	Wall (east)	Dining Rm	F104	0.005	0.248	0.014	16-3	24	0.08	1.92	102	4.8
E-2	304	Wall (north)	Bedroom #1	F104	-0.005	0.204	0.012						
				Average =	0.157	0.196	0.011				2.88		
				Std Dev.=	0.217	0.047	0.004				0.90		
E-2	311	Wall (east)	Dining Rm	B58+F104	0.518	0.259	0.007						
E-2	305	2nd Roof Line	N. Wall, NE corner	B58+F104	0.176	0.049	0.002						
E-1	106	Roof Line	N. Wall, NE corner	B58+F104	0.339	0.053	0.002						
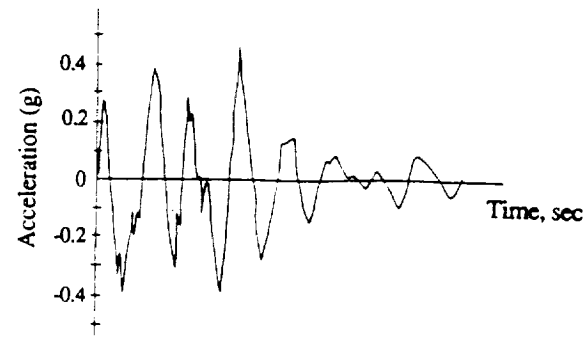
(a) F-104 Mission 16-3
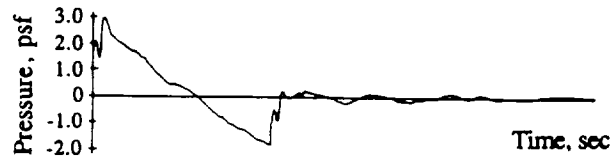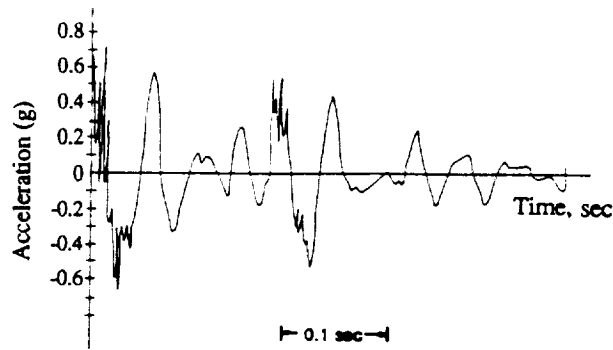
(b) B-58 Mission 16-1
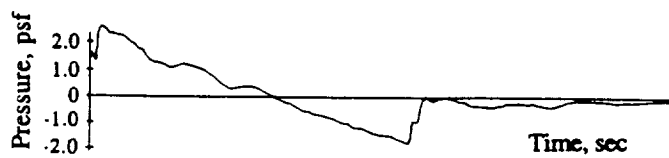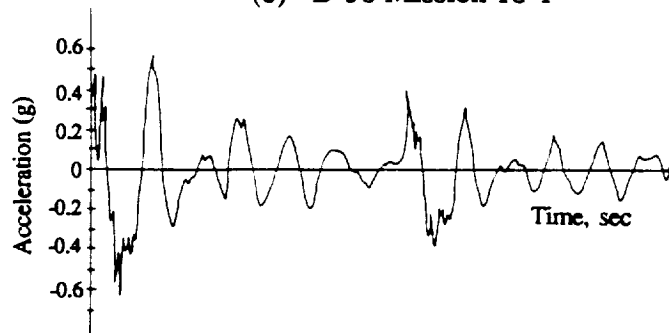
(c) XB-70 Mission 16-2

Figure B-1. Tracings of Time Histories of Sonic Boom Induced Acceleration of the East Dining Room Wall of House E-2 and Outside Pressure Signatures from Three Aircraft (Figures G-12, G-10, G-8, G-16, G-15 and G-14, Stanford, 1967).
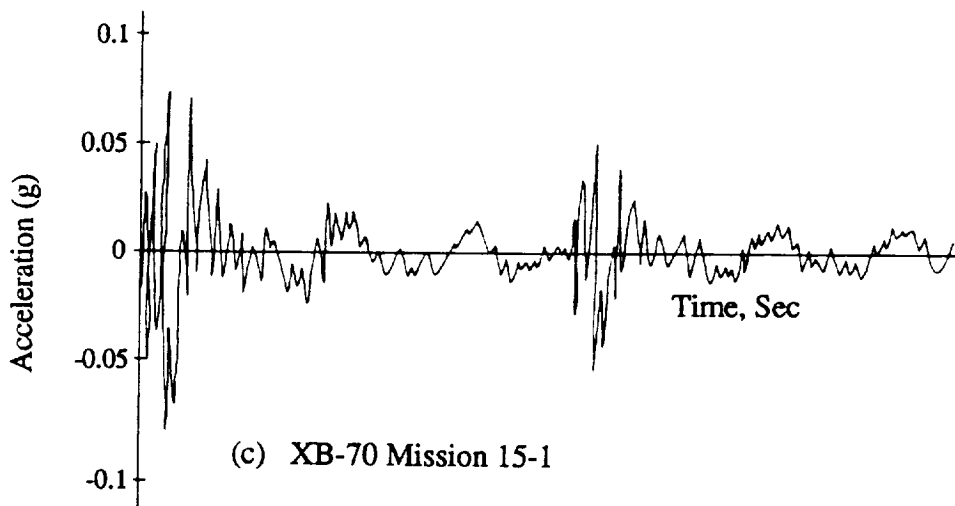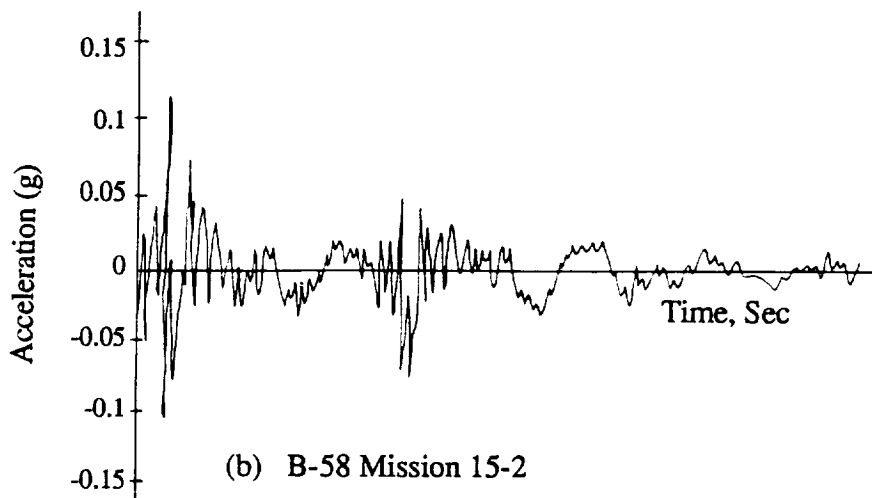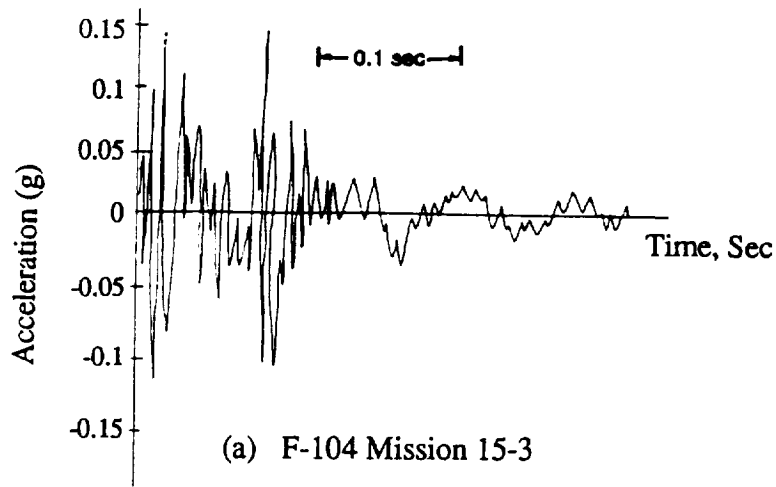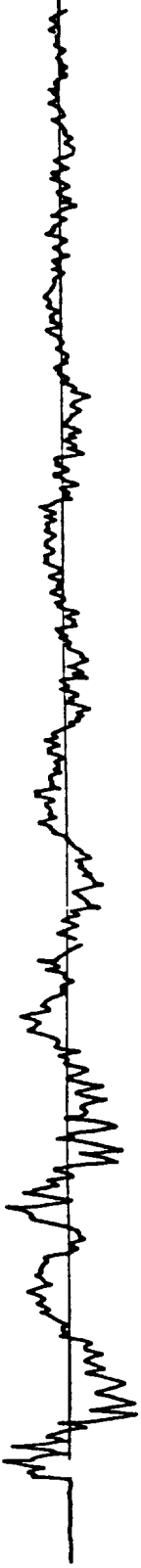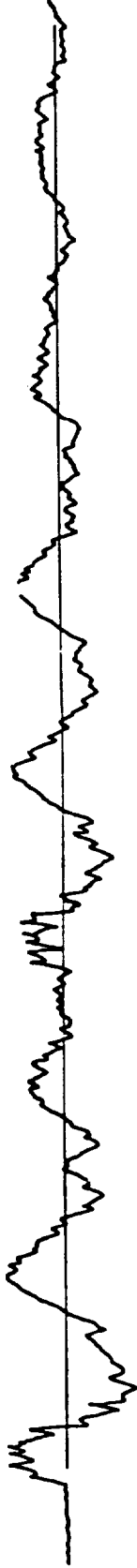
Figure B-2. Tracings of Times Histories of Sonic Boom Induced East-West Racking Acceleration at the Roof Line of the Northeast Corner of House E-1 from Three Aircraft (Figures 8-4, 8-3 and 8-2, Blume 1967).
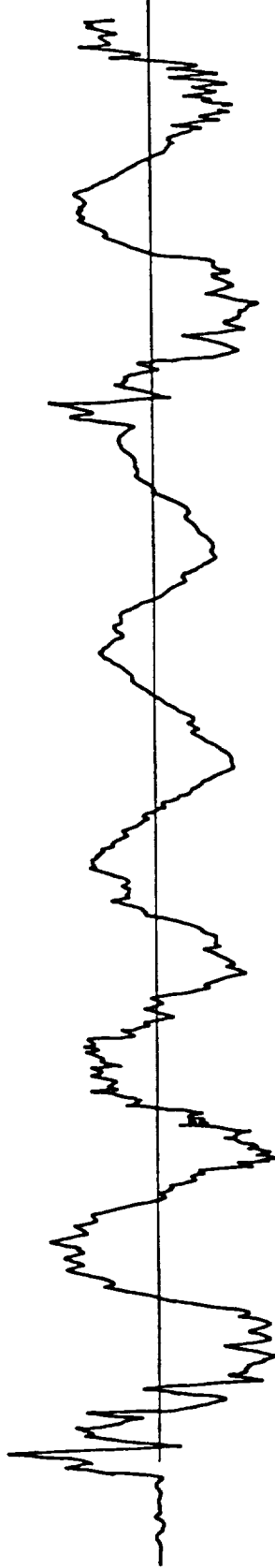
— 0.10 sec —

(a) F-104, Mission No. 37-B

(b) B-58, Mission No. 73-A

(c) XB-70, Mission No. 22

Figure B-3. Tracings of Time Histories of Sonic Boom Induced Acceleration Responses of the Bedroom East Wall of House E-1 from Three Aircraft (Figure G-4, Stanford, 1967).
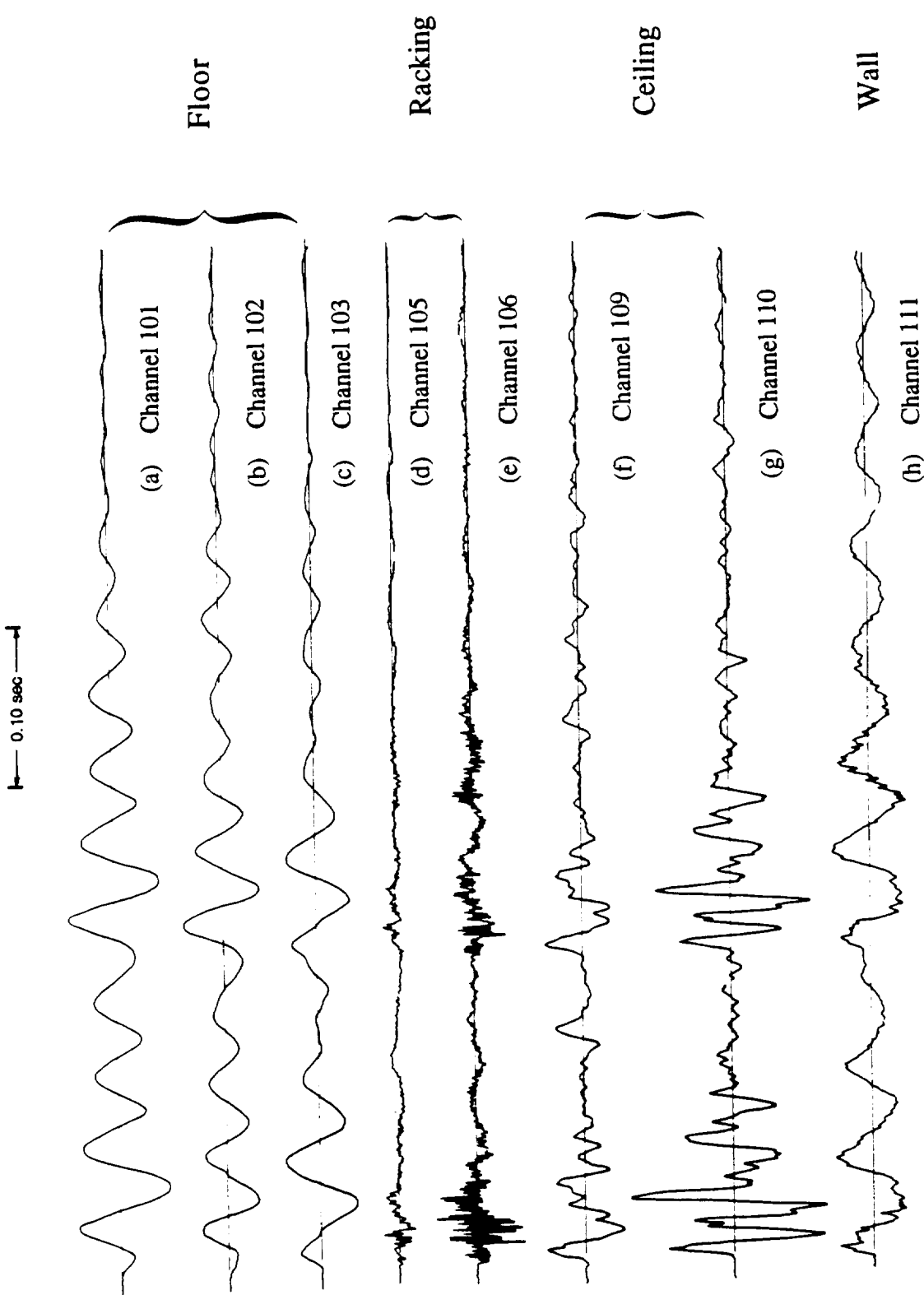
Figure B-4. Tracings of Time Histories of B-58 Sonic Boom Induced Acceleration Responses for Eight Transducer Locations in House E-1 for Mission 18-B (Figure G-3, Stanford, 1967).
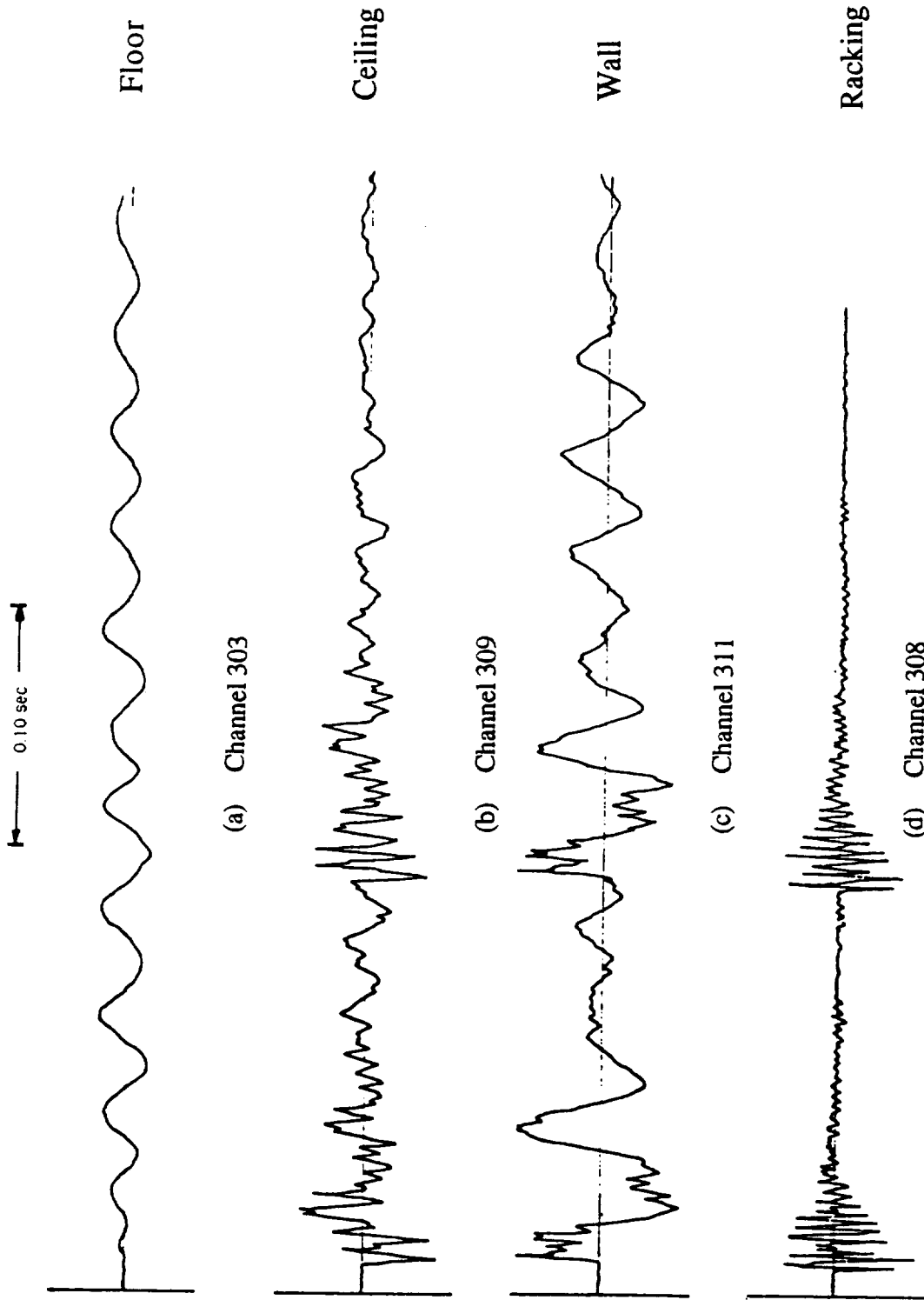
Figure B-5. Tracings of Time Histories of B-58 Sonic Boom Induced Acceleration Responses for Four Transducer Locations in House E-2 for Mission 80RB (Figure G-7, Stanford, 1967).

(a) Mission 86-B

(b) Mission 87-B

(c) Mission 80-B

(d) Mission 73-A

0.10 sec
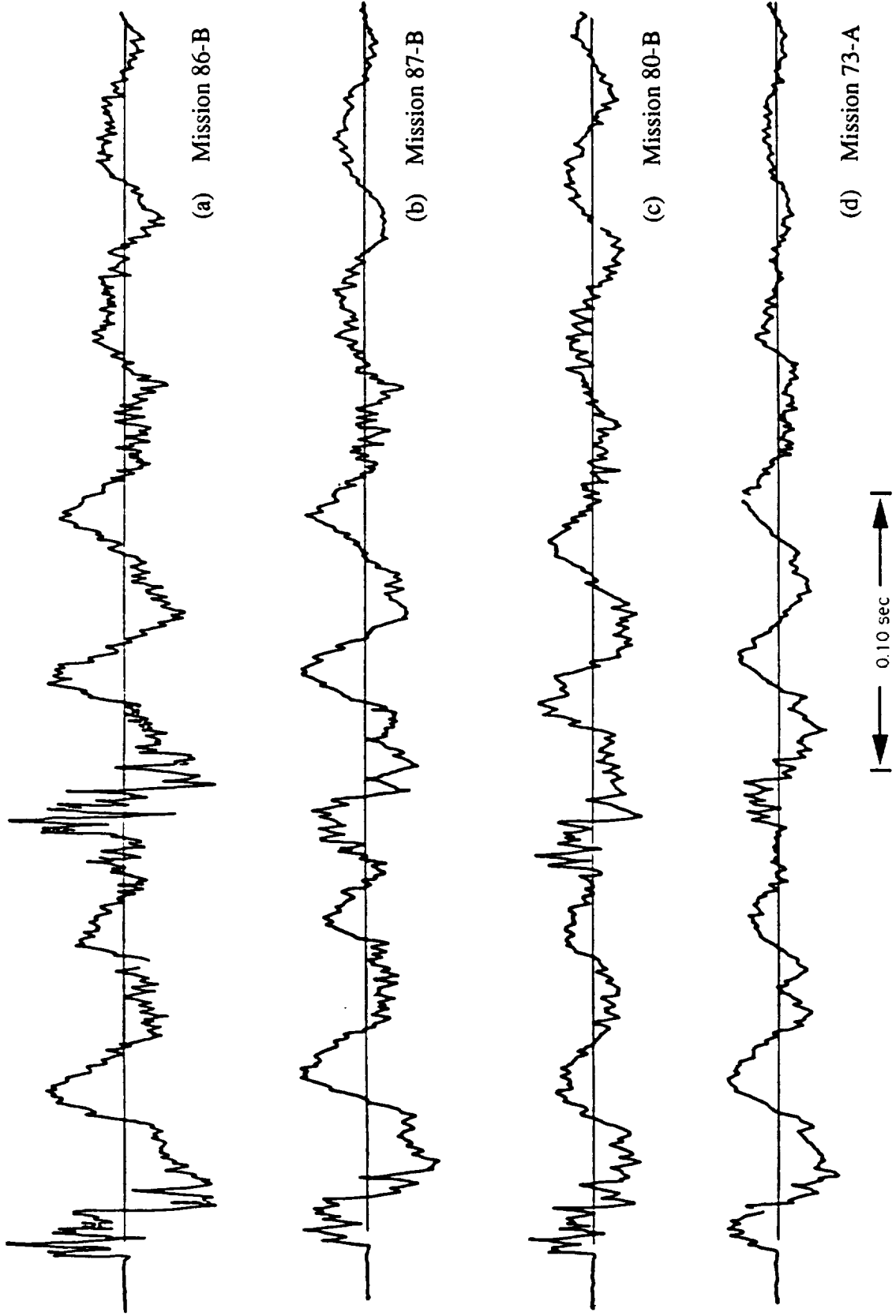
Figure B-6. Tracings of Time Histories of B-58 Sonic Boom Induced Acceleration Responses of the East Bedroom Wall of House E-1 for Several Different Missions (Figure G-5, Stanford, 1967).
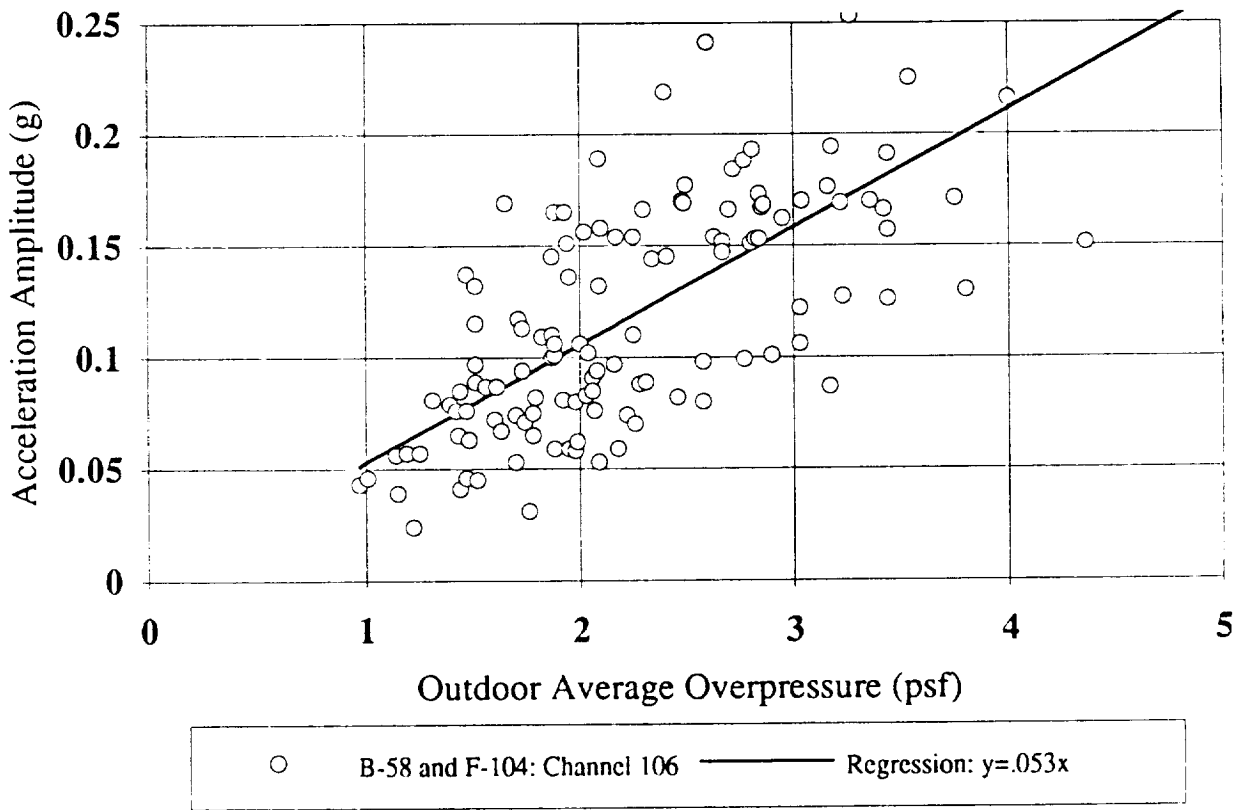
Figure B-7.   B-58 and F-104 Sonic Boom Induced East-West Racking Acceleration Response
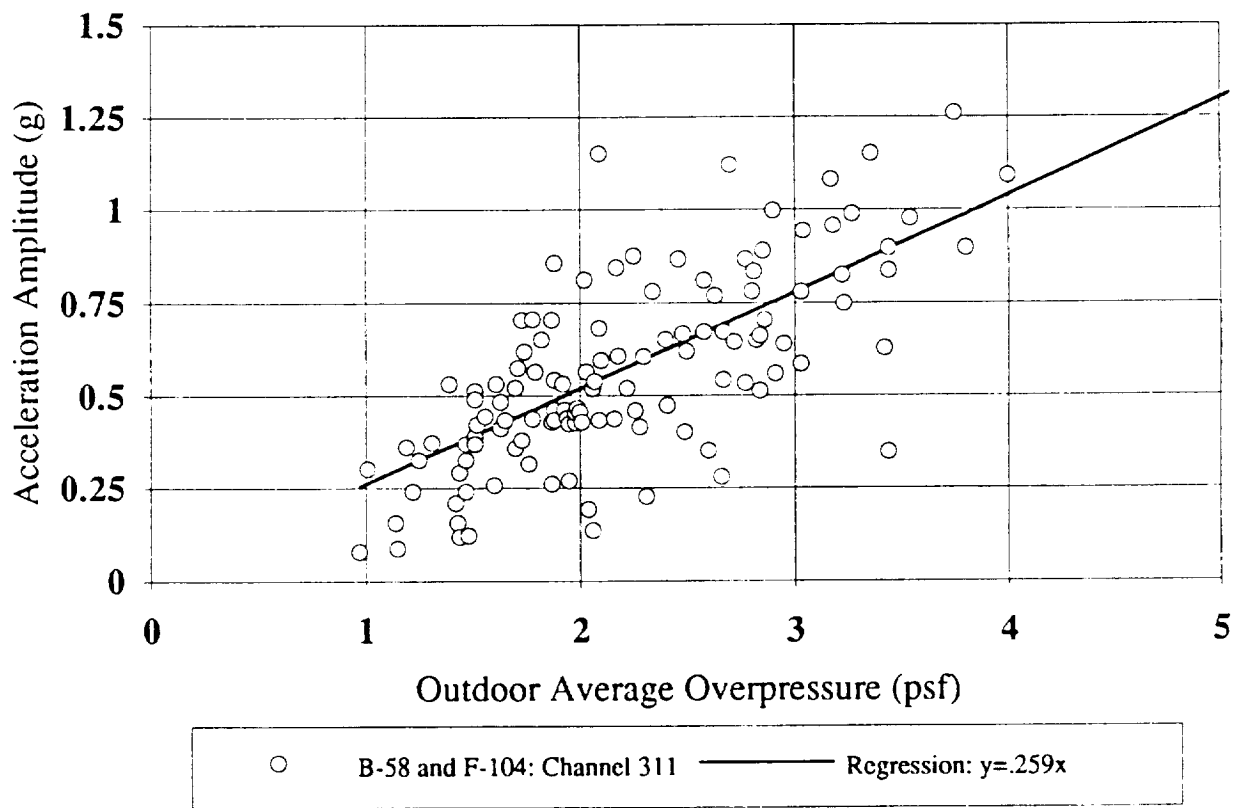of the Roof Line of House E-1 (Stanford, 1967).
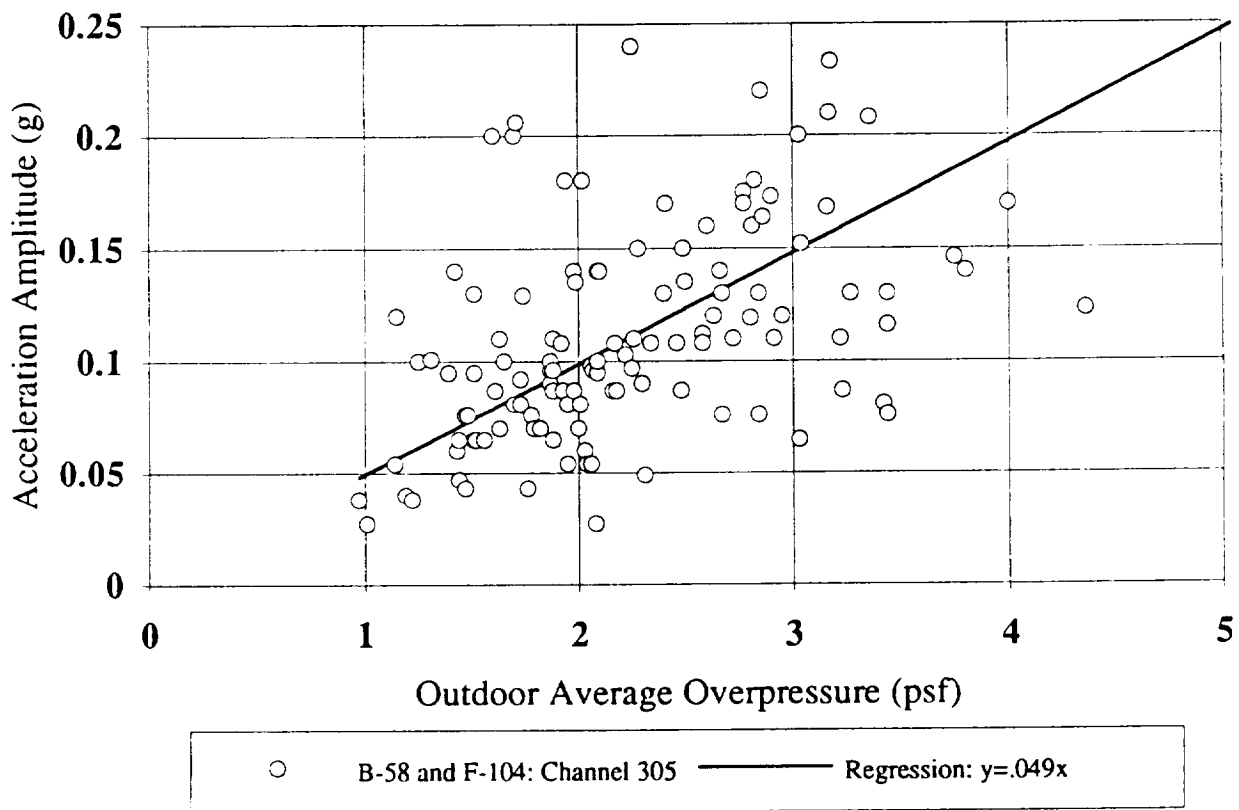
Figure B-8.   B-58 and F-104 Sonic Boom Induced East-West Racking Acceleration Response
of the Second-Story Roof Line of House E-2 (Stanford, 1967).

Figure B-9. B-58 and F-104 Sonic Boom Induced Horizontal Acceleration Response of the East Dining Room Wall of House E-2 (Stanford, 1967).
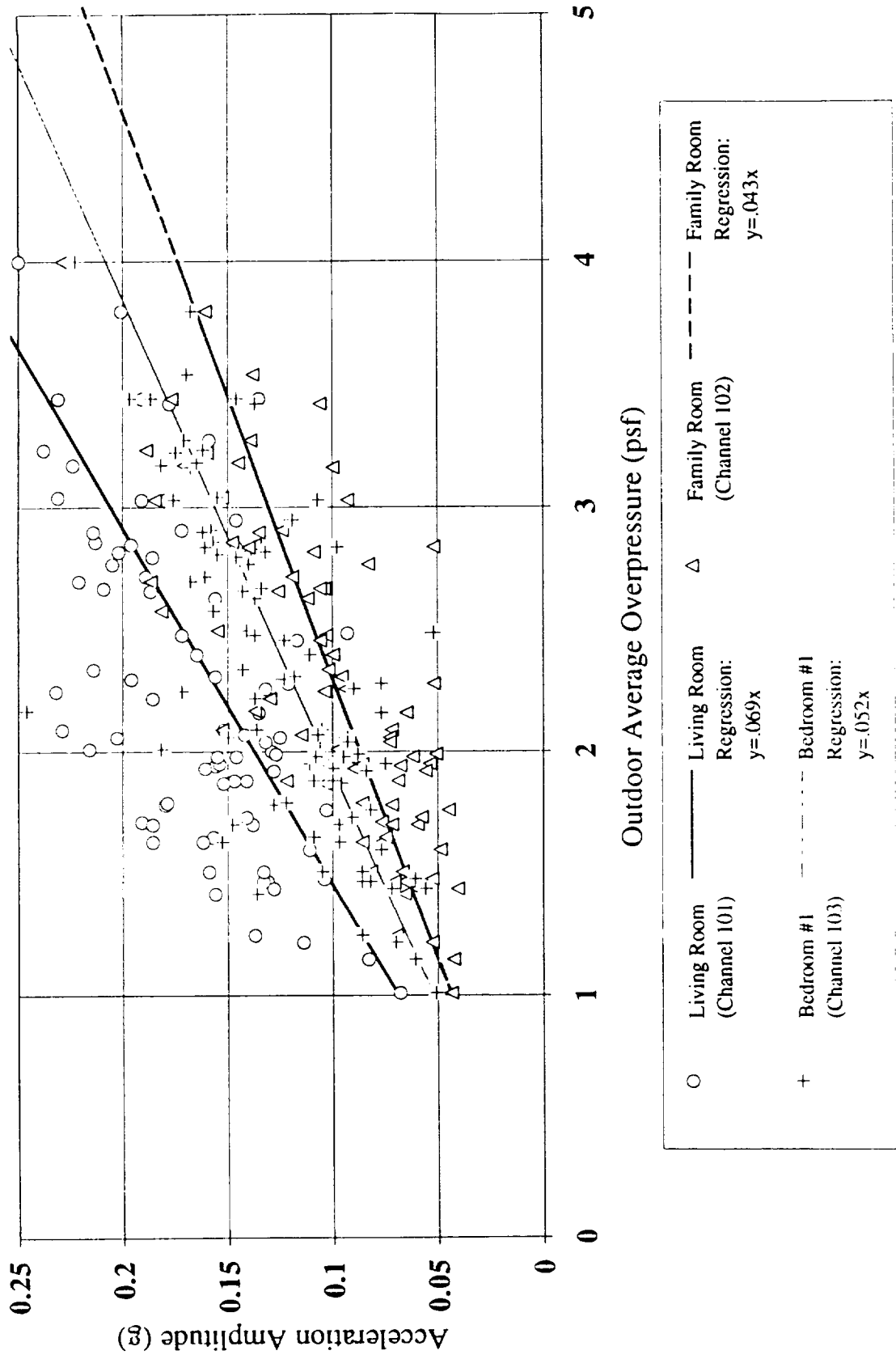
Figure B-10. B-58 Sonic Boom Induced Vertical Acceleration Response of Floors of House E-1 (Stanford 1967).
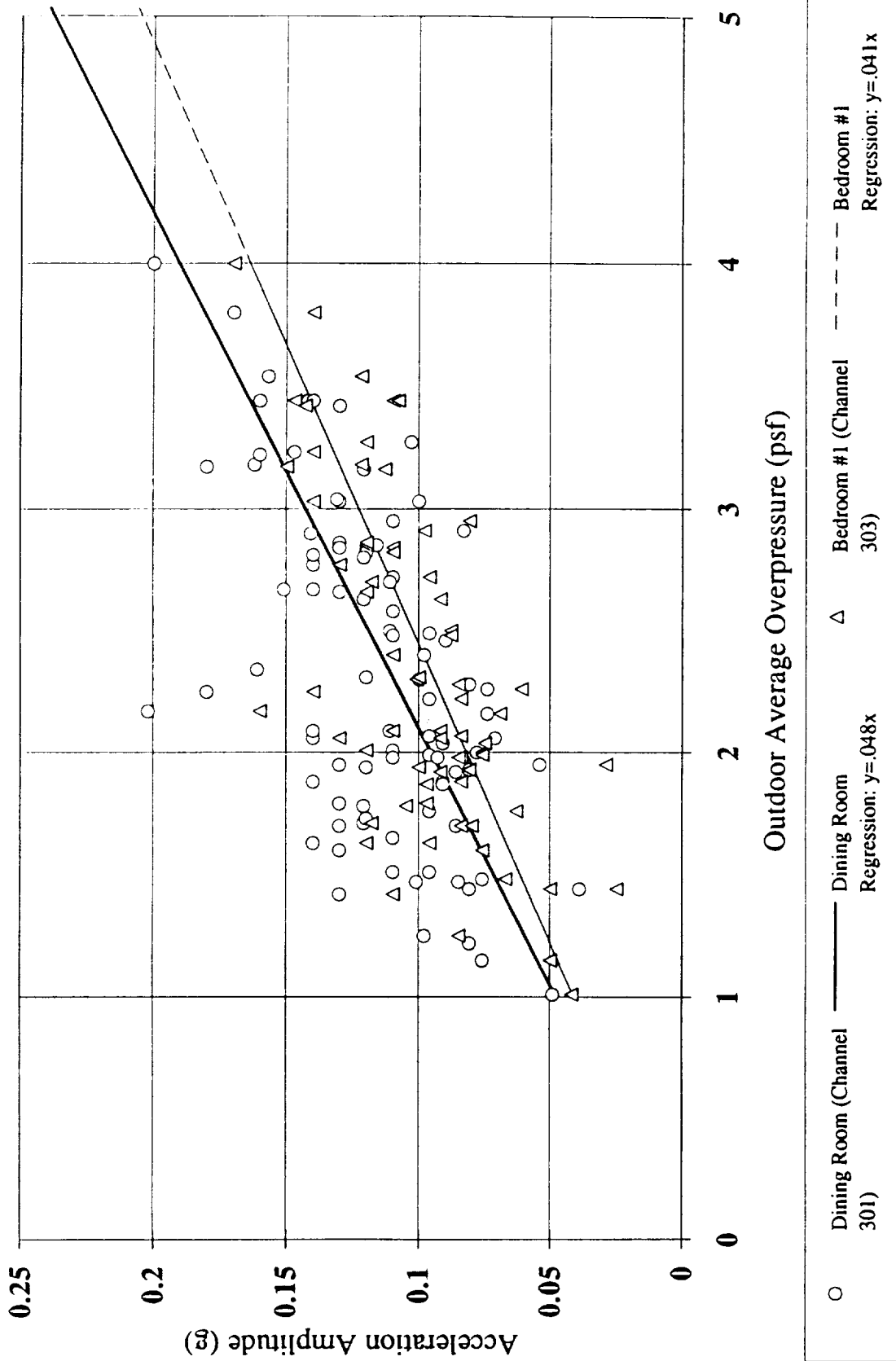
Figure B-11. B-58 Sonic Boom Induced Vertical Acceleration Response of Floors of House E-2 (Stanford 1967).
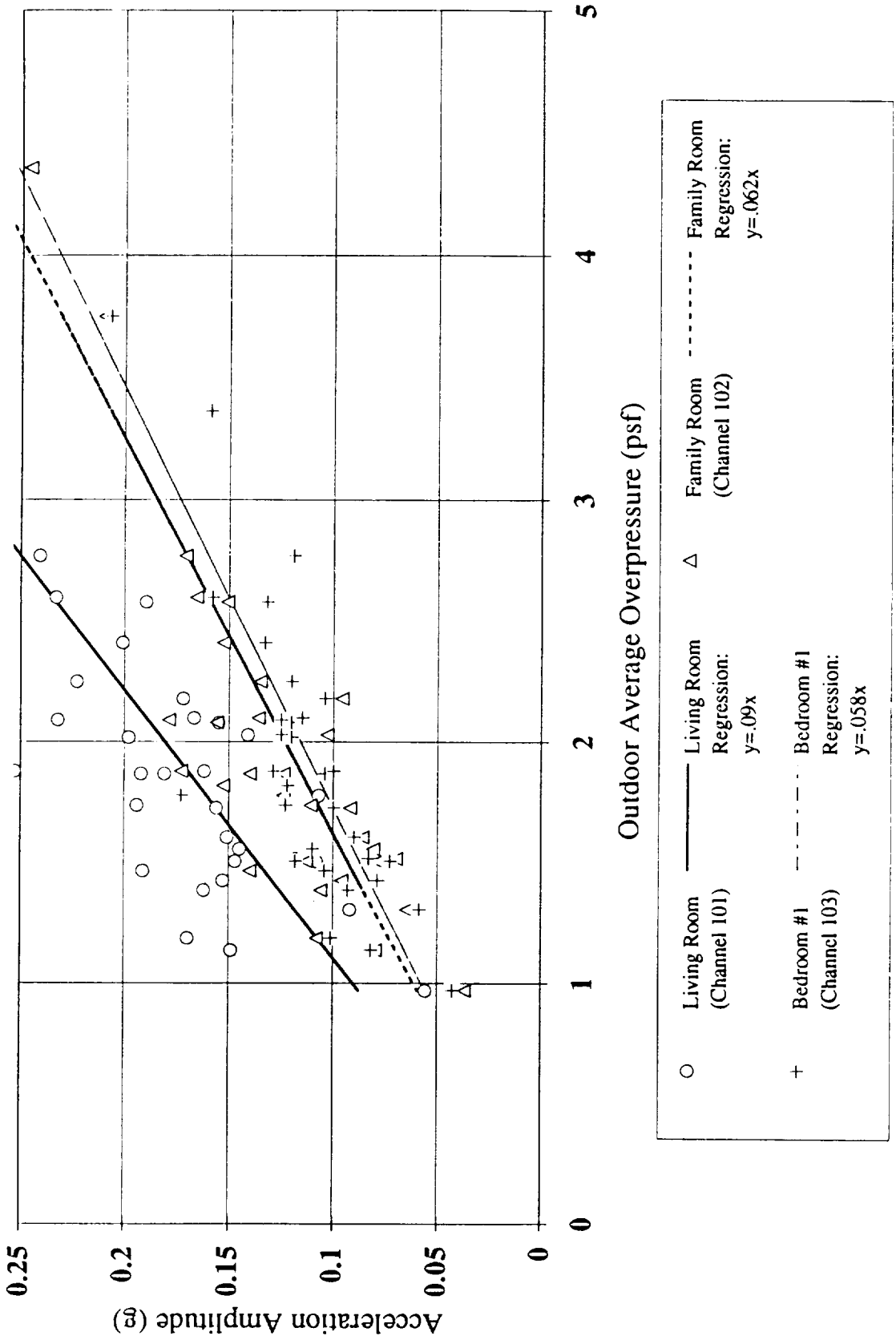
Figure B-12. F-104 Sonic Boom Induced Vertical Acceleration Response of Floors of House E-1 (Stanford, 1967).
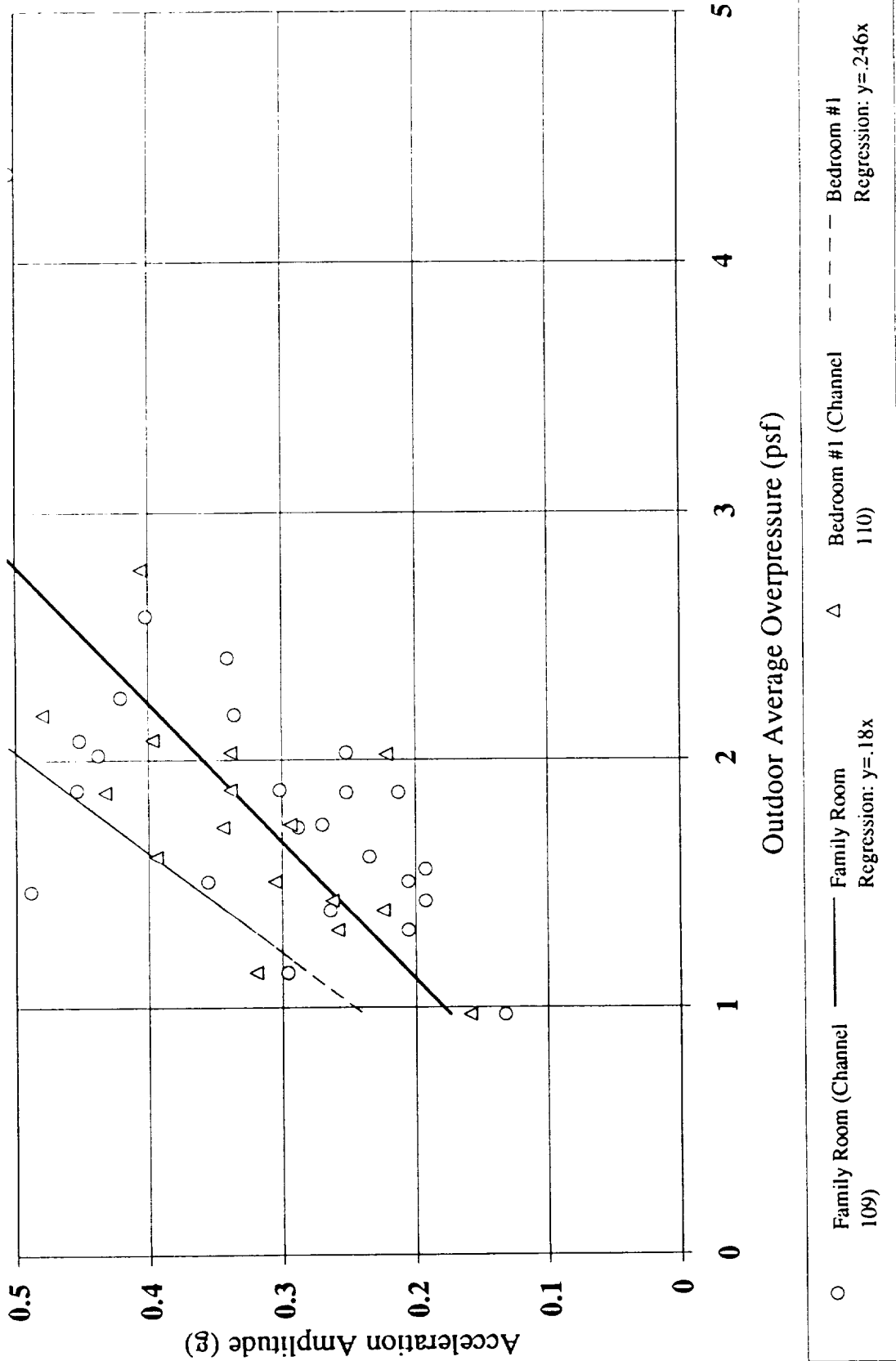
Figure B-15. F-104 Sonic Boom Induced Vertical Acceleration Response of Ceilings of House E-1 (Stanford 1967).

○   Family Room (Channel 109)   —— Family Room   △   Bedroom #1 (Channel 110)   – – – Bedroom #1

Regression: y=.18x   Regression: y=.246x